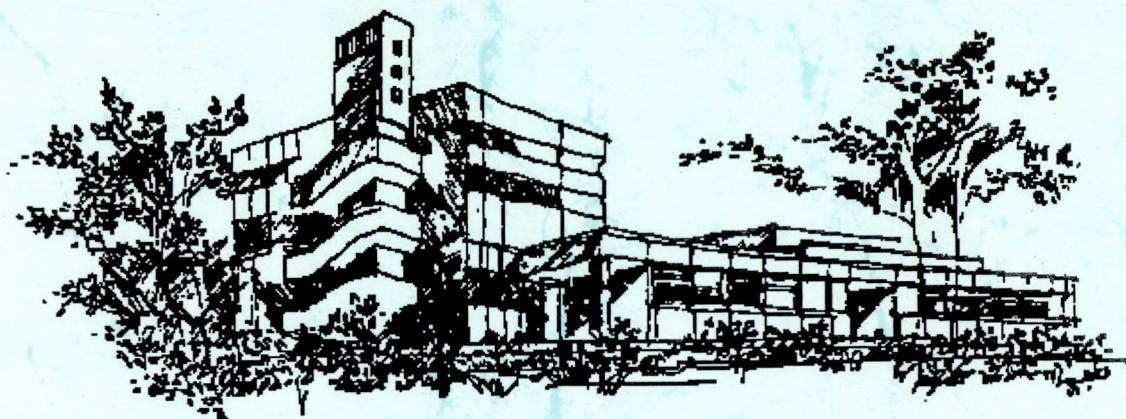


ATOMKI

ANNUAL REPORT

2001



INSTITUTE OF NUCLEAR RESEARCH
OF THE HUNGARIAN ACADEMY OF SCIENCES
DEBRECEN, HUNGARY



INSTITUTE OF NUCLEAR RESEARCH
OF THE HUNGARIAN ACADEMY OF SCIENCES
DEBRECEN, HUNGARY

ANNUAL REPORT
2001

ATOMKI

Postal Address:
P.O.Box 51
H-4001 Debrecen
Hungary

Editor:
I. Rajta

HU ISSN0 0231-3596

Preface

The first year of the millennium has passed smoothly. There was no U-turn in the life and management of the Institute though there were a few notable events.

In the Preface of the 2000 Annual Report I mentioned that a new major scheme had been launched by the government for the support and stimulation of research and development. The Institute had some stake in the first year, and was co-winner as consortium member in two projects: *Innovation Centre for Solar Cell Technology* and *Contamination of the environment by atmospheric aerosol*. In the former we have to support technological development work by analysing the surface of solar cells with the methods of photoelectron spectroscopy. The latter project involves us on account of the aerosol monitoring studies pursued for many years and our recent studies of the microstructure of the aerosol samples. This year we are participants of three major projects that have got to the final round and thus may be among the winners.

Two applied research projects of national significance concerning radioactive waste management in Hungary have been completed. We carry on innovative work on the monitoring of the potential environmental pollution of nuclear energy production in the country.

There has been an important development in the relationship of ATOMKI to the University of Debrecen. We used to have a Joint Department of Physics, whose activity was focussed on the teaching of environmental physics. The university used to have a Department of Isotope Techniques. Part of the latter has now been detached and merged into the Joint Department under the name of Joint Department of Environmental Physics, and moved to the premises of ATOMKI.

The subject of the Physics Days, the local 'public feast' of physics was the centenary of quantum physics. Some of the best popularizers of the country gave talks on the principles and peculiarities of quantum mechanics, on quantum teleportation, on some macroscopic-scale quantum phenomena and on recent attempts to go beyond quantum mechanics.

We held no international conferences this year, but the proceedings of those three held in the year before appeared this year. Moreover, there was a joint symposium with the participation of the Institute in Japan. As a concerted action with the University of Debrecen, back in 2000, we had signed an agreement of cooperation with Niigata University (Japan). The Debrecen signatories were the Faculty of Science and ATOMKI, while the Niigata partners were the corresponding faculty and graduate school. In May, 2001, there was a joint symposium held in Niigata to stimulate the cooperation between the two parties. There were six Debrecen participants. Professor Yasuyuki Suzuki, the mastermind of the cooperation agreement, was conferred an Honorary Degree at the University of Debrecen in November, 2001.

As for notable results, first I should mention a piece of instrument construction, a strong but recently declining tradition here. The light-charged-particle detector system DIAMANT, which was originally developed in Bordeaux, has been completely upgraded jointly with CENBG (Bordeaux). When combined with γ -ray detector arrays, DIAMANT thoroughly enhances their selectivity, and thus their utility. It may, e.g., give a better chance for hyperdeformed nuclear bands to show up. The most prominent features of the upgraded DIAMANT are fast, compact and sophisticated modern electronics and excellent particle discrimination. It is being used in combination with EUROBALL (Strasbourg), with EXOGAM (GANIL, Caen) and elsewhere.

A new perspective has been opened for electron spectroscopy by deployment of a Debrecen spectrometer at the Lund synchrotron. Auger electrons and photoelectrons are detected in coincidence, and complicated spectra coming from multiple initial states have been disentangled for the first time. The investigations of this type provide very detailed and thorough tests of atomic wave functions.

The group working on ion-beam analysis has started a program on the identification of light elements in samples. They have recognized that deuteron-induced γ -ray emission (DIGE) may be a

most efficient tool for this purpose, and started to measure excitation functions of this process for later use in analyses.

The small group working on perturbative quantum chromodynamics has been remarkably successful, and their results are rated high at CERN as well. They have recently constructed a numerical program for calculating multijet cross sections in deep inelastic scattering production at the next-to-leading order accuracy. They have calculated the three-jet differential distributions as functions of the momentum transfer, the Bjorken variable and the three-jet invariant mass. Adding the next corrections to the leading-order predictions, they found remarkable agreement with the data obtained at DESY, Hamburg.

It is also the result of last year's efforts that we have given a fully satisfactory microscopic description of the most famous halo nucleus, ^{11}Li , as a system of $\alpha+t+n+n+n+n$ clusters. It has been shown that the ^9Li 'core' is substantially distorted in ^{11}Li , which reduces the (still sizeable) neutron skin, and all measured nuclear properties are reproduced. The submodels also describe all of the nuclei $^7\text{--}^{11}\text{Li}$ successfully.

The Szalay Prize of the Institute for research in basic science was awarded to Dr. Béla Sulik for his experimental and theoretical studies of ionization processes and multiple scattering in ion-atom collisions. One of the 'Physics Awards' by the Academy of Sciences was received by Dr. Z. Trócsányi for his results in the application of perturbative quantum chromodynamics to particle physics. For my studies of nuclear clustering, I have been granted the 'Simonyi Fellowship', which is an award of high prestige established by a private donation.

We often say that ATOMKI has less reputation nationally than internationally. Our national reputation has however been boosted now by the fact that at last year's Assembly of the Academy of Sciences as many as four of our members have been invited to give review talks of their research field: Zs. Fülöp, A. Krasznahorkay, S. Ricz and B. Sulik. At this point it should be mentioned that Á. Kovách was re-elected last year as Secretary General of Eötvös Physical Society for another two years.

Last year I reported on a shock-wave of candidates for the DSc. degree in the pipeline. Now I can report that all of them (A. Krasznahorkay, A. T. Kruppa, E. Somorjai and T. Vertse) have been awarded the degree.

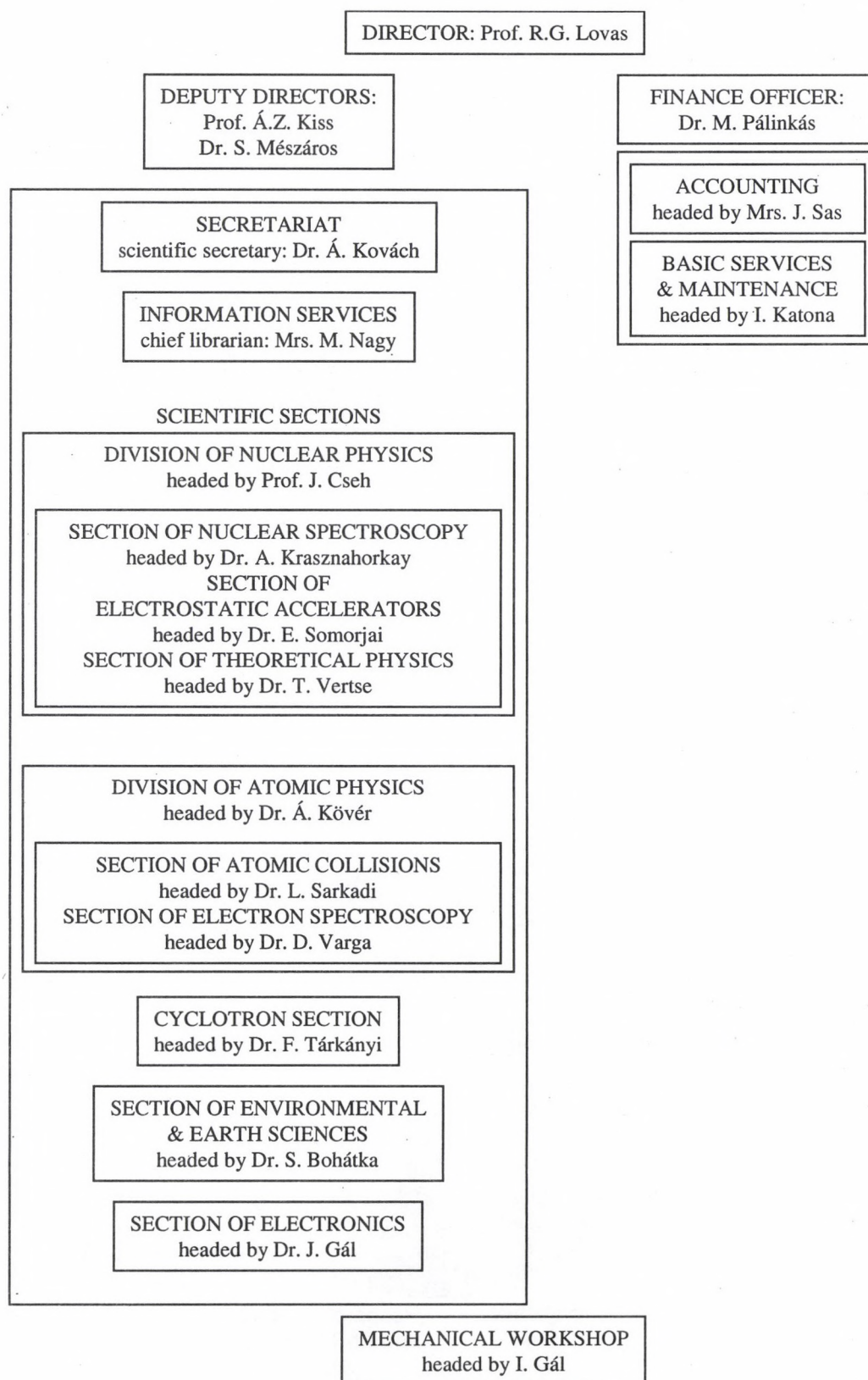
The financial and personnel conditions at the end of 2000 are given in the pie diagrams to follow this Preface.

This Annual Report has been prepared in \LaTeX , and will be available at the web-site at www.atomki.hu in HTML, DVI, PDF and PS(.GZ) formats.

Debrecen, 22 March 2002

Rezső G. Lovas
Director

Organizational structure of ATOMKI



Data on ATOMKI

At present the Institute employs 192 persons. The affiliation of personnel to units of organization and the composition of personnel are given below.

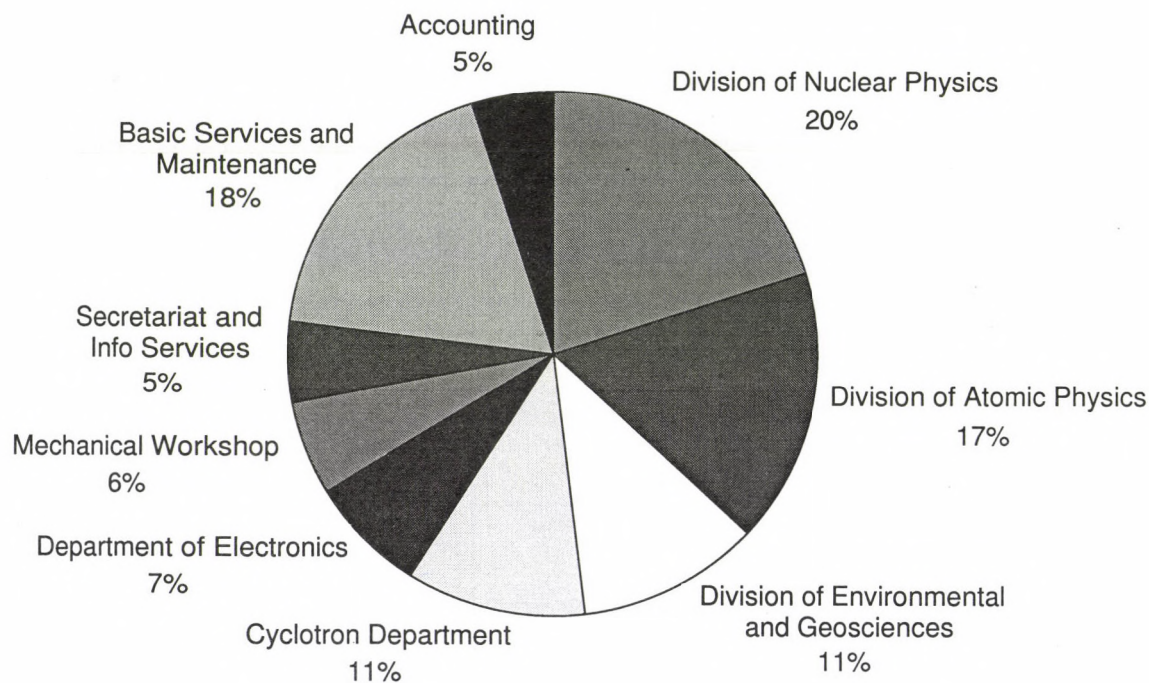


Figure 1. Affiliation of personnel to units of organization

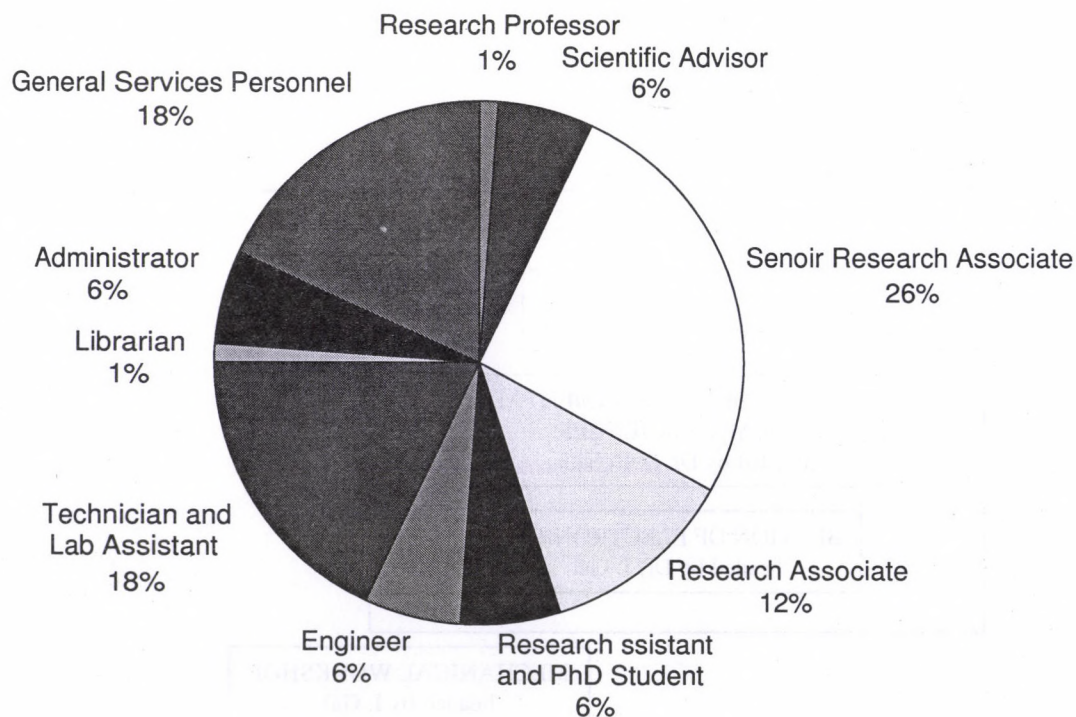


Figure 1. Composition of personnel

Finance

The total budget of the Institute for the year 2001 was 931 million Hungarian Forints. The composition of the budget and the share of personnel expenditure within the budget are shown below.

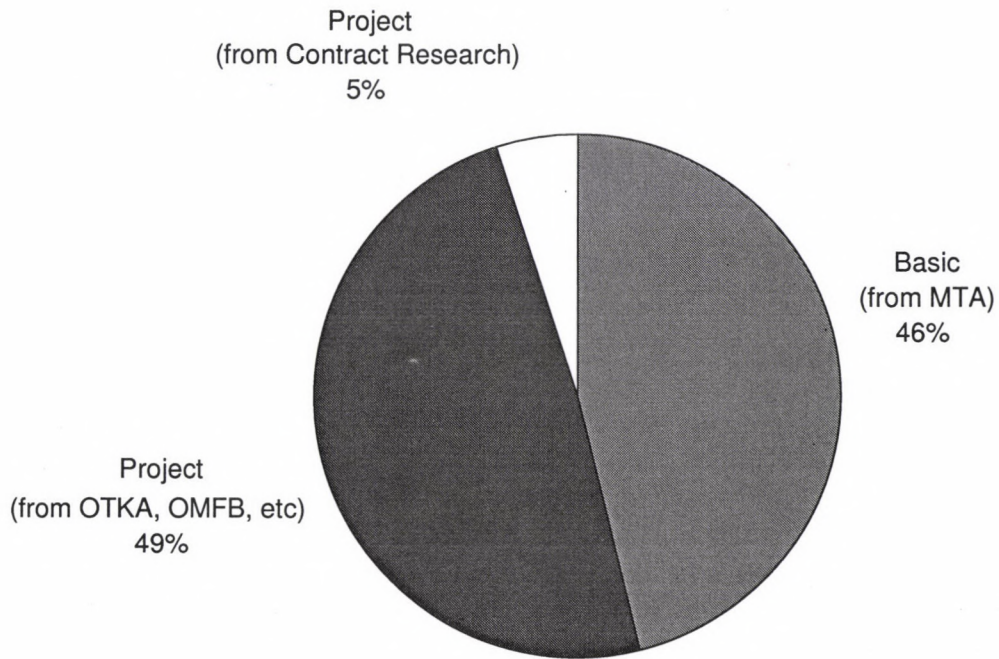


Figure 1. Composition of the budget of the Institute
MTA: Hungarian Academy of Sciences
OTKA: National Fund for Scientific Research
OMFB: National Committee for Technological Development

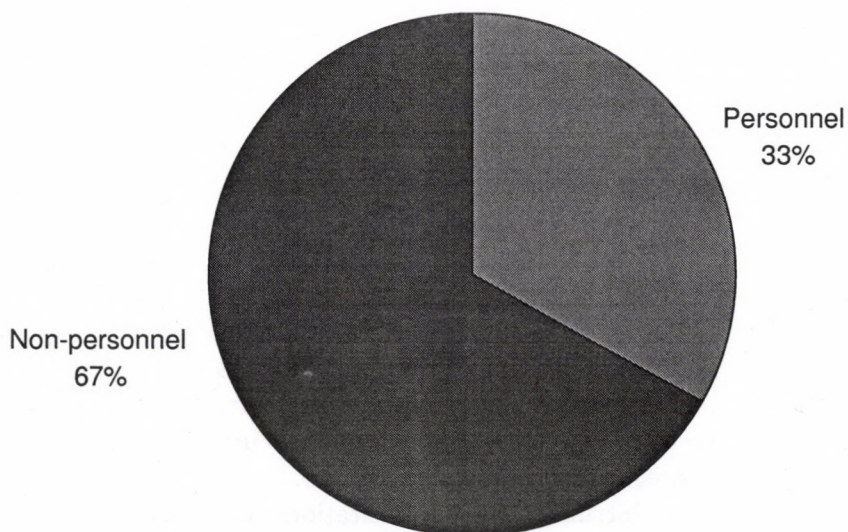


Figure 1. Breakdown of expenditure into personnel and non-personnel expenditures

Table of contents

Preface	i
Data on ATOMKI	iii
Table of contents	vi
1. General Physics	
1.1 Breakdown of \mathcal{PT} symmetry in solvable potential models	1
1.2 Spectral properties of an exactly solvable Natanzon-class potential	2
1.3 Composite dynamical symmetries	3
2. Subatomic Physics	
2.1 Astrophysical p-process studies on Se isotopes	4
2.2 Low energy cross section measurements	5
2.3 Temperature dependent BCS-gap-equations in the continuum	6
2.4 Perturbative Quantum Chromodynamics	7
2.5 Mass distribution of fission fragments from hyperdeformed states in $^{232}\text{Th}(n,f)$	8
2.6 Clusterization and configuration-mixed effective $SU(3)$ symmetries	9
2.7 Study of neutron excitations across the $N=50$ shell gap in ^{102}In	10
2.8 Study of shape evolution in the neutron-rich ^{40}S , ^{42}S and ^{44}S isotopes	11
2.9 Description of resonant states by analytic continuation	12
2.10 Installation of a new Total Absorption Spectrometer at ISOLDE/CERN mass separator	13
2.11 <i>Ab initio</i> versus cluster-model calculations	14
2.12 Microscopic multicluster description of ^{9-11}Li	15
2.13 New region of signature inversion in the $A\approx 100$ Rh and Ag isotopes	16
2.14 Low-lying levels and collective bands in doubly-odd ^{124}Cs	17
2.15 Magnetic dipole bands in ^{190}Hg	18
2.16 Measurement of Doppler shift attenuated gamma-rays from the $^{18}\text{O}(2_1^+)$ state	19
2.17 Production and chemical separation of ^{48}V radioisotope	20
3. Atomic Physics	
3.1 Study of the transfer ionization process by observing the electron cusp in $\text{He}^{2+}+\text{He}$ collisions	22
3.2 Postcollision interaction and two-centre effects in ionizing collisions	23
3.3 Calculation of ion-induced inner-shell ionization cross sections by applying the CTMC method	24
3.4 Theoretical study of cusp-electron emission from $\text{O}^{8+}+\text{Ar}$ collisions	25
3.5 Laser Spectroscopy of Antiprotonic Helium Atoms	26
3.6 Differential cross sections for positron impactexcitation of hydrogen	27
3.7 Application of the Landau-Zener model and the classical trajectory Monte Carlo method for capture processes in collisions of highly charged ions with light atoms	29
3.8 Improvement of atomic physics database is necessary to utilise the full potential of EDS X-ray spectrometry	30
3.9 Separation of extrinsic and intrinsic plasmon excitations in Ge KLL Auger spectra	31
3.10 Thickness determination of Germanium surface layers	32
3.11 Calculation of the Single Differential Cross Section of the $1s \rightarrow 2l$ Excitation of the Lithium-Like O^{5+} Ions in Collisions with He	33

3.12	Collision dynamics probed by convoy electron emission	34
3.13	Enhancement of Low-Energy Electron Ion Recombination in a Magnetic Field	35
3.14	Evidence for Fermi-Shuttle Ionization in $C^+ + Xe$ Collisions	36
3.15	Auger-electron lineshapes in electron impact ionization	37
3.16	Transmission of Ne^{7+} ions through nanocapillaries etched in polymer PET: Evidence for capillary guidance	38
3.17	Electron emission in highly-charged ion collisions on Li surfaces	39
4. Material Science and Analysis		
4.1	Micro-RBS characterisation of the chemical composition and particulate deposition on Pulsed Laser Deposited $Si_{1-x}Ge_x$ thin films	40
4.2	Formation and Stability of Metastable Pd(Zr) Solid Solution Developed During Ball Milling and/or Heat-Treatment of Pd_3Zr	41
4.3	Non-linearity of diffusion in amorphous Si-Ge multilayers	42
4.4	Magnetic relaxation and disordered magnetic phase in partially oxidized bulk nanocrystalline iron	43
4.5	Friction force of the highly charged ions at large distances from the metal surfaces	44
5. Earth and Cosmic Sciences, Environmental Research		
5.1	Geological and Biomedical Applications of Ion Beam Analysis Techniques	45
5.2	Radon exhalation of limestone bedrock and cave deposits	46
5.3	Representative indoor radon survey in Gyergyóremete, Romania	47
5.4	The origin of water in the vicinity of Püspökszilágy RWTDS	48
5.5	Excess tritium in observation wells around Püspökszilágy RWTDS	49
5.6	Modeling of the groundwater movement at Püspökszilágy RWTDS	50
5.7	Isotopic analysis of Hungarian thermal waters	51
5.8	^{226}Ra in bottled mineral waters of Hungary	52
6. Biological and Medical Researches		
6.1	Reduction of $[^{11}C]$ carbon dioxide to $[^{11}C]$ olefin over zeolite catalyst by hydrogenation	54
7. Development of Methods and Instruments		
7.1	Activities at the Van de Graaff Accelerator Laboratory	55
7.2	Status Report on the Cyclotron	56
7.3	3D Proton Beam Micromachining	57
7.4	Application for the excitation of medium energy (up to 10 keV) photoelectron and Auger lines used in the study of surface analytical applications*	58
7.5	Modeling and calibration of a double-crystal spectrometer for absolute x-ray wavelength measurements	60
7.6	Off-line production of 7Be radioactive ion beam	61
7.7	Spectral Artefacts with a Si-pin Photodiode X-Ray Detector: I. The Low Energy Case	62
7.8	Spectral Artefacts with a Si-pin Photodiode X-Ray Detector: II. The High Energy Case	63
7.9	Scintillation Detectors with Multilayer Polymer Mirror Reflector Based on Giant Birefringent Optics	64
7.10	Production of multiply charged fullerene and carbon cluster beams by the ECR ion source	65
7.11	Langmuir-probe data analysis including the complex nature of the ECR plasma	66

8. Publications and Seminars

8.1	Papers Published in 2000	67
8.2	Conference contributions, talks and reports	82
8.3	Theses	89
8.4	Diploma work	90
8.5	Book, chapter of book	91
8.6	Edited work	92
8.7	Hebdomadal Seminars in 2000	93

Author index	94
------------------------	----

1.1 Breakdown of \mathcal{PT} symmetry in solvable potential models

G. Lévai, M. Znojil^{a)}

Recently a number of complex one-dimensional quantum mechanical potentials have been found to possess real energy eigenvalues under rather general conditions. These potentials are not Hermitian, but they are invariant under the simultaneous action of the \mathcal{P} space and \mathcal{T} time reflection operations. These \mathcal{PT} -symmetric potentials have the property $[V(-x)]^* = V(x)$.

It was also found, that \mathcal{PT} symmetry does not necessarily lead to completely real spectrum, and examples have been found where part or all of the energy spectrum of a potential is complex. Since the Hamiltonian retains \mathcal{PT} symmetry, while the wavefunctions do not, this phenomenon has been interpreted as the spontaneous breakdown of \mathcal{PT} symmetry. In general, no criteria have been found for this breakdown of the symmetry, however, complex eigenvalues typically appeared when the imaginary part of the potential reached a critical strength. We analysed two different families of potentials [1,2] to formulate criteria for the breakdown of \mathcal{PT} symmetry.

Following an earlier work of us, in which we gave conditions for real energy eigenvalues in the \mathcal{PT} symmetric versions of shape-invariant potentials, we formulated conditions for having normalizable complex-energy solutions in the same potentials [1]. The potentials we analysed had the common feature that they could be made \mathcal{PT} symmetric by applying an imaginary coordinate shift $x \rightarrow x + i\epsilon$ to them, besides changing some of their parameters to imaginary values. Although this imaginary coordinate shift formally takes these potentials off the real x axis, they can still be considered as potentials defined on the real axis because the potential functions can be rewritten such that ϵ appears only in the redefined parameters of these potentials. This treatment could be applied to all shape-invariant poten-

tials (the simplest subset of the general Natanzon potential class) with the exception of the Coulomb and Morse potentials, in which cases \mathcal{PT} symmetry could be implemented only if these potentials were defined on a bent contour of the complex x plane. We have shown that with the exception of two cases (the Rosen-Morse II and the Eckart potentials) complex energy eigenvalues can appear at certain values of the potential parameters, and they always appear in complex conjugated pairs [1]. Furthermore, for these shape-invariant potentials the energy spectrum always contains either only real or only complex eigenvalues, so these two types of energy eigenvalues do not mix [1]. Our study confirmed earlier findings for two potentials (the hyperbolic Scarf and the harmonic oscillator potentials), and in every other cases it lead to new results.

In another study [2] we analysed the complex square well potential in order to find criteria for the spontaneous breakdown of \mathcal{PT} symmetry. This potential is defined in the $x \in (-1, 1)$ domain as $V(x) = \pm iZ$ for $\text{Re}(x) < 0$ and > 0 , respectively, where Z is a constant. We found [2] that all the energy eigenvalues are real if $|Z| < 4.48$, but then the lowest energy level splits into a pair of complex conjugated energy eigenvalues. The second critical point was found at $|Z| \sim 12.80155$: above this $|Z|$ value the second energy eigenvalue also split into two complex ones. It is to be noted that in contrast with the shape-invariant potentials studied in [1], the energy spectrum of the complex square well the energy spectrum can be mixed.

a) Nuclear Physics Institute of Academy of Sciences of the Czech Republic, Rež, Czech Republic.

[1] G. Lévai, M. Znojil, Mod. Phys. Lett. **A16** (2001) 1973.

[2] M. Znojil, G. Lévai, Mod. Phys. Lett. **A16** (2001) 2273.

1.2 Spectral properties of an exactly solvable Natanzon-class potential

G. Lévai, M. Znojil^{a)}, R. Roychoudhury^{b)}, P. Roy^{b)}

In non-relativistic quantum mechanics the most general class of exactly solvable potentials is Natanzon (or Natanzon confluent) potentials. The main feature of these potentials is that their bound-state solutions are expressed in terms of a single (confluent) hypergeometric function. They depend on six parameters, three of which are related to the variable transformation $z(r)$ connecting the wavefunctions $\psi(r)$ with (confluent) hypergeometric functions. In the most general case both the $z(r)$ function and the bound-state energy eigenvalues are determined by an implicit equation, which depend on the parameters.

An example for a potential with implicitly determined energy spectrum is

$$V(x) = -\frac{B}{z(x)} + \frac{A}{z^2(x)} - \frac{3}{4z^4(x)}, \quad (1)$$

where $z(x) = [1 + \exp(-2x)]^{1/2}$. This potential was generated from the shape-invariant Eckart potential in [1] by means of the point canonical transformation method, and it was identified as a conditionally exactly solvable (CES) potential, arguing that it is solvable only under the condition that the coupling parameter of the last term is a constant, $-3/4$.

A peculiarity of this potential is that its bound-state eigenvalues are obtained by solving a cubic algebraic equation for the principal quantum number n . Obviously, one expects then that only one of the three roots can lead to physically meaningful energy, however, this point has not been proven consistently in [1]. We analysed potential (1) and obtained the following results [2]:

- We proved that from the three roots the

middle one gives the physically acceptable energy eigenvalue.

- We gave a supersymmetric reinterpretation of this potential.
- We showed that (1) is, in fact, a Natanzon class potential, and therefore its interpretation as a CES potential is misleading.

The implicit nature of the energy spectrum also raises questions about the \mathcal{PT} symmetric version of (1). \mathcal{PT} symmetric potentials are complex and satisfy the relation $[V(-x)]^* = V(x)$, nevertheless, their energy eigenvalues are real under rather general conditions. In general, their solutions obey less strict boundary conditions, and therefore they have a richer energy spectrum than their Hermitian counterparts. We constructed the \mathcal{PT} symmetric version of (1) defined on a contour of the complex x plane [3], and showed that the number of bound states double, and this is secured by the fact that out of the three roots, now two lead to physically acceptable eigenfunctions. So, in addition to n , a parity-like quantum number, $q = \pm 1$ is also needed for the unambiguous classification of the states.

a) Nuclear Physics Institute of academy of Sciences of the Czech Republic, Řež, Czech Republic

b) Physics and Applied Mathematics Unit, Indian Statistical Institute, Calcutta, India

[1] R. Dutt, A. Khare, Y.P. Varshni, *J. Phys.* **A28** (1995) L107.

[2] R. Roychoudhury, P. Roy, M. Znojil, G. Lévai, *J. Math. Phys.* **42** (2001) 1996.

[3] M. Znojil, G. Lévai, P. Roy, R. Roychoudhury, *Phys. Lett.* **B290** (2001) 249.

1.3 Composite dynamical symmetries

J. Cseh

A quantum mechanical system is said to have a dynamical symmetry when its Hamiltonian can be expressed in terms of Casimir operators of a chain of nested subgroups:

$$G \supset G' \supset G'' \supset \dots \quad (2)$$

Let us consider a system of two components (1 and 2), each of them described by an algebraic model with group-structure G_1 and G_2 . If the particle number of the two components are conserved separately, then the algebraic model with group structure $G_1 \otimes G_2$ usually proves to be a successful approach, and it contains some dynamical symmetries.

Deeper symmetries, with essentially different nature arise from the embedding of the direct product group $G_1 \otimes G_2$ into a larger group:

$$G_0 \supset G_1 \otimes G_2. \quad (3)$$

Some generators of G_0 transform particles of type 1 into particles of type 2.

Famous examples for the composite dynamical symmetries are provided by the supersymmetric models of particle and nuclear physics. Then the two components are the bosonic and fermionic ones, and the supertransformations take bosons into fermions or vice versa. The group-structure of the model is given by a super (graded) Lie group: $U(n/m)$.

The typical supersymmetric models of particle physics contain Hamiltonians (Lagrangians) which are invariant with respect to some supertransformations [1], while the typical supersymmetric models of nuclear structure do not show such invariance [1,2]. Nevertheless, the multiplet structure of the latter case is also defined by the representations of the appropriate supergroup, and the physical operators establish well-defined connection

among the members of the supermultiplets. Due to this reason we talk about strong supersymmetry in the first (really superinvariant) case, and about weak supersymmetry in the second (not superinvariant) case.

From the mathematical viewpoint the difference is reflected by the subgroups describing the symmetry-breaking interactions: in case of strong supersymmetry there is (at least one) supergroup among the subgroups, while in the weak supersymmetry case only classical Lie groups appear.

Week and strong composite symmetries can be found among other composite dynamical symmetries as well. As an example for the week composite symmetries we refer to the proton-neutron (F-spin) symmetry of the quadrupole collective model of atomic nuclei, characterized by the

$$U(12) \supset U_p(6) \otimes U_n(6) \quad (4)$$

group-chain. In this case the two sectors of the model correspond to the proton and neutron systems, and no invariance is included with respect to the proton-to-neutron transformations.

On the other hand the recently proposed multichannel dynamical symmetry [3], which describes different clusterizations of the same nucleus turn out to be a strong composite symmetry, including real invariance with respect to some transformation between the two components (being the independent relative motions of a multicluster configuration in this case).

- [1] R. V. Jolos and P. von Brentano: *Phys. Rev.* **C60** (2000) 064318.
- [2] G. Lévai, J. Cseh, P. Van Isacker: *Eur. Phys. J.* **A12** (2001) 305.
- [3] J. Cseh: *Proc. XXIV. Symp. Nucl. Phys. Taxco, Mexico, 2001*, in press.

2.1 Astrophysical p-process studies on Se isotopes

Gy. Gyürky, Zs. Fülöp, E. Somorjai, I. Borbély-Kiss, S. Harissopulos^{a)}, M. Kokkoris^{a)}, S. Galanopoulos^{a)}, P. Demetriou^{a)}

As continuation of a systematic study of the astrophysical p-process [1], an experimental investigation of (p,γ) or (p,n) cross sections of several Se isotopes has been started. Calculation of the abundances of the p-process nuclides requires extensive reaction network. An important input parameter for these network calculations is the reaction rate of various reactions obtained from the cross section. Very few cross sections involving light ions on relatively heavy nuclei, have been measured at energies appropriate to astrophysics, leaving these reaction networks dependent upon theoretical estimates calculated through statistical models. The aim of our systematic study is to compare the experimental results with the predictions of statistical models and this way to check the reliability of the reaction network calculations and to put these calculations on a more firm base.

The experiments has been started both at the 5 MV van de Graaff accelerator of the ATOMKI, Debrecen and at the Dynamitron Accelerator at the University of Stuttgart, Germany in the framework of a Greek-Hungarian collaboration. In Debrecen activation method is used to determine the cross section of the $^{74,76}\text{Se}(p,\gamma)$ and $^{82}\text{Se}(p,n)$ reactions in the proton energy range between 1.5 and 3.4 MeV with steps of 100 to 300 keV covering the relevant Gamow-peak which spans from 1.3 to 3.8 MeV. The thickness of the evaporated natural Se targets has been determined with PIXE method and their stability has been

monitored with RBS during the long irradiations. The induced γ-radiation has been measured off-line with a calibrated HPGe detector shielded by 10 cm thick lead.

In the case of $^{78}\text{Se}(p,\gamma)$ and $^{80}\text{Se}(p,\gamma)$ the final nucleus is stable ($^{79,81}\text{Br}$), thus the activation technique is not applicable. Here the cross sections were determined using on-line γ-detection in Stuttgart. The details of the experimental set-up can be found in Ref. [2].

Hauser-Feshbach statistical model calculations were carried out for all stable Se isotopes using the MOST code. The obtained cross section data will be compared with the experimental results as soon as they are available.

Fig. 1 shows the relevant part of the chart of nuclides indicating the (p,γ) and (p,n) reactions as well as the decay of the final Br nuclides.

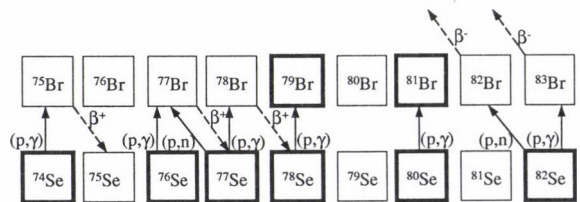


Figure 1. The proton capture reactions on Se isotopes and the decay of the reaction products. The stable nuclei are indicated by bold squares.

a) Institute of Nuclear Physics, NCSR "Demokritos", Athens, Greece

[1] Gy. Gyürky *et al.*, Phys. Rev. **C64** (2001) 065803.

[2] S. Harissopulos *et al.*, Phys. Rev. **C64** (2001) 055804.

2.2 Low energy cross section measurements

LUNA Collaboration^{a)} (Gy. Gyürky, Zs. Fülöp, E. Somorjai)

An accurate knowledge of thermonuclear reaction rates is important in understanding the generation of energy, the luminosity of neutrinos, and the synthesis of elements in stars. Due to the Coulomb barrier of the entrance channel, the reaction cross section drops nearly exponentially with decreasing energy. Thus it becomes increasingly difficult to measure $\sigma(E)$ and to deduce the astrophysical $S(E)$ factor. Although experimental techniques have improved significantly over the years, it has not been possible to measure $S(E)$ within the thermal energy window in stars, called the Gamow energy window. Instead, the observed $\sigma(E)$ data had to be extrapolated to thermal energies which can lead to considerable uncertainties.

The LUNA (Laboratory for Underground Nuclear Astrophysics) accelerator facilities installed at the Laboratori Nazionali del Gran Sasso, Italy offers unique possibilities for the studies of low cross section nuclear reactions owing to the extremely low cosmic background in the underground site.

Two low-energy, high current accelerators are available for cross section measurements with maximum energies of 50 and 400 keV. At the older 50 kV machine (LUNA 1), the investigation of the $p(d,\gamma)^3\text{He}$ reaction has been carried out from 22 down to 2.5 keV c.m. energy, well below the solar Gamow peak. This reaction is the second step of the pp-chain defining the equilibrium abundance of deuterium in an H-burning, low mass star. Moreover, this is the key reaction of the stellar evolution before the onset of the H-burning (proto-star phase). Hence a reliable knowl-

edge of the reaction rate down to a few keV (the Gamow window) is a fundamental prerequisite for these stellar models. The experimental set-up was based on a large solid angle, segmented BGO detector and a renewed windowless gas target system. The resulting astrophysical $S(E)$ factor within the Gamow peak is in good agreement with the value of one of the existing extrapolations based on data at higher energies [1].

The $^{14}\text{N}(p,\gamma)^{15}\text{O}$ reaction determines the velocity of the CNO cycle. Though the CNO cycle gives no significant contribution to the energy generation in the sun, it is important to know the neutrino flux produced by the decays of ^{15}O and ^{13}N in view of upcoming solar neutrino experiments like BOREXINO. At solar energies the cross section of $^{14}\text{N}(p,\gamma)^{15}\text{O}$ is dominated by a subthreshold resonance. Recently, some indirect measurements of this resonance have been performed and there are also some new calculations about its influence at solar energies. Thus direct measurements of this reaction at very low energies are needed.

The experiments have been started at the recently installed and tested 400 kV accelerator (LUNA 2). Different solid state N targets were prepared and tested in order to find the optimal targets for the measurements. The cross section is deduced from the induced γ -radiation measured with a high-efficiency HPGe detector. The measurements are still in progress.

a) For full authors' list, see: M. Aliotta *et al.*, Nucl. Phys. **A690** (2001) 790.

[1] G.J. Schmid *et al.*, Phys. Rev. **C56** (1997) 2565.

2.3 Temperature dependent BCS-gap-equations in the continuum

O. Civitarese^{a)}, R. J. Liotta^{a)}, and T. Vertse

An attempt is made for describing pairing correlations for excited nuclei near the proton (neutron)-drip line by using finite-temperature BCS equations including the continuum part of the spectrum[1]. In this model it is assumed that pairing can be calculated in the BCS approximation with nucleons moving either in bound orbits or in narrow resonances. Therefore the single particle states form a truncated Berggren representation[2] composed of real energy bound states and complex energy Gamow resonances. Due to the truncation broad resonances and all complex energy scattering states have been neglected. The BCS treatment in this basis is similar to the standard treatment however we have to use the generalized scalar product of the Berggren representation.

The thermal averaging procedure, for bound single particle (quasiparticle) states, can be generalized to include resonant single-particle states. The resulting picture is rather appealing because the quasiparticle motion can either "hit" resonant single particle states a) by the smearing out of the Fermi surface, due to pairing correlations or, b) by thermal occupation of high lying single-particle states.

We have performed BCS calculations for open shell proton-drip line nuclei around $N=50$ and $N=114$. The separable monopole pairing interaction has been parametrized by the a constant strength G . The BCS equations were solved in the Berggren basis. The correspond-

ing quasiparticle energies, for the active single particle states, were obtained for different proton numbers corresponding to different temperature values ($T = 0$ and $T > 0$). One can observe that the inclusion of thermal excitations does not change the $T = 0$ result considerably. The quasiparticle spectrum shows a limited spreading even for very large values of Z . The temperature dependence of $\Delta(T)$ shows the well known suppression of pairing correlations by thermal blocking effects. A smooth temperature dependence of the chemical potential λ has been observed. The relatively constant value of the gap indicates that the quasiparticle mean field is well defined, even for the very extreme situations considered in the present calculations i.e. in the proton-drip line region. In all the cases studied the imaginary parts of the calculated matrix elements were small therefore the interpretation of the corresponding real parts as the expectation values of the physical quantities lie on firm ground.

This work was partially supported by the Hungarian OTKA fund Nos. T26244, T29003

a) Dept. of Physics, Univ. of La Plata, c.c. 67 1900, La Plata, Argentina

b) Royal Institute of Technology, Physics Department Frescati, Frescativagen 24, S-10405, Stockholm, Sweden

[1] O. Civitarese, R.J. Liotta, and T. Vertse, Phys. Rev. **C64** (2001) 057305.

[2] T. Berggren, Nucl. Phys. **A109** (1968) 265.

2.4 Perturbative Quantum Chromodynamics

Z. Trócsányi and Z. Nagy^{a)}

Deep inelastic lepton-hadron scattering (DIS) has played a decisive role in our understanding of the deep structure of matter. The latest version of the experiment performed with colliding 27.5 GeV electrons or positrons and 820 GeV protons at HERA yields increasingly precise data so that not only fully inclusive measurements can be used to study the physics of hadronic final states. In fact, the study of multi-jet events and event shapes has become an important project at HERA.

One of the important theoretical tools in the analysis of hadronic final states is perturbative Quantum Chromodynamics (QCD). In order to make quantitative predictions in perturbative QCD, it is essential to perform the computations (at least) at the next-to-leading order (NLO) accuracy. In the case of DIS such computations have so far been completed for one-jet inclusive and two-jet cross sections. In our work [1] we computed various differential distributions of the three-jet cross section, defined using the inclusive k_{\perp} algorithm, that can be compared to recent data obtained by the H1 collaboration.

In order to make the comparisons, we used the same kinematic range as employed in the experiment, i.e., $5 \text{ GeV}^2 < Q^2 < 5000 \text{ GeV}^2$, $0 < x_{Bj} < 1$, $0.2 < y < 0.6$, $-1 < \eta_{\text{jet}}^{\text{lab}} < 2.5$, $E_{T,\text{jet}}^{\text{Breit}} > 5 \text{ GeV}$. The hard scale was chosen to be the average transverse momentum of the three-jets. The leading order curves were obtained using the CTEQ5L pdf's and α_s run from $\alpha_s(M_{Z^0}) = 0.127$ using one-loop running, and the NLO curves with CTEQ5M1 pdf's and α_s run from $\alpha_s(M_{Z^0}) = 0.118$ using two-loop running. The three-jet final states were selected using the inclusive k_T algorithm. The plot in Fig. 1 show the differential distribution in the momentum transfer squared. We can observe that the leading order prediction has different shape than the data: too low for small values of the variables and too high for large values. The radiative corrections bring theory

and experiment much closer. Taking into account the hadronization corrections, the NLO prediction gives a remarkably good description of the data.

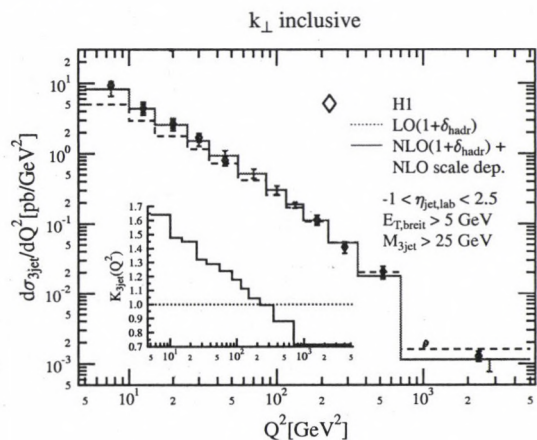


Figure 1. The three-jet differential distribution in the squared momentum transfer.

We should consider the impressive agreement with caution. For small values of Q^2 the radiative corrections are large (between 30 and 60%), so we may expect that the higher order corrections are also large, which is also indicated if we look at the dependence of the NLO prediction for the three-jet inclusive cross section on the renormalization and factorization scales. The scale dependence of the cross section at NLO is still large indicating potentially large higher order corrections. At high Q^2 we find that the renormalization-scale dependence is reduced significantly, while the originally not too strong factorization-scale dependence does not change substantially. Setting the two scales equal, at NLO we find a rather flat curve with a wide plateau around the chosen hard scale. If Q^2 is large, however, the NLO corrections are negative indicating that all order resummation of terms may be important.

a) Department of Physics, University of Durham, Durham DH1 3LE, England

[1] Z. Nagy and Z. Trócsányi, "Multi-jet cross sections in deep inelastic scattering at next-to-leading order," Phys. Rev. Lett. **87** (2001) 082001 [hep-ph/0104315].

2.5 Mass distribution of fission fragments from hyperdeformed states in $^{232}\text{Th}(n,f)$

M. Csatlós, Z. Gácsi, J. Gulyás, M. Heil^{a)}, Gy. Hegyesi, F. Käppeler^{a)}, A. Krasznahorkay, A. Krasznahorkay Jr., Z. Máté, N. Nenoff^{c)}, R. Reinfarth^{a)}, P.G. Thirolf^{b)}, J. Timár

In a previous work a substantial sharpening of the mass distribution has been observed in coincidence with the hyperdeformed (HD) states of ^{236}U [1]. The aim of this work was to study the fission of the HD resonance observed around $E_n = 1.6$ MeV in the $^{232}\text{Th}(n,f)$ reaction [2].

The ^{232}Th nucleus is excited into states by mono-energetic fast neutron leading subsequently fission. The neutrons are produced in a $^7\text{Li}(p,n)$ reaction at $E_p=3.4-3.7$ MeV bombarding energies. The Van de Graaff accelerator at Forschungszentrum Karlsruhe produced a $50 \mu\text{A}$ proton beam on a $200 \mu\text{g}/\text{cm}^2$ metallic Li target. The average neutron flux at the Th target was $\sim 1.8 \times 10^6$ neutron/ cm^2s .

The scattering chamber itself served as a detector, since it contained a twin ionization chamber constructed in ATOMKI, Debrecen. The design parameters were similar to those published by Budtz-Jorgensen et al. [3]. The large area (12.6 cm^2) and thin ($100 \mu\text{g}/\text{cm}^2$) $^{232}\text{ThO}_2$ target was placed into the center plane of this detector at 3-5 kV negative electric potential and both sides consisted of grid-
ded ionization chambers filled with a 90% Ar + 10% CH_4 mixture at 1 atm pressure.

The energies of the fission fragments are obtained from the anode pulse-heights, while the sum of the grid and anode signals is used for the determination of the fragment emission angle θ with respect to the symmetry axis of the chamber. The angle-dependent energy loss in the target was determined experimentally using this angular information.

Fission-fragment masses are determined with the double kinetic-energy method based on the conservation laws of mass and linear momentum. The mass distribution at each incident neutron energy was fitted with two Gaussians having the same height and width.

The widths (σ) of the Gaussians are shown in Fig. 1. as a function of the neutron energy.

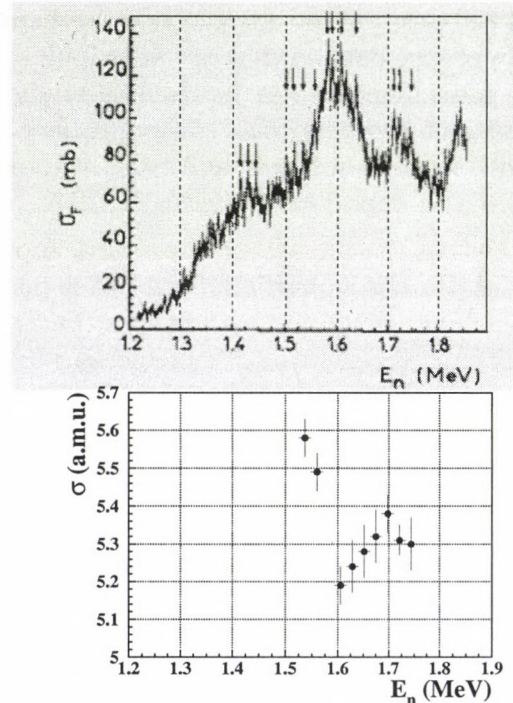


Figure 1. a) Hyperdeformed resonances in the $^{232}\text{Th}(n,f)$ reaction observed by Blons et al. [2]. b) Present results for the width of the corresponding mass distributions.

One can see a significant sharpening at 1.6 MeV neutron energy, which corresponds to a HD resonance in ^{233}Th .

a) Forschungszentrum Karlsruhe, Germany.

b) LMU, Muenchen, Germany.

c) Univ. Bonn, Germany.

[1] A. Krasznahorkay *et al.*, APH N.S. Heavy Ion Physics **13** (2001) 111.

[2] J. Blons *et al.*, Phys. Rev. Lett. **35** (1975) 1749.

[3] C. Budtz-Jorgensen *et al.*, Nucl. Instr. and Meth. **A285** (1987) 209.

2.6 Clusterization and configuration-mixed effective $SU(3)$ symmetries

P.O. Hess^{a)}, A. Algora^{b)} and J. Cseh

The effective symmetry [1] is one of the most general symmetry in quantum mechanics. It is a symmetry of the eigenvalue-equation, when neither the (Hamiltonian) operator is symmetric (scalar), nor its eigenvectors (transform according to some irreducible transformations). Yet the symmetry may act, and have important physical consequences.

The mathematical reason for this surprising situation is provided by the embedded representation [2]. An embedded representation is obtained by calculating the matrix elements of the operators between vectors which are special linear combinations of those belonging to irreducible representations. (The linear combinations are special in the sense that their coefficients are the same for several vectors.) When the summation and the internal product operations are exchangeable (either exactly, or approximately), then the matrices give (exactly or approximately) a representation, called embedded representation.

In physical terms the embedded representation describes the adiabatic coupling; and it explains why some models can be successful, when they (seemingly) have no right to be so.

In nuclear physics the effective $SU(3)$ symmetry proved to be valid in heavy nuclei, where the real $SU(3)$ symmetry is badly broken due to the spin-orbit and other interactions [1]. If a symmetry exists, it has several important physical consequences, e.g. it provides us with selection rules.

Selection rules can be very useful in studying nuclear fragmentations, like e.g. spontaneous fission, or clusterization in general. In light of the recently discovered neutronless cold fission, these questions are of utmost interest in the structural study of heavy nuclei.

Jarrio et.al. showed a way, how to deter-

mine the effective $SU(3)$ symmetry of heavy nuclei in the region, where the asymptotic Nilsson quantum numbers are valid [1]. Based on their method we have carried out symmetry-considerations concerning the relative preference of different exotic binary clusterizations of the ground state of the ^{252}Cf nucleus [3]. The possible clusterizations, however, include not only strongly deformed nuclei, but other types as well. Therefore, some sort of extension of the method of [1] is highly needed for systematic studies.

We propose an interpolation method for the determination of the effective $SU(3)$ symmetry between zero and large quadrupole deformations [4]. It is based on the numerical expansion of the Nilsson-states of a given deformation in terms of asymptotic basis, and applying the procedure of [1] for these linear combinations. This method is not based on a rigorous proof, it should be considered as a recipe for the interpolation. Nevertheless, selfconsistency arguments show that it gives reliable results both in the case of some light nuclei (where the real $SU(3)$ symmetry is valid), and in the case of heavy nuclei.

The extended method may prove to be a useful tool in the cluster studies of heavy nuclei, where it is essential to incorporate the effects of deformation as well as that of the Pauli exclusion principle.

a) Instit. Cienc. Nucl. UNAM, Mexico

b) Univ. Valencia, Spain and ATOMKI

[1] M. Jarrio, J.L. Wood and D.J. Rowe, Nucl. Phys. **A528** (1991) 409.

[2] D.J. Rowe, P. Rochford and J. Repka, J. Math. Phys. **29** (1988) 572.

[3] A. Algora, J. Cseh, and P.O. Hess, J. Phys. **G24** (1998) 2111.

[4] P.O. Hess, A. Algora and J. Cseh, in preparation.

2.8 Study of shape evolution in the neutron-rich ^{40}S , ^{42}S and ^{44}S isotopes

D. Sohler, M. Stanoiu^{a)}, Zs. Dombrádi, O. Sorlin^{b)}, J. Timár, F. Azaiez^{b)}, F. Amorini^{b)}, D. Baiborodin^{c)}, A. Bauchet^{d)}, F. Becker^{e)}, M. Belleguic^{b)}, C. Borcea^{f)}, C. Bourgeois^{b)}, Z. Dlouhy^{g)}, C. Donzaud^{b)}, J. Duprat^{b)}, M. Girod^{h)}, D. Guillemaud-Mueller^{b)}, F. Ibrahim^{b)}, M.J. Lopez^{a)}, R. Lucasⁱ⁾, S.M. Lukyanov^{c)}, V. Maslov^{c)}, J. Mrazek^{g)}, C. Moore^{j)}, F. Nowacki^{k)}, B.M. Nyakó, Yu.-E. Penionzhkevich^{c)}, L. Petizon^{b)}, M.G. Saint-Laurent^{a)}, F. Sarazin^{a)}, J.A. Scarpaci^{b)}, G. Sletten^{l)}, C. Stodel^{b)}, M. Taylorⁱ⁾, C. Theisen^{e)}, G. Voltolini^{a)}

The higher lying excited states in neutron-rich $^{40,42,44}\text{S}$ nuclei were studied using in-beam γ -spectroscopy technique associated to fragmentation reactions of a 60 MeV $\cdot\text{A}$ ^{48}Ca beam on a thin Be target. Energies, intensities and coincidence relationships of the transitions, as well as, γ -ray angular distributions for the first time at intermediate energy were measured for these isotopes. The level schemes previously containing only a single γ transition are extended, and spin values are proposed for the new states. The $E_{4_1^+}/E_{2_1^+}=2.5$ ratio in ^{40}S was found to be consistent with that of an anharmonic vibrator or a γ -soft rotor. In ^{42}S

the $E_{4_1^+}/E_{2_1^+}=3.0$ and $E_{2_2^+}/E_{2_1^+}=3.1$ ratios are characteristic for a triaxial rigid rotor. Furthermore, the low lying 0_2^+ state proposed for ^{44}S indicates shape-coexistence in this isotope.

- a) GANIL, Caen, France
- b) IPN, IN2P3-CNRS, Orsay, France
- c) FLNR, JINR, Dubna, Russia
- d) CSNSM, IN2P3-CNRS, Orsay, France
- e) CEA-Saclay, Gif sur Yvette, France
- f) IAP, Bucharest-Magurele, Romania
- g) NPI, Rez, Czech Republic
- h) CEA, Bruyères-le-Chatel, France
- i) IPN, Lyon, France
- j) OLL, Univ. of Liverpool, Liverpool, UK
- k) Univ. L. Pasteur, Strassbourg, France
- l) NBI, Copenhagen, Denmark

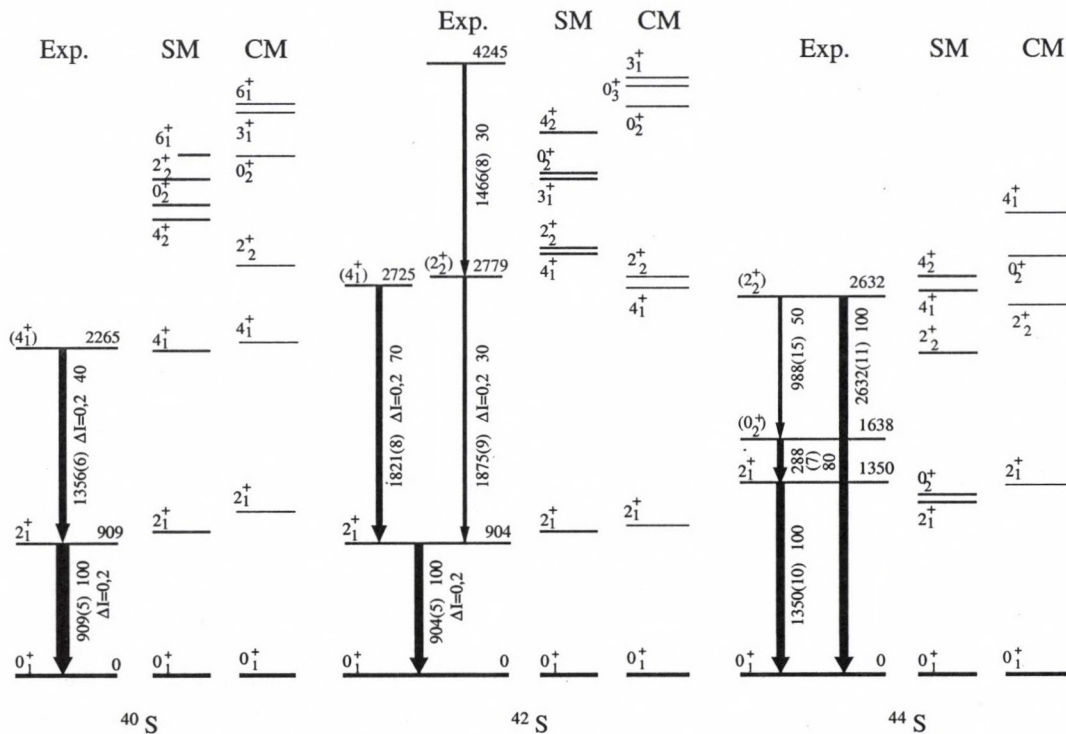


Figure 1. Proposed level schemes of $^{40,42,44}\text{S}$ from the present experiment in comparison with the results of shell model (SM) and microscopic collective model (CM) calculations. γ -ray energies (with uncertainties) multipolarities and relative intensities are given.

2.9 Description of resonant states by analytic continuation

J.Zs. Mezei, R.G. Lovas and Y. Suzuki^{a)}

The description of nuclei cannot be complete without the description of unbound states, including resonances and virtual states. Unbound states are especially important for drip-line nuclei, which have very few bound states or none. The theoretical methods to describe unbound states, the localization of the S-matrix poles, the determination of the energies and widths, the calculation of the wave functions and physical matrix elements, are based mostly on bound-state methods [1]. We are experimenting with a powerful method, the so-called ‘analytic continuation in the coupling constant’ [1]. This involves an extrapolation of the trajectory of the S-matrix pole as a function of a potential strength (‘the coupling constant’) from the bound-state region to the unbound-state region.

To test the approach, at present we consider a simple model problem [2] consisting of chargeless and unit-mass particles interacting via a potential $V = -8\lambda e^{-(r/2.5)^2} + B e^{-(r/5)^2}$, where λ is the coupling constant. It is useful [1] to choose $x = \sqrt{\lambda - \lambda_0}$ to be the variable of extrapolation, where λ_0 is the value of λ at the bifurcation point, the point where the pole trajectory leaves the $\text{Im } k$ axis. The advantage of this is that the (complex) wave-number $k (= \sqrt{E})$ of an unbound state as a function of x is linear ($k \sim x$) around $\lambda \approx \lambda_0$. The extrapolation is done by a Padé approximation of type II.

The eventual aim is to use the method for calculating matrix elements of physical quantities of few-body systems. The tests are made for a two-particle problem. The calculated energies and widths are in very good agreement with the results of a direct numerical solution produced by the *Gamow* code [3], not only for narrow but for broad resonances as well.

As a second step, we tried to con-

tinue bound-state wave functions analytically by pointwise extrapolation to the unbound-state region. A result is shown in Fig. 1, again compared with the results produced by *Gamow*. Although the well-known asymptotic behaviour of the resonance states (Gamow states) is not very well reproduced, for the radial interval in which the wave function is not known *a priori*, the agreement with the direct numerical integration is satisfactory. We are nevertheless working on improving the extrapolation procedure. We are also testing the wave function by comparing some matrix elements.

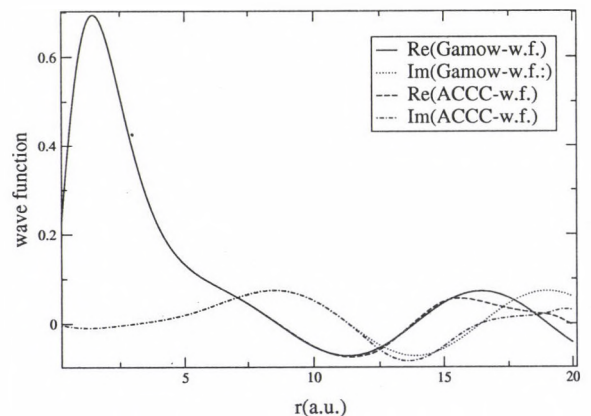


Figure 1. Wave functions of a narrow resonance state, for a barrier of the interaction potential $B = 2$.

a) Department of Physics, Faculty of Science, Niigata University, Niigata 950-2181, Japan.

[1] V.I. Kukulin, V.M. Krasnopol'sky and J. Horáček: *Theory of Resonances* (Kluwer, Dordrecht, 1989).

[2] R.G. Lovas, N. Tanaka, Y. Suzuki, K. Varga, *Few-Body Sys. Suppl.* **13** (2001) 76.

[3] T. Vertse, K.F. Pál and Z. Balogh, *Comput. Phys. Commun.* **27** (1982) 309.

2.10 Installation of a new Total Absorption Spectrometer at ISOLDE/CERN mass separator

A. Algora, M.J.G. Borge^a, D. Cano-Ott^b, S. Courtin^c, Ph. Dessagne^c, L.M. Fraile^d, A. Gadea^e, W. Gelletly^f, A. Jungclaus^a, F. Maréchal^c, Ch. Miehé^c, E. Nácher^g, F. Perrot^c, E. Poirier^c, B. Rubio^g, J.L. Tain^g, O. Tengblad^a and the ISOLDE collaboration^d

We report on the installation of a new Total Absorption γ Spectrometer (TAGS) *Lucrecia* at the ISOLDE/CERN mass separator. The new TAGS is based on a large (38cm diameter, 38cm long) NaI(Tl) crystal (one piece) with cylindrical symmetry (see Fig. 1). It has a radial hole of 7.5 cm which gives the possibility to take the sources to the geometric centre of the detector and also to introduce additional ancillary detectors. The crystal is viewed by eight, five-inch photomultiplier tubes, and the stability of the light collection is monitored using an LED (light emitting diode). A tape transport system, operated under vacuum, is used to move the radioactive sources to the measuring position and to remove the remaining activity. This system has two possible collection modes: the first, which is used for very short lived nuclear species, collects the sources in the centre of the crystal and then transports the measured source after one measur-

ing cycle outside the TAS; in the other possible setup the sources are collected outside the TAS and taken to the centre of the spectrometer for measurement.

The first experiment using this new setup was performed in June 2001. We studied the decay of the $^{72-75}\text{Kr}$ isotopes. The goal of these measurements is to extract information on the ground state deformation of these nuclei from the shape of the B(GT) in their respective beta decay daughter nuclei [1]. As a continuation of this programme, we plan to study the decays of $^{76-80}\text{Sr}$ in the near future.

- a) IEM, Madrid, Spain
- b) CIEMAT, Madrid, Spain
- c) IRES, Strassbourg, France
- d) ISOLDE, CERN, Switzerland
- e) LNL, INFN, Legnaro, Italy
- f) Univ. Surrey, Guildford, U.K.
- g) IFIC, Valencia, Spain

[1] P. Sarriguren *et al.*, Nucl. Phys. **A658** (1999) 13.

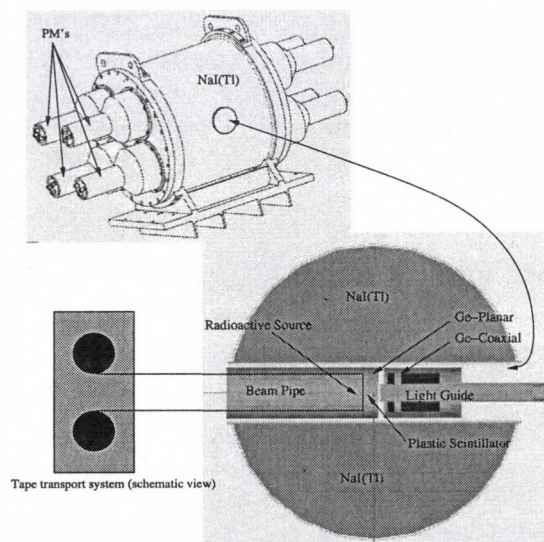


Figure 1. Schematic view of the TAS (*Lucrecia*) installed at ISOLDE.

2.11 *Ab initio* versus cluster-model calculations

K. Varga^a, R.G. Lovas and Y. Suzuki^b

A nuclear model may be regarded as a solution of the many-body problem on a truncated basis. Therefore, as the basis is made complete, the effective force should converge to the bare nucleon–nucleon force. In practice, however, the effective force is mostly fixed. Recent progress has made it possible to use almost complete bases for light nuclei, which makes the use of effective forces questionable.

This progress has taken place owing to the introduction of correlated Gaussian bases used in a stochastic variational method (SVM). This approach was introduced as a cluster model [1], and was subsequently reduced to a few-body approach [2]. Nevertheless, it has been found that a refined cluster model with an effective force gives an almost perfect description of light nuclei [3]. Since, however, a few-body calculation cannot be considered realistic unless it involves a realistic (bare) force, these calculations need to be repeated with realistic forces. That is the aim of the present work.

When applied to $A \leq 4$ nuclei as a few-body method, the SVM turns out to be ‘numerically exact’. This encouraged us to attack the problem of ${}^6\text{Li}$. The Argonne V18 (AV18) force [4] was combined with the Urbana IX (UIX) three-body terms [5]. No convergence has been reached, and the results are shown in Table 1. The Green’s function Monte Carlo method (GFMC) performs quite well, but the variational Monte Carlo (VMC) and the SVM are inferior. Moreover, the variational ground states seem to be unbound with respect to $\alpha+d$ disintegration. The difficulty lies in reproducing the correlations implied by the strong repulsive core of the Argonne force.

Table 1. Energy of ${}^6\text{Li}$ (in MeV) calculated with the AV18+UIX interaction with different techniques.

VMC [6]	GFMC [6]	SVM	Exp.
−28.09	−31.2	−28.79	−31.99

With the supersoft-core (SSC) interaction [7], convergence has not been reached, but a binding of $\varepsilon = E_{6\text{Li}} - E_\alpha - E_d = -0.5$ MeV (experiment: -1.4 MeV) has been produced and the radii and the quadrupole moment are close to the realistic values. The $\alpha+d$ spectroscopic amplitude is close to the prediction of the cluster model, but its tail is too small in spite of the fact that the energy ε is not deep enough. That is so since more binding is missing from the energy $E'_\alpha + E'_d$ of the clusters in ${}^6\text{Li}$, defined by pulling the clusters far apart, than from $E_{6\text{Li}}$ itself. Thus the approximate ${}^6\text{Li}$ is actually overbound with respect to the $E'_\alpha + E'_d$ threshold. The *ab initio* calculation is inaccurate just asymptotically.

Pure $\alpha+d$, $t+h$ and $\alpha+p+n$ cluster models as well as their mixtures have also been produced. These are perfect in the respective asymptotic regions, and yet no binding has been reached due to inaccuracies inside.

In conclusion, the *ab initio* calculations with bare nucleon–nucleon forces are feasible with the SVM, and the results show complementarity to the cluster models. It is likely that, with full convergence, the *ab initio* description would be fully realistic.

- a) Present address: Solid State Division, Oak Ridge National Laboratory, Oak Ridge, Tennessee 37830, USA.
- b) Department of Physics, Faculty of Science, Niigata University, Niigata 950–2181, Japan.
- [1] K. Varga, Y. Suzuki and R.G. Lovas, Nucl. Phys. **A571** (1994) 447.
- [2] K. Varga and Y. Suzuki, Phys. Rev. **C52** (1995) 2885.
- [3] K. Arai, Y. Suzuki and R.G. Lovas, Phys. Rev. **C59** (1999) 1432.
- [4] R.B. Wiringa, S. Pieper, J. Carlson and V.R. Pandharipande, Phys. Rev. **C62** (2000) 014001.
- [5] B.S. Pudliner, V.R. Pandharipande, J. Carlson and R.B. Wiringa, Phys. Rev. Lett. **74** (1995) 4396.
- [6] S.C. Pieper and R.B. Wiringa, Ann. Rev. Nucl. Part. Sci. **51** (2001) 53.
- [7] R. De Tourreil, B. Rouben and D.W.L. Sprung, Nucl. Phys. **A242** (1975) 465.

2.12 Microscopic multicluster description of ${}^9\text{-}^{11}\text{Li}$

K. Varga^a, R.G. Lovas and Y. Suzuki^b

The nucleus ${}^{11}\text{Li}$ is known to have a two-neutron halo. It is most often described as a ${}^9\text{Li}+n+n$ three-body system, with a passive ${}^9\text{Li}$ core, although ${}^9\text{Li}$ is not really stiff. The Pauli principle may also have non-trivial effects. Indeed, in such a model, it seems impossible to get enough binding for ${}^{11}\text{Li}$ ($\epsilon = E_{11\text{Li}} - E_{9\text{Li}} \simeq -0.25$ MeV). A truly microscopic treatment is thus indispensable.

The isotopes ${}^7\text{-}^9\text{Li}$ have been described reasonably well [1] in $\alpha+t$, $\alpha+t+n$ and $\alpha+t+n+n$ cluster models, respectively. Going beyond these cases along the same line requires $\alpha+t+n+n+n$ for ${}^{10}\text{Li}$ and $\alpha+t+n+n+n+n$ for ${}^{11}\text{Li}$. That is attempted now, and we give a preliminary report on the results.

The effective nucleon-nucleon force is the same as was used for the lighter Li isotopes [1]. The ${}^9\text{Li}$ core is described in an $\alpha+t+n+n$ model as before, but with a smaller basis of 50 elements, with a more thorough optimization. The core is assumed to have the same angular-momentum structure as the free nucleus ${}^9\text{Li}$, but its motion in ${}^{10,11}\text{Li}$ is otherwise not frozen. The bases for ${}^{10,11}\text{Li}$ are constructed by coupling a single neutron or two neutrons to each of the basis elements used for ${}^9\text{Li}$, with essentially no restriction on the relative motions. For ${}^{11}\text{Li}$, the description of the ${}^9\text{Li}+n+n$ motion can be depicted by showing the types of Jacobi coordinates that are included (Fig. 1).

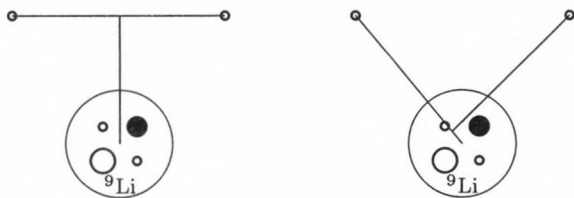


Figure 1. Jacobi coordinates for ${}^9\text{Li}+n+n$. Notation: α : \bullet ; t : \bigcirc ; neutron: \circ .

The level sequence obtained for ${}^{10}\text{Li}$ is 1^+ ($\epsilon=0.39$ MeV), 2^+ (0.55 MeV), 2^- (1.56 MeV), 1^- (1.74 MeV), 0^+ (2.12 MeV). All are unbound states approximated by square-

integrable wave functions. The positive-parity states come from the p-orbits of the ${}^9\text{Li}-n$ relative motion and correspond to the experimentally observed levels. Negative-parity states may come from s-orbits, which may be virtual states. The virtual states actually belong to negative energies, but bound-state-like bases shift them to the positive-energy region.

The ${}^{11}\text{Li}$ basis contains more than 3600 elements. There are 8 ${}^9\text{Li}+n+n$ angular-momentum combinations included, and each ${}^9\text{Li}$ basis function is multiplied by at least 9 different relative-motion states for each angular momentum. This basis is large enough for the relative motion and allows for a major part of the core distortion. The results are summarized in Table 1.

Table 1. Properties of ${}^9\text{Li}$ and ${}^{11}\text{Li}$

	ϵ (MeV)	r_p (fm)	r_n (fm)	r_m (fm)	Q (efm ²)	μ (μ_N)
${}^9\text{Li}$	-5.91	2.12	2.54	2.41	-3.37	3.40 ¹
Exp.	-6.09	2.18	2.30	2.32	-2.74	3.44
${}^{11}\text{Li}$	-0.34	2.43	3.09	3.03	-3.71	3.23
Exp.	-0.25	2.88	3.21	3.10	3.12	3.66

A comparison of the respective properties shows that ${}^9\text{Li}$ and ${}^{11}\text{Li}$ are described simultaneously pretty well. The model ${}^9\text{Li}$ is slightly more deformed and has a thicker neutron skin than is found by experiment. The quoted value of the experimental proton radius of ${}^{11}\text{Li}$ contradicts the halo picture, and is not supported by theory. Single-configuration calculations show that the s-wave-type configurations give slightly deeper bindings than p-wave-type configurations. This indicates that the s-wave-like subspaces must have a somewhat larger weight than the p-wave-like subspaces.

a) Present address: Solid State Division, Oak Ridge National Laboratory, Oak Ridge, Tennessee 37830, USA.

b) Department of Physics, Faculty of Science, Niigata University, Niigata 950-2181, Japan.

[1] K. Varga, Y. Suzuki and I. Tanihata, Phys. Rev. C52 (1995) 65.

2.13 New region of signature inversion in the $A \approx 100$ Rh and Ag isotopes

J. Timár, J. Gizon^{a)}, A. Gizon^{a)}, D. Sohler, B. M. Nyakó, L. Zolnai, D. Bucurescu^{b)}, Gh. Căta-Danil^{b)}, A.J. Boston^{c)}, D. T. Joss^{c,d)}, E. S. Paul^{c)}, A. T. Semple^{c)}, C. M. Parry^{e)}

In $\Delta I=1$ rotational bands, the two signature branches are usually not equivalent energetically. Due to the Coriolis force acting on the valence particles, one of them, called favoured, is lower in energy than the other branch. The favoured signature is determined by the configuration and can be obtained in terms of a simple rule. Some two- and three-quasiparticle bands, however contradict this simple rule at low spin: the expected favoured signature branch becomes energetically unfavoured. This so-called signature inversion has recently attracted a lot of attention both in experimental and theoretical aspects.

In order to gather more information about this phenomenon in new mass regions the $\pi g_{9/2}\nu h_{11/2}$ and $\pi g_{9/2}\nu(h_{11/2})^2$ bands were studied in the $A \approx 100$ nuclei [1]. It has been revealed that signature inversion systematically occurs in these bands. Two types of signature inversion have been observed in this region. The first one is found only in the $\pi g_{9/2}\nu h_{11/2}$ band of ^{98}Rh . It has a large signature splitting and the inversion spin is close to the $j_n + j_p = 10\hbar$ value. All the other cases belong to the second type which has a small signature splitting and an inversion spin considerably higher than $j_n + j_p = 10\hbar$. The $\pi g_{9/2}\nu h_{11/2}$ bands belonging to this type are very similar to each other, they all have the same inversion spin of $I=15\hbar$. The behaviour of the inversion spin can be qualitatively understood as a competition between the Coriolis and the proton-neutron interaction, as it was proposed by Zheng et al. for the $A \approx 160$ region, if we take the variation of the moment of inertia into account. According to this scenario the big difference between the signature inversions in ^{98}Rh and in the other doubly odd nuclei is caused by a big change in the deformation.

- a) ISN, IN2P3-CNRS/UJF, Grenoble, France
- b) HHNIP, Bucharest, Romania
- c) OLL, Univ. Liv., Liverpool, UK
- d) Staffordshire Univ., Stoke-on-Trent, UK
- e) Univ. York, Heslington, York, UK

- [1] A. Gizon *et al.*, Eur. Phys. J. **A2** (1998) 325;
J. Gizon *et al.*, Nucl. Phys. **A658** (1999) 97;
J. Timár *et al.*, Nucl. Phys. **A696** (2001) 241.
- [2] R. Zheng *et al.*, Phys. Rev. **C64** (2001) 014313.

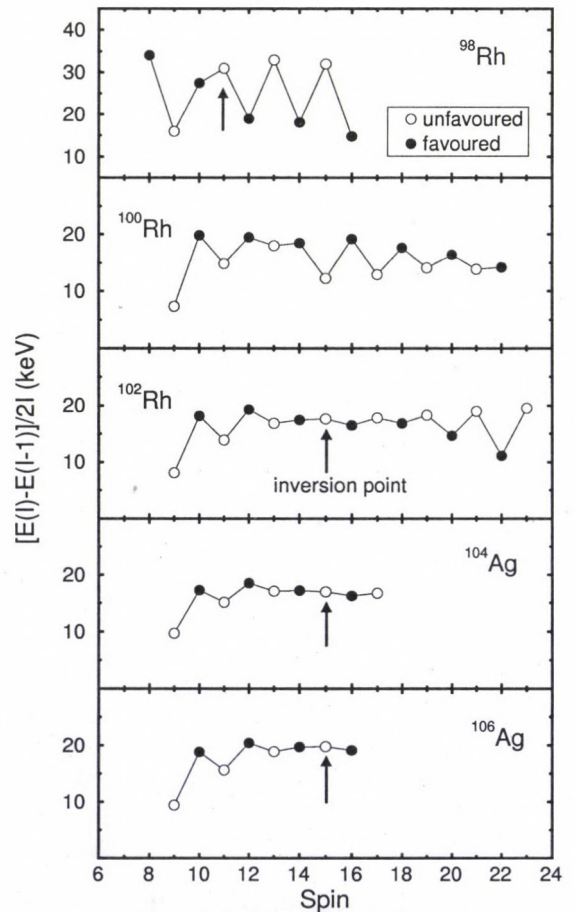


Figure 1. Energy difference plots of $\pi g_{9/2}\nu h_{11/2}$ bands in the $A \approx 100$ mass region.

2.14 Low-lying levels and collective bands in doubly-odd ^{124}Cs

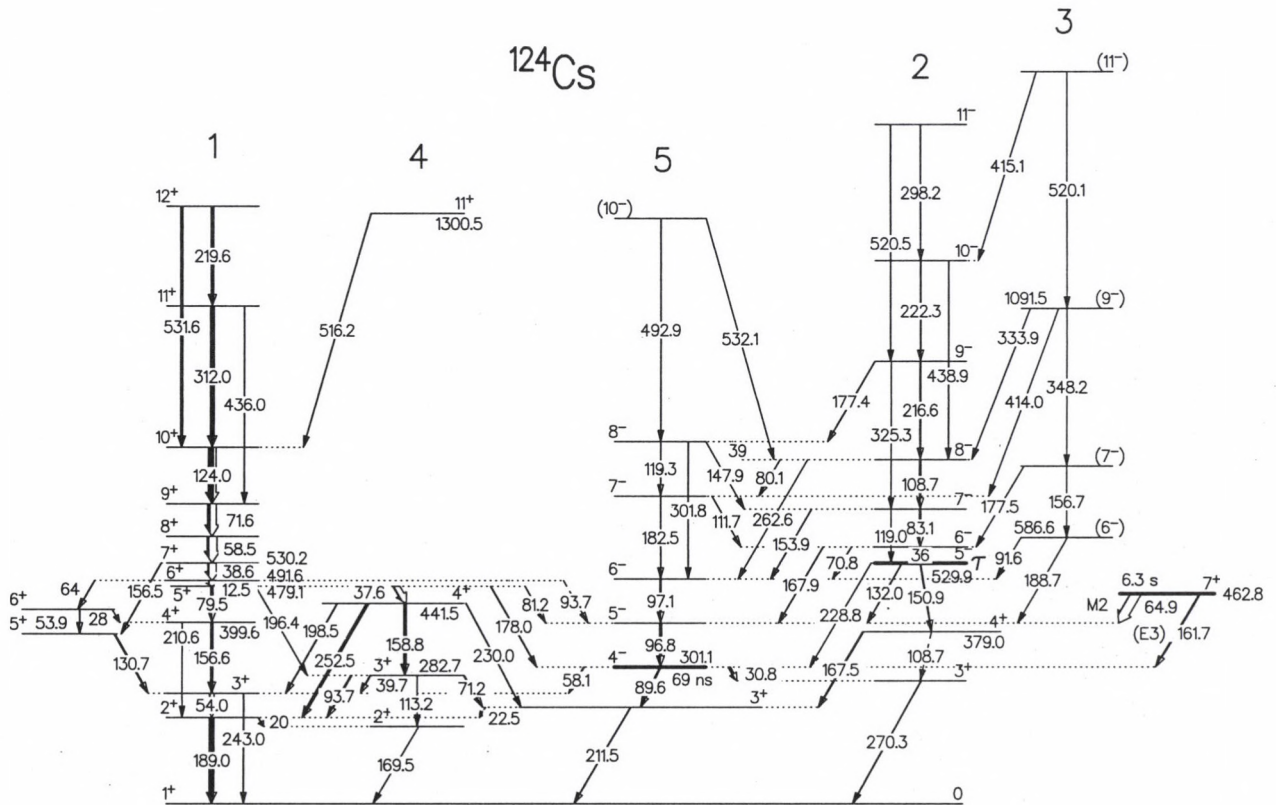
A. Gizon^{a)}, J. Timár, J. Gizon^{a)}, B. Weiss^{a)}, D. Barnéoud^{a)}, C. Foin^{a)}, J. Genevey^{a)}, F. Hannachi^{b)}, C.F. Liang^{b)}, A. Lopez-Martens^{b)}, P. Paris^{b)}, B.M. Nyakó, L. Zolnai, J.C. Merdinger^{c)}, S. Brant^{d)}, V. Paar^{d)}

The nucleus ^{124}Cs has been studied by in-beam γ - and e^- -spectroscopy techniques with the fusion-evaporation reaction $^{115}\text{In}(^{12}\text{C}, 3n\gamma)$ at 57 MeV. Multipolarities of the main low-energy transitions have been deduced from electron spectra. A level scheme is proposed with firm I^π assignments. Low-spin low-lying levels and high-spin states have been investigated. New high-spin bands were found and the known ones extended up to higher spins. The new spin values determined for the $\pi h_{11/2}\nu h_{11/2}$ band is in agreement with the expected signature inversion found sys-

tematically in the odd-odd nuclei in this region. The low-spin levels and two quasiparticle bands were interpreted by using the interacting boson-fermion-fermion model. The band structures were also discussed in the frame of the cranked shell model. The results are published in Ref. [1].

- a) ISN, IN2P3-CNRS, Grenoble, France
- b) CSNSM, IN2P3-CNRS, Orsay, France
- c) IReS, IN2P3-CNRS, Strasbourg, France
- d) Univ. Zagreb, Zagreb, Croatia

[1] A. Gizon *et al.*, Nucl. Phys. **A694** (2001) 63.



2.15 Magnetic dipole bands in ^{190}Hg

A.N. Wilson^{a)}, J. Timár, I. Ahmad^{b)}, A. Astier^{c)}, F. Azaiez^{d)}, M. Bergström^{e)}, D.J. Blumenthal^{b)}, B. Crowelly^{b)}, M.P. Carpenter^{b)}, L. Ducroux^{c)}, B.J.P. Gall^{f)}, F. Hannachi^{g)}, H. Hubel^{h)}, T.L. Khoo^{b)}, R.V.F. Janssens^{b)}, A. Korichi^{g)}, T. Lauritsen^{b)}, A. Lopez-Martens^{g)}, M. Meyer^{c)}, D. Nisius^{b)}, E.S. Paul^{e)}, M.G. Porquet^{g)}, N. Redon^{c)}, J.F. Sharpey-Schafer^{e)}, R. Wadsworth^{a)}, J.N. Wilson^{e)}, I. Ragnarssonⁱ⁾

An experiment aimed at studying high-spin states in ^{190}Hg was performed with the EUROGAM II array at CRN, Strasbourg. The data collected have revealed the presence of cascades of magnetic dipole transitions with some very unexpected properties. Unlike the previously known M1 bands in the Hg isotopes, these structures have extremely large $B(\text{M1})/B(\text{E2})$ ratios, which indicate both a large magnetic dipole moment and a small deformation. The properties of these bands cannot be explained within the standard Donau and Frauendorf formalism assuming high-K configurations. An alternative explanation could lie in the magnetic rotation scenario; however this is not a phenomenon predicted to occur in the Hg isotopes. The observation of a third dipole band with much lower $B(\text{M1})/B(\text{E2})$ values in the same spin/excitation energy regime suggests that the bands may represent configurations occurring in a different minimum in the nucleus's potential energy surface. Comparisons are made with configuration-dependent cranked Nilsson-Strutinsky calculations. It is proposed that these bands are based on configurations where one proton is excited across the $Z = 80$ shell gap. The results are published in Ref. [1].

- a) Univ. York, Heslington, York, UK
- b) ANL, Cass Ave, Argonne, IL, USA
- c) IPN, Lyon, France
- d) IPN, Orsay, France

- e) OLL, Univ. Liverpool, Liverpool, UK
- f) IReS, Strasbourg, France
- g) CSNSM, Orsay, France
- h) ISKP, Univ. Bonn, Germany
- i) Lund Inst. Tech., Lund, Sweden

[1] A.N. Wilson *et al.*, Phys. Lett. **B505** (2001) 6.

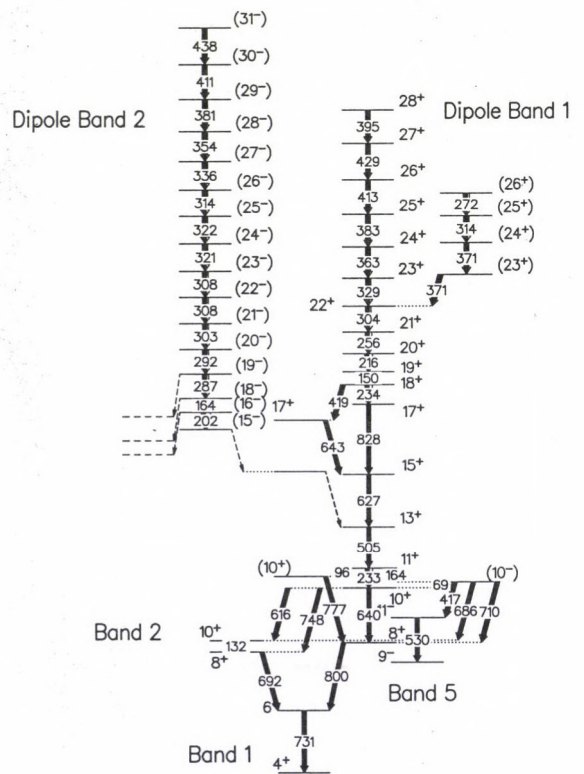


Figure 1. Partial level scheme showing dipole bands in ^{190}Hg .

2.16 Measurement of Doppler shift attenuated gamma-rays from the $^{18}\text{O}(2_1^+)$ state

N. Imai^{a)}, N. Aoi^{a)}, H. Sakurai^{a)}, K. Demichi^{b)}, H. Kawasaki^{b)}, H. Baba^{b)}, Zs. Dombrádi, Z. Elekes, N. Fukuda^{c)}, Zs. Fülöp, A. Gelberg^{d)}, T. Gomi^{b)}, H. Hasegawa^{b)}, H. Iwasaki^{e)}, E. Kaneko^{b)}, S. Kanno^{b)}, T. Kishida^{c)}, Y. Kondo^{f)}, T. Kubo^{c)}, S. Michimasa^{e)}, T. Minemura^{b)}, M. Miura^{f)}, T. Motobayashi^{b)}, T. Nakamura^{f)}, M. Notani^{e)}, T. Ohnishi^{a)}, H.J. Ong^{a)}, A. Saito^{b)}, S. Shimoura^{e)}, T. Sugimoto^{f)}, S. Takeuchi^{b)}, K. Yoneda^{c)}, H. Watanabe^{c)}, M. Ishihara^{c)}

The $B(E2; 0_{g.s.}^+ \rightarrow 2_1^+)$ values in even-even neutron-rich nuclei have been successfully measured at intermediate energies by using the Coulomb excitation method [1, 2]. However, this technique is not suitable for nuclei with $Z < 8$, since the nuclear excitation competes with the Coulomb excitation for low Z projectiles. As an alternative way, we propose a mean life measurement of the $2_{g.s.}^+ \rightarrow 0_1^+$ transition using the Doppler shift attenuation method. Here we report the first attempt to apply this method to fast projectiles.

In this experiment, we use a thick target and the projectile velocity is degraded in the target. Accordingly, the Doppler shifted gamma-ray energy is spread over a certain range. The energy of the gamma-ray emitted inside the target is distributed continuously, while that of emitted outside the target is constant since the projectile does not change its velocity any more. The longer the mean life becomes, the larger the latter component is. When we choose properly the target thickness and the projectile energy so that the time for the projectile to pass through the target is comparable with mean life of its excited state, the mean life can be determined from the shape of the energy spectrum of 500 gamma-ray events with $\pm 10\%$ uncertainty.

As a test, we applied this method to the $^{18}\text{O}(2_1^+)$ state the mean lifetime of which is precisely known to be 2.79 ± 0.07 ps [3]. This test experiment was performed in RIKEN. Figure 1 shows the schematic view of the experimental setup. A 48.2 MeV/u energy ^{18}O beam from the RIPS fragment separator [4] hits a 580 mg/cm² thick ^{197}Au target. The de-excitation gamma-rays from the inelastically excited ^{18}O nuclei were detected by four Clover detectors. Each Clover was located 30 cm upstream from

the target at 150 degrees with respect to the beam direction. The scattering angle was measured by three Parallel Plate Avalanche Counters (PPAC), two of which were located upstream and the third one downstream of the target. The particle identification of the scattered particle was carried out with a silicon telescope by using ΔE - E method. The silicon telescope was placed 30 cm downstream from the target covering an angular acceptance of 9.6 degrees. It consisted of five layers of silicon detectors with thicknesses of 0.5, 1.0, 0.5, 1.0 and 0.5 mm, respectively. In order to prevent background gamma-rays from the silicon detectors, we put 5 cm thick lead shield between the Clovers and the silicon telescope. Data analysis is in progress.

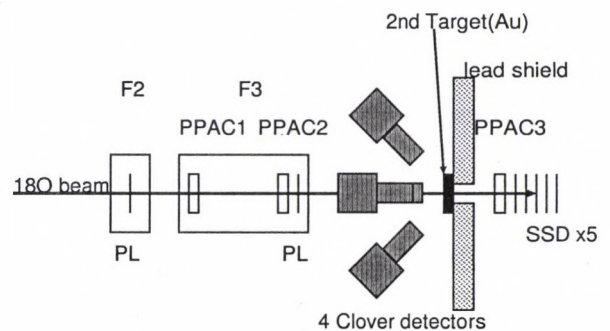


Figure 1. The layout of the detection system

- a) University of Tokyo, Tokyo, Japan
 - b) Rikkyo University, Tokyo, Japan
 - c) RIKEN, Wako, Saitama, Japan
 - d) University of Köln, Köln, Germany
 - e) CNS, University of Tokyo, Tokyo, Japan
 - f) Tokyo Institute of Technology, Tokyo, Japan
- [1] T. Motobayashi *et al.*, Phys. Lett. **B346** (1995) 9.
 [2] T. Glasmacher, Ann. Rev. Nucl. Part. Sci. **48** (1998) 1.
 [3] J.A. Hermans *et al.*, Nucl. Phys. **A255** (1998) 221.
 [4] T. Kubo *et al.*, Nucl. Instr. and Meth. **B70** (1992) 309.

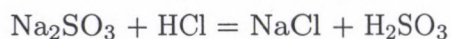
2.17 Production and chemical separation of ^{48}V radioisotope

Z. Szűcs^{a,b}), D. Dudu^b), C. Campeanu^b), A. Luca^b), E. Duta^b), M. Sahagia^b)

The positron emitter ^{48}V isotope ($T_{1/2}=16\text{d}$, γ -lines: 511 keV(100%), 983.5(100%), 1312(97.6%)) deserves interest in several fields of science. This is available for the transmitting scanning in the validation process of PET-camera by its positron emission, can be used for as an industrial monitor isotope by its γ -photons having high energy and intensity and is also suitable for biological study since it is the only radioisotope of the biological trace element, of V, which can be a radiotracer by its longer half-life.

The ^{48}V was produced by $^{nat}\text{Ti}(d,xn)^{48}\text{V}$ nuclear reaction in the U-120 cyclotron with activity of 6 mCi. The energy of irradiating beam was 13 MeV, its intensity was 5 μA , and the metallic Ti target dimension was $16\times 11\times 2$ mm. For target cooling the circulated water in back side was used. After 3 cooling days only the ^{48}V and some ^{46}Sc ($T_{1/2}=84\text{d}$) produced by the side nuclear reaction, $^{48}\text{Ti}(d,\alpha)^{46}\text{Sc}$ were found in the target. For the preparation of source of ^{48}V , the Ti target was dissolved in HF and in sulfuric acid too. The ionexchange separation was developed for both dissolving methods:

The dissolution of the chemically resistant Ti target [1] is so violent in concentrated (35% m/m) HF, that it is necessary to carry out in polyethylene tube because of avoiding of the splash of the dissolved target. An anion exchanging column, DOWEX1-8 (size 100-200 mesh, length 12 cm, ID 10mm, treated 1 day earlier, prepared fresh) was used for separation in HF media. The reduced ionic form of Ti bond to the resin, therefore the dissolved target was saturated with sulfure-dioxid produced in Kipp-equipment by the above chemical reaction:



The treated solution was diluted to concentration of 2 mol/l of HF and the same concentration of the HF was used as an eluent for separation. Flow rate of the elution

was 1ml/min. The eluate was collected fractionally. The fractions were measured by g-spectrometry, which detected only ^{48}V . The advantages of this method are the easy dissolution of the target and the quick, complete separation of ^{48}V . The disadvantage are the avoiding glassware, all lab-equipments must be produced of HF-resistant plastic material and the final product difficult to use due to the aggressive HF media.

The sulfuric acid with concentration of 6 mol/l [2] can also dissolve the target, however it is much more difficult than by the HF: It needs heating under reflux for 6 hours. During the dissolution was forming the solid salt of Ti in high amount. Only 50% of the stoichiometric necessary amount of sulfuric acid for fully dissolution was used because of avoid of dissolution of that part of the target, in which the nuclear reaction wasn't produced. After the dissolution the liquid and solid faze was separated and solid salts was dissolved by 0.01 mol/l sulfuric acid. This soft acidic circumstance is necessary for effective separation on the Amberlit CG-50 column. The higher oxidation stage and the peroxid-complex of Ti is guaranty for remaining of Ti on the cationexchange column. Therefore 1% H_2O_2 in 0.01 mol/l nitric acid was added to the sample. The orange color is demonstrated the successful chemical reaction. For ionexchange separation this solution was used. The elution was carried out by 1% H_2O_2 in 0.01 mol/l nitric acid as an eluent. The radio-chromatogram was determined by the same method which was mentioned in the case of the separation in HF media. The chemical yield of the separation was more than 95%.The radionuclide impurity of ^{46}Sc was less than 0.02% determined by g-spectrometry. The chemical purity of ^{48}V was 99.8% in according to Ti determined by VIS-spectrophotometry using the absorbance of peroxid complex of Ti in 420 nm approximately. The advantages of this method are

the softer chemical circumstances and the easy to use final product. The disadvantages are the long dissolution time, the several made by hand steps and the less separation ratio compared with the separation in HF media.

For application of any methods in production of ^{48}V with high amount of radioactivity would be necessary some modifications to fit the method for work in shielded box by ma-

nipulators.

- a) Institute of Nuclear Research of the Hungarian Academy of Sciences, Debrecen, Hungary
 - b) Horia Hulubei National Institute of Physics and Nuclear Engineering, 76900 Bucharest, P.O.Box MG-6, Romania
- [1] U. Schindewolf, J.W. Irvine, *Anal. Chem.* **30** (1958) 906.
- [2] S.K. Zeisler, T.J. Ruth, *Radioanal. Nucl. Chem. Lett.* **200** (1995) 283.

3.1 Study of the transfer ionization process by observing the electron cusp in $\text{He}^{2+} + \text{He}$ collisions

L. Sarkadi, L. Lugosi, K. Tőkési, L. Gulyás and Á. Kövér

We investigated the cusp-electron emission in He^{2+} on He collisions in the energy range 25–75 keV amu^{-1} [1]. By detecting the electrons in coincidence with the charge-state analysed outgoing He^{2+} and He^+ ions, we identified the processes of electron capture to the continuum (ECC), and ECC accompanied by bound-state capture (transfer ionization, TI), respectively. The ratios of yields for the TI and ECC cusp are found to increase steeply with decreasing projectile energy. At 25 keV amu^{-1} the obtained TI/ECC ratio (1.42 ± 0.14) is almost two times larger than the corresponding ratio measured in a previous experiment for Ar target at the same impact energy [2]. We compared the measured data with calculations carried out in the independent particle model (IPM) with use of the classical trajectory Monte Carlo method (CTMC) and a hybrid version of the continuum-distorted-wave (CDW-EIS) theory.

The experimental and theoretical TI/ECC ratio values are plotted in Fig. 1. Both theory fail to reproduce the steep increase of the measured data with decreasing projectile energy. Searching for the reason of the discrepancy, we derived an upper limit for the TI/ECC cross section ratio within IPM in the range of small collision velocities:

$$\left(\frac{\sigma_{\text{TI}}}{\sigma_{\text{ECC}}} \right)^{\text{upper limit}} = (N - 1) \frac{p_c^{\text{max}}}{1 - p_c^{\text{max}}}.$$

Here N is the number of the electrons in the regarded target atomic shell, and p_c^{max} is the maximum of the impact-parameter-dependent one-electron capture probability function, $p_c(b)$. To determine the value of p_c^{max} for the $\text{He}^{2+} + \text{He}$ system, we used the Landau-Zener model in the molecular-orbital (MO) description of atomic collisions. At small collision velocities the Landau-Zener model resulted in $p_c^{\text{max}} \approx 0.5$. Using this, the above

equation for He target ($N = 2$) yields a value of 1 for the upper limit of the TI/ECC ratio in IPM (see Fig. 1). Since the measured value 1.42 ± 0.14 at 25 keV amu^{-1} is considerably larger than 1, we may conclude that the cusp production via transfer ionization in the low-energy $\text{He}^{2+} + \text{He}$ collisions cannot be understood within the framework of IPM, i.e., the process is probably influenced by electron correlation effects.

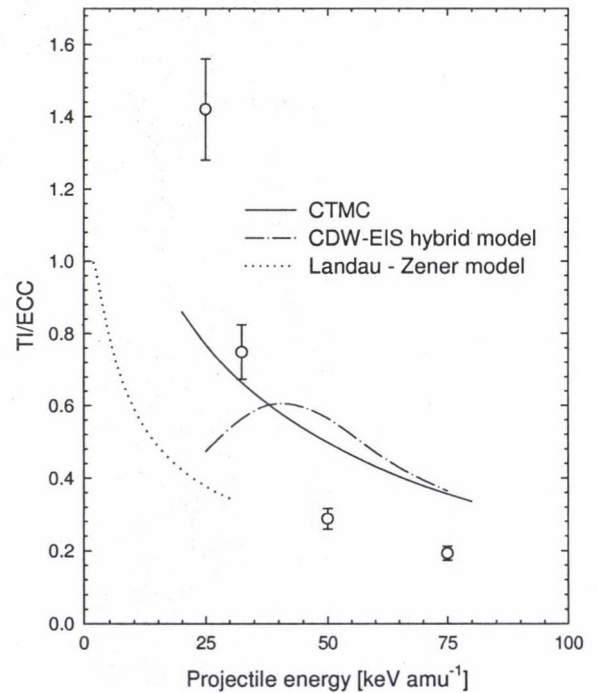


Figure 1. Cusp-electron production by TI relative to ECC as a function of the impact energy.

- [1] L. Sarkadi, L. Lugosi, K. Tőkési, L. Gulyás and Á. Kövér, *J. Phys. B: At. Mol. Opt. Phys.* **34** (2001) 4901.
- [2] L. Víkor, L. Sarkadi, J.A. Tanis, A. Báder, P.A. Závodszky, M. Kuzel, K.O. Groeneveld and D. Berényi, *Nucl. Instr. Meth.* **B124** (1997) 342.

3.2 Postcollision interaction and two-centre effects in ionizing collisions

L. Sarkadi, L. Gulyás and L. Lugosi

We report on a theoretical investigation of the process of ‘electron capture to the continuum’ (ECC) in which we attempted to interpret the recent experimental results obtained by An et al. [1]. These authors performed a kinematically complete experiment on single ionization for 75-keV $H_2^+ + He$ collisions by combining the techniques of the projectile energy loss spectrometry and the recoil ion momentum spectroscopy. In the experiment the momentum vectors of all the collision fragments were determined at a fixed (0°) projectile scattering angle, and the *centroids* of the longitudinal and transverse momentum distributions for both the recoil ions and ejected electrons were analysed as a function of the energy loss of the projectile. It was found that the momentum distributions of the collision products, especially for the electron, show clear signatures of ECC (or, more generally, the postcollision interaction effect, PCI).

An et al. explained their experimental findings only qualitatively, without comparing the data with theoretical calculations. In the present work we gave a quantitative analysis of the problem by performing calculations within the framework of the *classical trajectory Monte Carlo* (CTMC) model and the *continuum distorted wave* (CDW-EIS) theory. We showed that although the gross tendencies of the momentum distributions as a function of the energy loss of the projectile can simply be explained by kinematical effects, the rapid changes of the momentum centroids observed in the experiment at the energy loss value corresponding to the matching velocity $v_e = v_p$ are indeed signatures of PCI. (see Fig. 1). In our analysis we could determine the effects of PCI in the momentum distributions by repeating the CTMC calculations with a *short-range* interaction potential between the electron and the projectile ion. These calculations were made at several interaction length values. In

addition to PCI, we investigated also the contributions due to two-centre character of the electron emission. In order to identify these latter effects, we compared the results of the CDW calculations with those obtained in the first-Born approximation (i.e., a theory that accounts only for the one-centre electron emission).

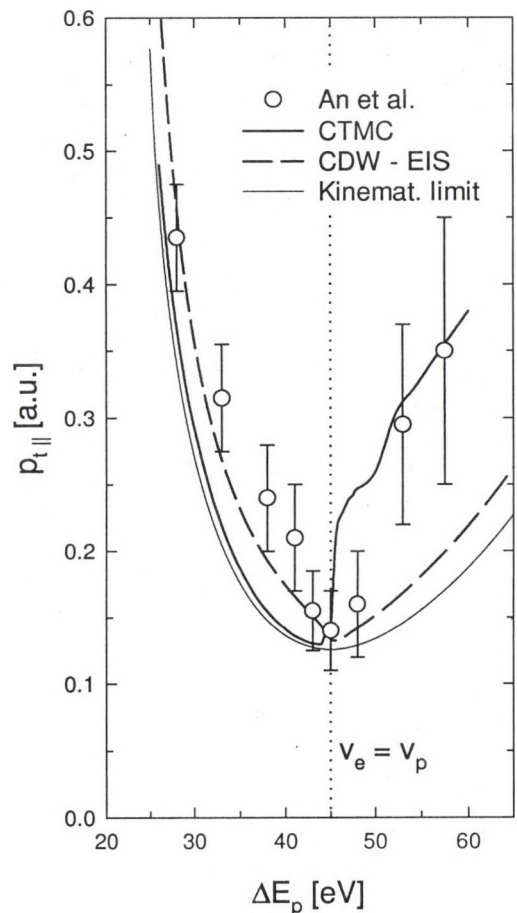


Figure 1. Centroid of the momentum distribution of the recoil target ion as a function of the projectile energy loss for 75-keV $H_2^+ + He$ collisions.

[1] L. An, Kh. Khayyat and M. Schultz, Phys. Rev. **A63** (2001) 030703(R)

3.3 Calculation of ion-induced inner-shell ionization cross sections by applying the CTMC method

L. Sarkadi

The ionization of the inner atomic shells by ion impact is an important field of the physics of atomic collisions both from theoretical and practical point of view. For light-ion projectiles the process can be treated perturbatively using first-order theories, like the plane-wave Born approximation (PWBA) and the semiclassical approximation (SCA). In most cases the states of the inner-shell electrons can be well represented by screened hydrogenlike wave functions.

In the present work we applied the *classical trajectory Monte Carlo* (CTMC) method [1] for calculation of inner-shell ionization cross sections. The method is based on the numerical solution of Newton's classical equation of motion for a large number of trajectories under randomly chosen initial conditions. CTMC describes the motion of all particles classically. The initial bound electronic states of the target atom are represented by elliptic Kepler orbits.

So far CTMC has been used mainly for collision systems involving light atoms. For collisions involving heavier atoms the method has generally been used to determine the contributions of the outer atomic shells, therefore the information about the applicability of CTMC for inner-shell problems is very scarce.

We tested the performance of CTMC for inner shells by calculation of K- and L-shell ionization cross sections for proton on argon collisions in the energy range 0.5–2 MeV. The many-electron target atom was replaced by a one-electron atom, representing the ion core by a model potential developed by Green et al. [2] based on Hartree-Fock calculations. The potential has the following form for a neutral atom (in atomic units):

$$V(r) = -[(Z - 1)\Omega(r) + 1]/r,$$

where Z is the nuclear charge and

$$\Omega(r) = \{(\eta/\xi)[\exp(\xi r) - 1] + 1\}^{-1}.$$

The values of η and ξ were taken from Garvey et al. [3]: $\eta = 3.50$ and $\xi = 0.957$. Concerning the choice of the random initial parameters, we followed the procedure proposed by Reinhold and Falcón [4] for non-Coulombic interaction.

The cross sections obtained for the K, L_1 and L_{23} shell are compared with the predictions of the ECPSSR theory [5] in Fig. 1. The latter theory is known to be an efficient theory of inner-shell ionization. The agreement between the two theories is reasonable.

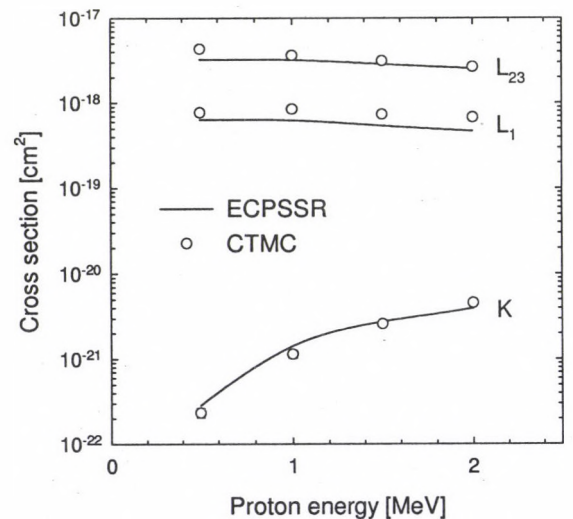


Figure 1. Cross sections for inner-shell ionization of argon by proton impact calculated by the CTMC and the ECPSSR theory.

- [1] R. Abrines and I.C. Percival, Proc. Phys. Soc. **88** (1966) 861.
- [2] A.E.S. Green, D.L. Sellin and A.S. Zachor, Phys. Rev. **184** (1969) 1.
- [3] R.H. Garvey, C.H. Jackman and A.E.S. Green, Phys. Rev. **A12** (1975) 1144.
- [4] C.O. Reinhold and C.A. Falcón, Phys. Rev. **A33** (1986) 3859.
- [5] W. Brandt and G. Lapicki, Phys. Rev. **A20** (1979) 465. and **A23** (1981) 1717.

3.4 Theoretical study of cusp-electron emission from $O^{8+} + Ar$ collisions

L. Sarkadi

In ion-atom collisions the emission of continuum electrons along the ion beam direction with the velocity of the beam (the so-called *cusp electrons*) is a problem of fundamental interest. The cusp-electron emission associated with target ionization is known as *electron capture to the continuum* (ECC). ECC may be accompanied by bound-state capture of an additional electron (or electrons) from the target to the projectile. The latter process is called *transfer ionization* (TI). TI is particularly interesting, because as a two- (multi-) electron process it may provide information about the role of electron-electron interaction (correlation) in atomic collisions.

The present work is connected to our previous systematic experimental investigations dealing with cusp-electron emission via TI (for a review see [1]). These studies were carried out with H^+ , He^+ , He^{2+} , O^{7+} and O^{8+} projectile ions in a broad range of the collision velocity (from 4.4 keV amu^{-1} to 1.5 MeV amu^{-1}). The experiments resulted in a large amount of measuring data. However, for long time the theoretical interpretation of the obtained results was missing. First quantitative description of the process was attempted only recently [1]: The energy spectra of the cusp peak and the TI/ECC cusp-intensity ratios for the $He^{2+} + He, Ar$ collision systems were determined in the independent particle model (IPM) by applying the classical trajectory Monte Carlo (CTMC) method and a hybrid version of the continuum-distorted-wave (CDW-EIS) theory.

We continued the theoretical study of TI by CTMC calculations carried out for $O^{8+} + Ar$ collisions in the energy range of $0.5\text{--}2.0 \text{ MeV}$. An interesting experimental finding observed for this collision system [2] is that the TI/ECC ratio as a function of the collision energy exhibits a slight maximum at about 0.9 MeV amu^{-1} . As a possible explanation, it was assumed that the maximum is due to the increasing contribution of the *inner shells* (first of all,

the L shell) to the cusp-electron production with increasing collision velocity.

The preliminary results of the CTMC simulations made for the L and M shell of Ar support the above assumption: At 1 MeV amu^{-1} collision energy the contribution of the L shell to the total cusp-electron emission is 59% and 81% for ECC and TI, respectively. Energy spectra of the ECC and TI cusp are shown in Fig. 1. The calculated TI/ECC ratio is 0.51, in good agreement with the experimental value, 0.58 ± 0.18 . This indicates that the electron correlation plays a minor role in TI (the calculations were made in IPM).

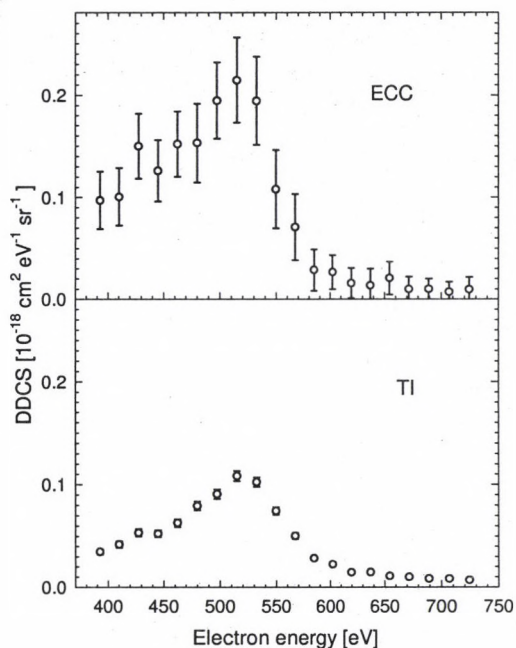


Figure 1. Energy spectra of the ECC and TI cusp calculated by the CTMC method for 1 MeV amu^{-1} $O^{8+} + Ar$ collisions.

- [1] L. Sarkadi, L. Lugosi, K. Tókési, L. Gulyás and Á. Kövér, *J. Phys. B: At. Mol. Opt. Phys.* **34** (2001) 4901.
- [2] P.A. Závodszy *et al.*, XIX. ICPEAC, Abstr.: p. 311. (1995)

3.5 Laser Spectroscopy of Antiprotonic Helium Atoms

D. Horváth, B. Juhász, E. Takács (ASACUSA collaboration)

In 2001, laser spectroscopy studies of antiprotonic helium atoms ($\bar{p}-e^{-}-\text{He}^{2+} \equiv \bar{p}\text{He}^{+}$) were carried out at the Antiproton Decelerator (AD) of CERN between July and September. The experiments used both the direct AD antiproton beam (energy: 5.3 MeV) and the decelerated beam (energy: 20–120 keV) which was produced using the Radio Frequency Quadrupole Decelerator (RFQD), a unique device which both decelerates and focuses the antiproton beam.

The studies included:

- Precision measurements of the wavelengths of transitions between pairs of metastable and short-lived antiprotonic states in ^4He . These measurements provided the most precise determination of the mass and charge of the antiproton to date, a test of the *CPT* invariance [1].
- Investigation of the influence of collisions with D_2 molecules on the lifetime of metastable antiprotonic states in comparison with that of H_2 studied earlier. A significant isotope effect was observed [2].
- Determination of the hyperfine splitting of an antiprotonic state using a laser-microwave-laser triple resonance method [3,4]. This hyperfine splitting is caused by the interaction of the electron spin and the antiproton's orbital magnetic moment.
- Discovery of 10 new laser resonant transitions between antiprotonic states, 4 of them in ^4He and 6 of them in ^3He . The wavelengths of these transitions were also measured.
- Determination of the density shifts and

zero-density wavelengths of 9 transitions in ^3He .

- Determination of the initial populations of metastable antiprotonic states in ^3He and ^4He by measuring the time dependence of the resonance intensity of the transitions [5].
- Observation of laser induced transitions at ultra low densities of He, about three orders of magnitude lower than before. These measurements used the low energy beam after the RFQD. At such low target densities, the measured transition wavelengths are practically the zero-density wavelengths therefore no density shift correction is needed.
- First observation of a two-photon transition between states of $\bar{p}\text{He}^{+}$.
- Determination of Auger rates of short-lived antiprotonic states [6].

Another remarkable achievement of 2001 was the capture, cooling and extraction of antiprotons using an antiproton trap inside of a superconducting magnet. We this trap, we could capture appr. 10^5 - 10^6 antiprotons coming from the RFQD, cool them using a cold electron cloud and rotational compression, and extract appr. 10^2 - 10^3 to the end of a 3 meter long beamline at energies of 10–250 eV.

Almost all of the support structures of the experimental devices were designed and manufactured in Hungary.

[1] M. Hori *et al.*, Phys. Rev. Lett. **87** (2001) 093401.

[2] B. Juhász *et al.*, Eur. Phys. J. D (in press)

[3] E. Widmann *et al.*, in preparation.

[4] J. Sakaguchi *et al.*, in preparation.

[5] M. Hori *et al.*, submitted to Phys. Rev. Lett.

[6] H. Yamaguchi *et al.*, in preparation

3.6 Differential cross sections for positron impact excitation of hydrogen

L. Lugosi and K. Tórkési

The study of the energy and angular distributions of the ejected electrons and scattered projectiles provides a sensitive test of various theories in atomic collision physics [1]. The most extensive and thorough investigations of positron-atom scattering have been made for atomic hydrogen. Noteworthy contributions on the elastic scattering, positronium formation, discrete excitation and ionization processes in positron-hydrogen collisions can be found both theoretically and experimentally, for example, in the works of Walters [2], Kernoghan et al. [3], Zhou et al. [4] and Jones et al. [5].

In this paper a *distorted wave polarized orbital* (DWPO) model and the *classical trajectory Monte Carlo method* (CTMC) are used to calculate singly differential excitation cross sections for positron impact induced 1s-2s transitions in hydrogen at 50, 100 and 200 eV incident energies. For the simple close-coupling approximation the coupled radial Schrödinger equations are

$$\frac{1}{2} \left[\frac{d^2}{dr^2} - \frac{l(l+1)}{r^2} + k_i^2 \right] u_i^l(r) = \sum_{j=1}^2 [V_{ij}(r) + V_{pol}(r)\delta_{ij}] u_j^l(r), \quad i = 1, 2. \quad (1)$$

The boundary conditions for the radial wave functions $u_i^l(r)$ can be written

$$\begin{aligned} u_i^l(r=0) &= 0, \\ u_i^l(r \rightarrow \infty) &= \frac{(2l+1)i^l}{k_i} \left[k_i r \cdot j_l(k_i r) \delta_{ij} + \sqrt{\frac{k_j}{k_i}} \exp \left[i \left(k_i r - \frac{l\pi}{2} \right) \right] T_{ij}^l \right], \end{aligned} \quad (2)$$

where T_{ij}^l denote the partial transition matrix elements, k_1 and k_2 are the magnitude of the momentum of the incident and scattered positrons, $j_l(x)$ is the spherical Bessel functions, respectively. The perturbation between

the incident positron and the atom is

$$V_H(\vec{r}, \vec{x}) = \frac{1}{r} - \frac{1}{|\vec{r} - \vec{x}|}, \quad (3)$$

so that the repulsive static matrix potential $V_{ij}(r) = \langle \phi_i(\vec{x}) | V_H(\vec{r}, \vec{x}) | \phi_j(\vec{x}) \rangle$, where \vec{r}, \vec{x} are the position vectors of the positron and electron referred to the proton, i and j labels the 1s and 2s eigenfunctions of the H-atom, respectively. In eq. (1) $V_{pol}(r)$ is the Callaway-Temkin [6] polarization potential that describes the interaction between the positron projectile and the neutral polarizable hydrogen atom in multipole order. The distorted wave model is useful when the coupling between the channels is small. Using the Green's function technique, the inelastic partial transition matrix elements in the framework of DWPO model can be expressed as

$$\begin{aligned} T_{21}^l &= -\frac{2}{\sqrt{k_1 k_2}} \exp[i(\delta_1^l + \delta_2^l)] \times \\ &\times \int_0^\infty g_2^l(r) V_{21}(r) u_1^l(r) dr, \end{aligned} \quad (4)$$

where $g_2^l(r)$ satisfies the differential equation

$$\begin{aligned} \frac{1}{2} \left[\frac{d^2}{dr^2} - \frac{l(l+1)}{r^2} - V_{22}(r) - \right. \\ \left. - V_{pol}(r) + k_2^2 \right] g_2^l(r) = 0 \end{aligned} \quad (5)$$

with the boundary conditions

$$g_2^l(r \rightarrow \infty) = \sin \left(k_2 r - \frac{l\pi}{2} + \delta_2^l \right). \quad (6)$$

Here $\delta_{1,2}^l$ are the partial-wave phase shifts. Thus we obtain the differential cross section for excitation of hydrogen as

$$\begin{aligned} \frac{d\sigma_{21}}{d\Omega} &= \frac{2}{k_1^3 k_2} \left| \sum_{l=0}^\infty (2l+1) \exp[i(\delta_1^l + \delta_2^l)] \times \right. \\ &\times \left. \int_0^\infty g_2^l(r) V_{21}(r) u_1^l(r) dr \cdot P_l(\cos \Theta) \right|^2. \end{aligned} \quad (7)$$

Here $P_l(x)$ denote the Legendre's polinomial of the first kind of order l and Θ is the scattering angle. The $u_1^l(r), g_2^l(r)$ functions were propagated using a Numerov algorithm with energy-dependent radial mesh with step-size ranging from 10^{-3} to 10^{-2} atomic units. The converged values of the T -matrix were determined by summing a set of partial waves belonging to low l values (usual up to $l_{max} = 10..15$). For higher l values the effective range formulas were applied

$$\begin{aligned} \tilde{\delta}_i^l &= -2k_i \int_0^\infty r^2 j_l^2(k_i r) V_{i,i}(r) dr \\ \tilde{T}_{21}^l &= -2\sqrt{k_1 k_2} \int_0^\infty r^2 j_l(k_1 r) j_l(k_2 r) V_{21}(r) dr, \\ \Omega &= \tilde{\delta}_1^l + \tilde{\delta}_2^l, \quad T_{21}^l = \tilde{T}_{21}^l \exp[i\Omega]. \end{aligned} \quad (8)$$

Fig. 1 shows the differential cross sections for 1s-2s excitation at three incident energies. At 50 eV the present CTMC results are very close to the second order distorted wave Born (DWB2) data of Bubulev and Madison [7]. For small scattering angles the different theoretical calculations give the same values except the data of the present DWPO model. At large scattering angle the coupled-channel optical model (CCOM) of Bransden et al [8] predicts smaller cross section values than the other calculations. At 100 eV our data are in good agreement with results obtained by DWB2 approximation and the multi-state close coupling (MCC) calculation of Walters [2]. At 200 eV the CTMC data overestimate the results of previous and present quantum mechanical calculations.

This work is supported by OTKA No.T032306, the grant "Magyary".

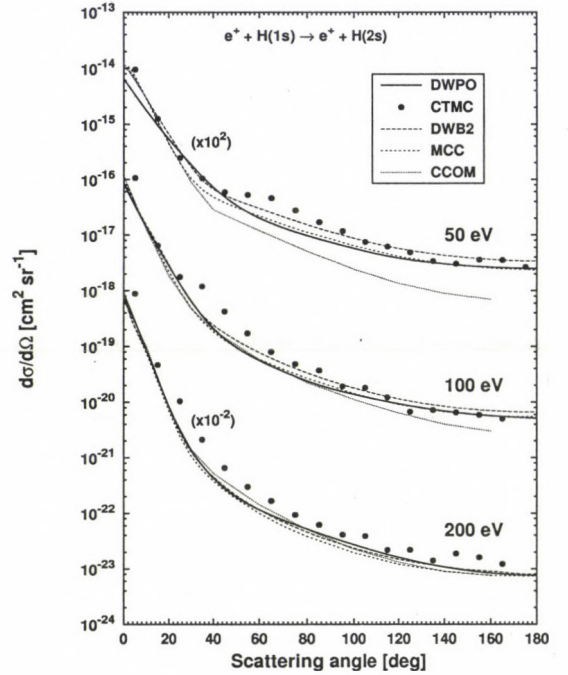


Figure 1. Differential cross sections for positron excitation of the 2s state of hydrogen at 50, 100 and 200 eV bombardment energies.

- [1] B. Matterstock, R. Huster, B. Paripás, A.N. Grum-Grzhimailo, W. Mehlhorn, *J. Phys.* **B28** (1995) 4301.
- [2] H.R.J. Walters, *J. Phys.* **B21** (1988) 1893.
- [3] A.A. Kernoghan, D.J.R. Robinson, M.T. McAlinden, H.R.J. Walters, *J. Phys.* **B29** (1996) 2089.
- [4] S. Zhou, H. Li, W.E. Kauppila, C.K. Kwan, T.S. Stein, *Phys. Rev.* **A55** (1997) 361.
- [5] G.O. Jones, M. Charlton, J. Slevin, G. Laricchia, Á. Kövér, M.R. Poulsen, S. Nic Chormaic, *J. Phys.* **B26** (1993) L483.
- [6] R.J. Drachman and A. Temkin, in: E.W. McDaniell and M.R.C. McDowell (Eds.), *Case Studies in Atomic Collisions Physics*, vol. II, North-Holland, Amsterdam, p.400. (1972).
- [7] V.E. Bubulev and D.H. Madison, *J. Phys.* **B25** (1992) 3229.
- [8] B.H. Bransden, I.E. McCarthy and A.T. Stelbovics, *J. Phys.* **B18** (1985) 823.

3.7 Application of the Landau-Zener model and the classical trajectory Monte Carlo method for capture processes in collisions of highly charged ions with light atoms

L. Lugosi and L. Sarkadi

Single and double electron transfer processes in slow collisions of multiply charged ions with light neutral atoms are one of the most basic reactions in a few-body Coulomb system. The cross sections of these collision systems are not only fundamental data in atomic physics, astrophysics, plasmaphysics and fusion-plasma research but also help to understand ion-atom collisions in the low-energy region ($E < 25$ keV amu⁻¹). In this work we investigate the single and double electron capture processes in collisions of C⁶⁺, N⁷⁺, O⁸⁺ and Ne¹⁰⁺ with H or He targets using the semi-classical two-state Landau-Zener-Stueckelberg (LZ) model and the three-body classical trajectory Monte Carlo method at low impact velocities ($v < 1$ au).

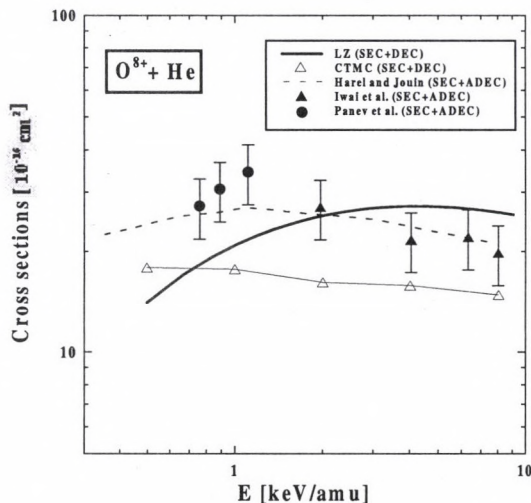


Figure 1. Cross sections of capture in $O^{8+} + He$ collisions as a function of the impact energy.

In describing the collision dynamics of processes SEC and DEC (single and double electron capture, respectively) in case of the He target we applied the one active electron approximation with a single-centre effective potential for calculations of the dominant (n,l)-level state selective and total charge exchange

cross sections. For He target part of the di-excited states of the projectile ions produced by DEC decay by Auger emission of one electron. This autoionizing double capture channel (ADEC) is not taken into account in the present work.

In the LZ approximation, the single electron transition probabilities P^{LZ} after two passages through the crossing region are given by the

$$p = \exp \left[- \frac{2\pi \Delta^2(R)}{v_R \cdot \Delta F(R)} \right]_{R=R_c},$$

$$P^{LZ} = 2p(1 - p) \quad (9)$$

equations in the adiabatic molecular orbital basis. Here R_c is the diabatic curve-crossing distance, ΔR is the splitting of the corresponding adiabatic energies, $\Delta F(R) = d/dR \Delta(R)$ and v_R is the radial velocity. For calculation of the total cross sections in the two-electron cases we have applied the modified IPM model of Errea et al. [1] which is a nonequivalent independent electron treatment in the framework of the LZ approximation. An example of our calculations are shown in Fig. 1 for the $O^{8+} - He$ system together with the close-coupling calculation of Harel and Jouin [1] and experimental data of Iwai et al. [3] and Panov et al. [4]. In our present approach the LZ cross sections are given in a fully analytical form. The obtained values of the LZ as well as the CTMC capture cross sections are in a reasonable agreement with the experimental data and the results of other theoretical calculations.

- [1] L.F. Errea, A. Macias, L. Mendez and A. Riera. Phys. Rev. **A64** (2001) 032714.
- [2] C. Harel and H. Jouin, J. Phys. **B25** (1992) 221.
- [3] T. Iwai *et al.*, Phys. Rev. **A26** (1982) 105.
- [4] M.N. Panov *et al.*, Physica Scripta **T3** (1983) 124.

3.8 Improvement of atomic physics database is necessary to utilise the full potential of EDS X-ray spectrometry

I. Török, T. Papp

Despite of the generally accepted opinion, that X-ray analytical methods, like e. g. PIXE (Particle induced X-ray emission) are matured, the utilisation of the full potential of the method is far from reaching its limit. One of the possible reasons for this is, that either the atomic process, or the detection mechanism is not considered in necessary depth. E.g. there are large number of lines with small relative intensity, which in certain circumstances are larger than negligible, and in addition some of them could depend on the chemical states of the sample. These lines are in the neighbourhood of the diagram lines, which are used in analytical measurements, and they are not resolved by semiconductor detectors. Moreover many times in the evaluation of the X-ray spectra they are not involved into the model spectrum. This can lead to unwanted analytical errors. By WDS the energies and intensities of such weak lines can be measured, and these energies and intensities can be used in construction of the model spectrum for spectrum evaluation. Such evaluations give more precise and reliable analytical results. We have measured and collected from the literature some of these data: The intensity of $K\beta_5$ [1, 2], the energies of $K\alpha L^i$ and $K\beta L^i$ multiple ionization satellites (in this case we could deduce simple semi-empirical formulae for the energies of the i -th satellites of a given element: [3] for $K\alpha L$ and [4] for $K\beta L$ satellites). Now a similar work is in process for the intensities of these multiple ionization satellites for elements $11 \leq Z \leq 50$ for cases when the projectile is 1-4 MeV proton [5]. Such compilation and experimental

works can help EDS to reach more precise analytical results. E.g. the newer versions of the GUPIX, an X-ray spectrum evaluation program package (developed at the Guelph University, Canada) widely used in PIXE [6,7,8], now either already use these results, or the use of them is in preparation.

The work was supported by OTKA No. T016636.

- [1] I. Török, T. Papp, J. Pálinkás, M. Budnar, A. Mühleisen, J. Kawai, J.L. Campbell, *Relative intensity of the $K\beta_5$ x-ray line*. Nucl. Instr. and Meth. **B114** (1996) 9.
- [2] I. Török, J. Pálinkás, M. Budnar, M. Kavcic, A. Mühleisen, J. Kawai, *Forgotten(?) X-ray intensity enhancement in solids at lines related to not completely filled shells*. In Application of Accelerators in Research and Industry: Proceedings of the Fourteenth International Conference, Denton, Texas, November 1996, ed.: J.L. Duggan, I.L. Morgan, (AIP Conference Proceedings, No. 392, Woodbury New-York 1997), p.153.
- [3] I. Török, T. Papp and S. Raman, *Energy systematics of the multiple ionization $K\alpha L^i$ satellites*. Nucl. Instr. and Meth. **B150** (1999) 8.
- [4] I. Török, T. Papp, S. Raman, *An improved description of the multiple ionization $K\beta L^i$ satellite energy spacings*. ATOMKI Annual Report 1999 (2000) p.38.
- [5] Matjaz Kavcic, privat communication.
- [6] J.A. Maxwell, W.J. Teesdale, J.L. Campbell, *The Guelph PIXE software package*. Nucl. Instr. and Meth. **B43** (1989) 218.
- [7] J.A. Maxwell, W.J. Teesdale, J.L. Campbell, *The Guelph PIXE software package II*. Nucl. Instr. and Meth. **B95** (1995) 407.
- [8] J.L. Campbell, Th. Hopman, J.A. Maxwell, Z. Nejedly, *The Guelph PIXE software package III: Alternative proton database*. Nucl. Instr. and Meth. **B170** (2000) 193.

3.9 Separation of extrinsic and intrinsic plasmon excitations in Ge KLL Auger spectra

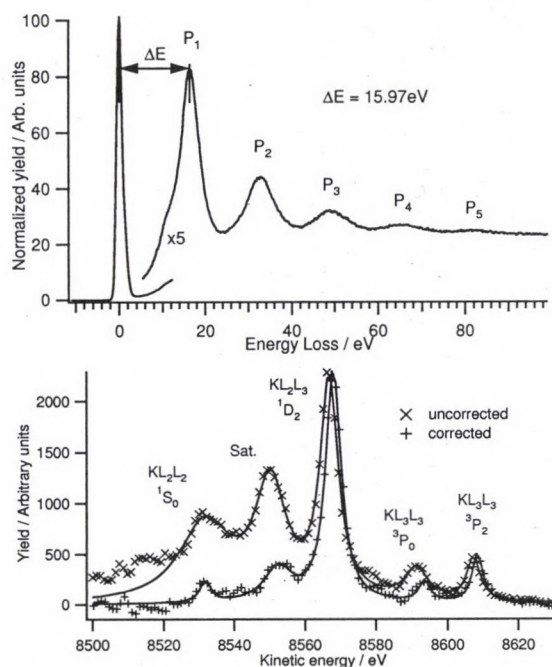
Z. Berényi, B. Aszalós-Kiss, A. Csik, J. Tóth, L. Kövér and D. Varga

The nature of the Ge satellite structure and the contributions from extrinsic and intrinsic processes were investigated using the ESA-31 electron spectrometer [1]. These measurements are providing the first high energy resolution Ge KLL data.

Plasmons are commonly defined to be the oscillations of the free electron gas in conductors, however, some semiconductors appear to show similar phenomenon. In an earlier work on the Ge KLL Auger spectra the presence of a strong satellite was identified as due to the effect of inelastic electron scattering [2]. The *reflected electron energy loss* (REELS) spectrum of Ge also shows the well-known periodic plasmon excitation structure (fig. 1). The plasmon excitation can be originated at any sudden change in the electric potential field. In *photo- and Auger electron spectroscopy* (XPS/AES) we usually distinguish between two excitation mechanisms, the so-called 'intrinsic' process, due to the creation of a core vacancy e.g. in XPS and the 'extrinsic' excitation when the presence of the outgoing photo- or Auger electron modifies the equilibrium potential in the solid. Both excitation mechanisms contribute to the energy loss structure, however, their effects can be separated using the differential inelastic scattering cross section extracted from REELS spectra [3]. Since in REELS experiments only extrinsic plasmons are produced, using this cross section one can eliminate the extrinsic part of the plasmon peak in the KLL spectrum [4]. Ge KLL spectra, excited by Cu x-rays (bremsstrahlung) were measured by the home built ESA-31 electron spectrometer based on a 180° hemispherical analysis, using 2.6 eV energy resolution at 8.5 keV electron energy. Energy loss spectra of 5 and 7 keV energy primary electrons were produced using a VG

LEG 62 electron gun. During measurements the vacuum was better than 2×10^{-9} mbar. The measured and the corrected KLL spectra can be seen on figure 2. The structures were fitted by sets of Lorentzians at both cases. The intensity ratio of the plasmon peaks induced by intrinsic and extrinsic excitation processes is found to be:

$$\frac{I_{int}}{I_{ext}} = 0.44 \pm 0.03 \quad (10)$$



- [1] L. Kövér, D. Varga, I. Cserny, J. Tóth, K. Tókési, *Surf. Interface. Anal.* **19** (1992) 9.
- [2] E. Sokolowski, C. Nordling, *Arkiv för Fysik* **14** (1958) 557.
- [3] S. Tougaard, J. Kraaer, *Phys. Rev.* **B43** (1991) 1651.
- [4] S. Tougaard *QUASES: Software Package for Quantitative XPS/AES of Surface Nanostructures by Peak Shape Analysis* (ver. 4. 4.) Univ. of Southern Denmark: Odense, Denmark, 2000.

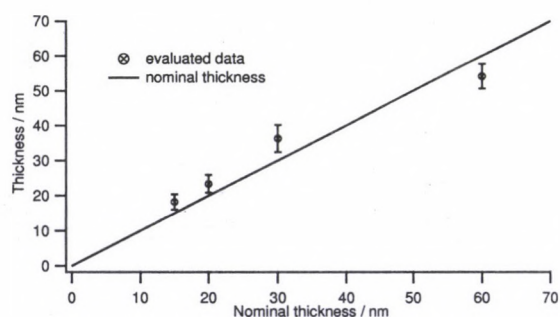
3.10 Thickness determination of Germanium surface layers

Z. Berényi, B. Aszalós-Kiss, A. Csik, J. Tóth, L. Kövér and D. Varga

In the electron spectra of solid samples with finite thickness there is always a distortion due to the energy losses of the outgoing electrons during inelastic scattering events. The strength of this distorting effect strongly depends on the pathlength of the electrons in the solid, so on the sample's geometry. The thicknesses of Ge surface layers on Si substrate were determined with a method based on inelastic electron scattering model using high-resolution photoelectron spectra of the sample. An attempt was made to complement the QUASESTM spectrum analyzer package with quantitative thickness evaluation method.

For the elimination of the inelastic scattering effect Tougaard *et al.* developed the QUASESTM program package [1]. As input, it requires the electrons' inelastic mean free path (IMFP) and inelastic scattering cross section in the studied material, as well as the geometrical parameters of the sample. The evaluation results in an energy distribution that is supposed to be free from inelastic distorting effects, i.e. the source spectrum, which is emitted by the atoms into the solid. The aim of the present work is to establish a reliable method for the optimization of the sample's morphology parameters while all other inputs and a reference source function are given. Assuming a certain geometrical setup, the shape of the resulting source spectrum can be compared to the reference source function and the goodness of the matching can be quantified through a parameter similar to the χ^2 function. The optimum is reached for the real morphological data of the sample. The reference source function can be obtained from the evaluation of the electron spectrum of any samples with known morphology. The most convenient way is to use a semi-infinite reference sample, because in this case the elimination of the inelastic background is simpler (e.g. no need to use IMFP). Ge layers with various thickness

(monitored by a quartz crystal microbalance) were deposited onto Si substrates by d.c. magnetron sputtering technique, forming flat and amorphous surface layers. For the evaluation the photoelectron spectra of the Ge 2p region were used, because its structure is free from the inelastic tail from any higher energy peak. We used Cu $K\alpha_{1,2}$ excitation and the ESA-31 high-resolution hemispherical spectrometer [2]. The IMFP values were taken from reference [3] and were checked by own measurements. The differential inelastic scattering cross sections were obtained from our *reflected electron energy loss spectrometry* (REELS) experiments on samples prepared in the same manner as described above and were evaluated with the method suggested by Tougaard *et al.* [4]. For each sample the optimal thickness and also its error can be determined well from the shape of the χ^2 curve [5]. Figure 1 shows the summary of the surface layer thickness determination results for all of the studied samples.

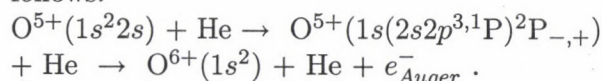


- [1] S. Tougaard QUASES: *Software Package for Quantitative XPS/AES of Surface Nanostructures by Peak Shape Analysis* (ver. 4. 4.) Univ. of Southern Denmark: Odense, Denmark, 2000.
- [2] L. Kövér, D. Varga, I. Cserny, J. Tóth, K. Tökési, *Surf. Interface. Anal.* **19** (1992) 9.
- [3] C.J. Powell, A. Jablonski, *J. Phys. Chem. Ref. Data* **28** (1999) 19.
- [4] S. Tougaard, J. Kraaer, *Phys. Rev.* **B43** (1991) 1651.
- [5] G. Cowan: *Statistical Data Analysis*, Clarendon press, Oxford, 1998.

3.11 Calculation of the Single Differential Cross Section of the $1s \rightarrow 2l$ Excitation of the Lithium-Like O^{5+} Ions in Collisions with He

A. Orbán, B. Sulik and T.J.M. Zouros^{a)}

New calculations of single $1s \rightarrow 2p$ excitation cross sections have been performed in the second order semiclassical approximation (SCA). Two types of intermediate states, $1s2s^2\ ^2S$ and $1s^22p\ ^2P$, are considered and compared with existing state-selective Auger electron production cross section data [1] measured earlier in collisions of $O^{5+}(1s^22s)$ with He targets. The considered transitions are as follows:



In the calculations the electronic screening effect of the target is taken into account by using a $1s$ type H-like screening potential [2], while the projectile initial and final states are described with Hartree-Fock-Slater (HFS) wavefunctions.

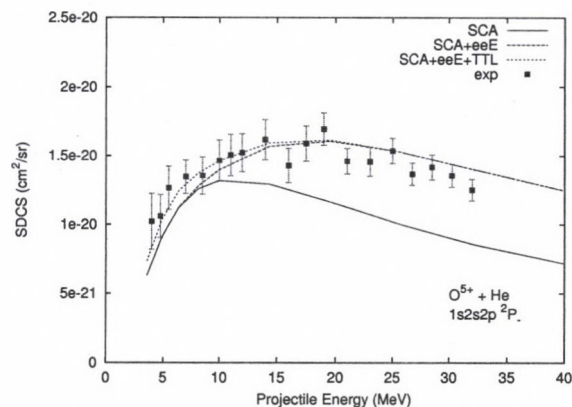


Figure 1. Single differential cross section as a function of the projectile (O^{5+}) energy. The present calculation is marked by SCA, eeE stands for a 1^{st} Born calculation and TTL shows the contribution of the transfer-loss process calculated elsewhere [5].

The impact parameter dependent excitation

probabilities $P(b)$ are calculated within the framework of the time dependent perturbation theory. The Auger e^- emission cross sections at 0° from the doublet initial state i ($^2P_-$ or $^2P_+$) to the ground state, were calculated in the following manner [3]:

$$\frac{d\sigma_i(0^\circ)}{d\Omega} = \frac{a_i}{4\pi} [(1 + 2D_2)\sigma_0 + (2 - 2D_2)\sigma_1]$$

where a_i is the Auger yield for the decay from the state i to the ground state, D_2 is the dealignment coefficient and σ_0 and σ_1 are the single excitation cross sections for $1s \rightarrow 2p(m=0)$ and $1s \rightarrow 2p(m=1)$ transitions. Different B1 and B2 calculations have been previously reported using screened H-like projectile wavefunctions for the same system [4], but these calculations overestimated the experimental data by a factor of 2–3. Our new results are in much better agreement with experimental data. In the present calculations, we also have taken into account the TL process [5]. We treat the dielectronic interaction (eeE) within the framework of the 1^{st} Born approximation.

- a) Department of Physics, University of Crete & I.E.S.L-F.O.R.T.H., Heraclion, Crete, Greece
- [1] T.J.M. Zouros, D.H. Lee, J.M. Sanders and P. Richard, Nucl. Instr. & Meth. Phys. Res. **B79** (1993) 166.
 - [2] S. Ricz, B. Sulik, N. Stolterfoht, I. Kádár, Phys. Rev. **A47** (1993) 1930.
 - [3] N. Stolterfoht, A. Mattis, D. Schneider, G. Schiwietz and B. Sulik, Phys. Rev. **A48** (1993) 2986.
 - [4] T.J.M. Zouros, D.H. Lee, P. Richard, U. Thumm and B. Sulik, Scientific Program and Abstract of Contributed Papers (TH129), XX. ICPEAC, 23-29 July 1997, Vienna, Austria.
 - [5] A. Orbán, T.J.M. Zouros, L. Gulyás and B. Sulik, Program Schedule & Abstract Book (3D-015), ICES8, 8-12 August 2000, Berkeley, USA.

3.12 Collision dynamics probed by convoy electron emission

M. Seliger^{a)}, *K. Tókési*, *C.O. Reinhold*^{b)}, *J. Burgdörfer*^{a)}, *Y. Takabayashi*^{c)}, *T. Ito*^{c)}, *K. Komaki*^{c)}, *T. Azuma*^{d)}, and *Y. Yamazaki*^{c,e)}

We have probed the description of the collision mechanisms by the emission of convoy electrons as a result of the transport of an Ar^{17+} ion with an energy of 390 MeV/amu through self-supporting amorphous carbon foils of thickness varying from 25 to 9190 $\mu\text{g}/\text{cm}^2$. We have on one hand performed a classical trajectory Monte Carlo (CTMC) simulation of the random walk of the electron initially attached to the relativistic hydrogenic Argon ion. On the other hand we have performed measurements of the final kinetic energy of the emitted convoy electrons at the Heavy Ion Medical Accelerator in Chiba (HIMAC).

By varying the target foil thickness we have the opportunity to scan different regions of collision dynamics: electrons emitted from very thin targets have suffered only few hard elastic collisions. With increasing target foil thickness higher excited states become populated and hence contribute to an increased flux of electrons into low lying continuum states. This transition is dominated by inelastic collisions transferring small amounts of momentum. The third region is the post ionization transport of continuum electrons that is governed by angular straggling due to elastic collisions and energy stopping as a result of inelastic interactions with target electrons.

Electrons emitted from very thin targets show a broad almost isotropic velocity distribution (Fig. 1). With increasing foil thickness emission from higher excited states becomes dominant. The width of the velocity distribution of the emitted electrons decreases with increasing foil thickness in both directions, parallel and perpendicular. Since the minimum width in the parallel velocity distribution is reached for targets of a thickness of 248 $\mu\text{g}/\text{cm}^2$ and for the perpendicular later, the overall distribution shows an elliptic form.

The effects of post ionization transport become apparent for thicker foils: Both velocity distributions, parallel and perpendicular, are

broadened. Inelastic collisions are decreasing the parallel velocity resulting in an increased width and a shift towards lower energies. The perpendicular velocity is mostly effected by elastic collisions. The so called "Newton Circle" is clearly visible for the thickest foils in Fig. 1.

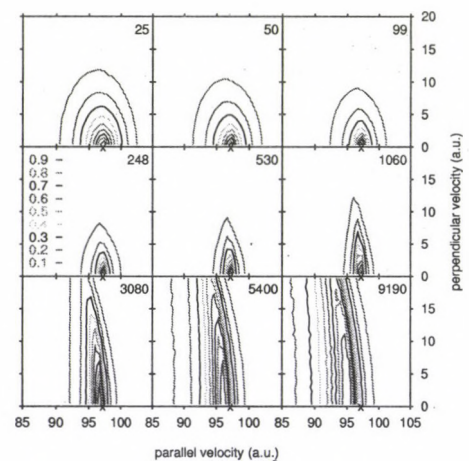


Figure 1. Velocity distribution of simulated convoy electrons emitted by an Ar^{17+} in transport through a carbon foil of different thickness. Figures show contour plots of the velocity distributions in the parallel versus the perpendicular directions with respect to initial projectile ion velocity. The foil thickness is denoted for every graph in units of $\mu\text{g}/\text{cm}^2$. Intensities have been normalized to one.

This work is supported by FWF, OTKA No.T032306, the grant "Magyary", and the "Stiftung Aktion Österreich-Ungarn" (45öu6).

- a) Institute for Theoretical Physics, Vienna University of Technology, Austria.
- b) Physics Division, Oak Ridge National Laboratory, Oak Ridge, Tennessee.
- c) Institute of Physics, Graduate School of Arts and Sciences, University of Tokyo.
- d) Department of Physics, Tokyo Metropolitan University, Hachioji, Tokyo.
- e) Atomic Physics Laboratory, RIKEN, Wako, Saitama, Japan

3.13 Enhancement of Low-Energy Electron Ion Recombination in a Magnetic Field

M. Hörndl^{a)}, S. Yoshida^{a)}, K. Tókési, and J. Burgdörfer^{a)}

Electron-ion recombination in cold magnetized plasmas shows a dramatic enhancement of the radiative recombination rate for bare high Z ions relative to what standard radiative recombination rates predict. Several proposals have been put forward to explain this surprising discrepancy with theory for one of the supposedly well-understood elementary quantum-electrodynamic processes. They range from the influence of three-body recombination and density enhancement due to plasma screening effects to transient electric field induced recombination. None of these models can, so far, account quantitatively for the observed enhancement.

We developed an alternative model which focuses on the classical chaotic dynamics of the electron in the combined Coulomb field of the ion and the magnetic guiding field in the cooler. The phase space structure of this irregular scattering problem is such that generalized deflection functions, specifically the visit function, are dramatically changed compared to the pure Coulomb case. As a result, the net flux of electrons towards the immediate vicinity of the ion is enhanced.

As a first application we compare our simulation with the experimental data [1] for C^{6+} . The electron temperatures in this experiment are $k_B T_{\parallel} \approx 0.06$ meV and $k_B T_{\perp} \approx 5$ meV, and the magnetic guiding field of the electron beam is $B = 42$ mT. Fig. 1 shows the recombination rate as a function of the average relative energy between electrons and ions. The dashed line corresponds to the standard RR theory. The solid line represents the experimental data [1] and the circles the enhanced recombination rate according to our present CTMC calculations.

The calculation appears to reproduce the enhancement quite well, both in terms of the energy dependence and the overall magnitude of the effect. In fact, the present calculation seems to overestimate the enhancement by 20

to 30 %. Several effects in the experiment not taken into account within the theory may account for this overestimate. The simulation assumes a perfectly homogeneous magnetic field neglecting any inhomogeneity or fluctuation. The velocity distribution may not be perfectly Maxwellian as assumed in our theory. Moreover, fluctuating fields and perturbations due to neighbouring ions and electrons, *i.e.* many-body effects in the plasma are ignored. Furthermore, future investigations should include non-adiabatic switch-on and switch-off effects of the magnetic field at the entrance and the exit of the cooler which may have an influence on the recombination rate [2].

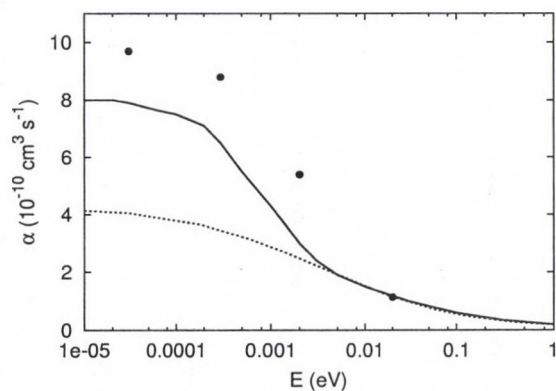


Figure 1. Radiative recombination rate for C^{6+} and $B = 42$ mT as a function of relative energy between electrons and ions. The standard RR theory with $n_{max} = 10$ (dashed line), the experimental measurements [1] (solid line), and CTMC results (\circ) are plotted.

This work is supported by FWF, and the "Stiftung Aktion Österreich-Ungarn" (45öu6).

a) Institute for Theoretical Physics, Vienna University of Technology, Austria.

[1] G. Gwinner *et. al.*, Phys. Rev. Lett. **84** (2000) 4822.

[2] G. Gwinner *et. al.*, XXII-ICPEAC, Abstracts of Contributed Papers (2001) 326.

3.14 Evidence for Fermi-Shuttle Ionization in $C^+ + Xe$ Collisions

B. Sulik, Cs. Koncz, K. Tórkési, A. Orbán and D. Berényi

In $C^+ + Xe$ collisions, clear evidence has been found for the consecutive projectile-target-projectile (P-T-P; triple) and projectile-target-projectile-target (P-T-P-T; quadruple) scattering of the electrons before their ejection. This type of multiple scattering is often referred to as Fermi-shuttle mechanism, which provides ping-pong electrons. Originally, the model has been introduced by Fermi [1] to give a possible explanation of the origin of cosmic rays. He supposed that giant magnetic fields moving in space against each other, can accelerate charged particles up to extremely high energies in a long set of elastic collisions. It was pointed out later that even the microscopic fields of molecules or atoms might play this kind of ping-pong game with electron balls. Such processes may contribute to the spectra of electrons, emitted in collisions of energetic particles with matter. The high-energy tail of these spectra is important for many reasons. The observation of such hot electrons is of fundamental importance for basic research. Energetic (few keV) electrons form a rather long-range secondary radiation which has a crucial role in the interaction of radiation with biological tissues, relevance in astrophysics, plasma physics and also in analytic methods or ion-beam technologies.

Ionization in ion-atom collisions may include a sequence of backscatterings of an electron between the incoming projectile ion and the target core. The velocity of the electron is increased by approximately $2V$, in every 180° elastic scattering with the incoming projectile, while only the direction of the electronic motion is changed by a scattering with the target:

The cross section ratios are shown in Fig. 4. Distinct broad peaks appear at $2V$ in backward angles and close to $4V$ in both forward and backward angles. The integrated experimental relative P-T : P-T-P : P-T-P-T yields are 10,000 : 280 : 16. The large fractions backscattered by the xenon core in the fourth scattering ($\sim 6\%$) might be considered as an in-

dication for a trapping mechanism. Fig. 4 also shows the results of classical trajectory Monte Carlo (CTMC) calculations, performed for all shells of the C^+ ion (electron loss), and for the $4d$, $5s$ and $5p$ subshells of Xe. It is clearly seen that experiment and CTMC calculations provide very similar peak structures. Moreover, an analysis of the associated recoil ion momenta shows that at least 97% of the "CTMC electrons" in the peaks at $4V$ are emitted in P-T-P processes at forward, and in P-T-P-T processes at backward observation angles. These results provide an independent confirmation that the experimental peaks at about $4V$ also originate from the indicated processes.

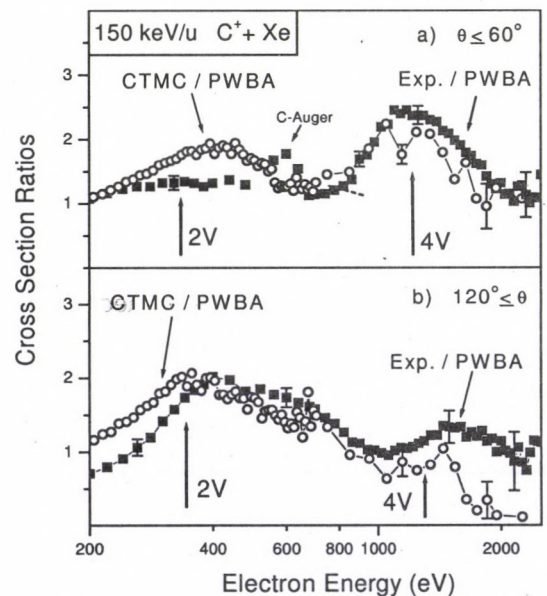
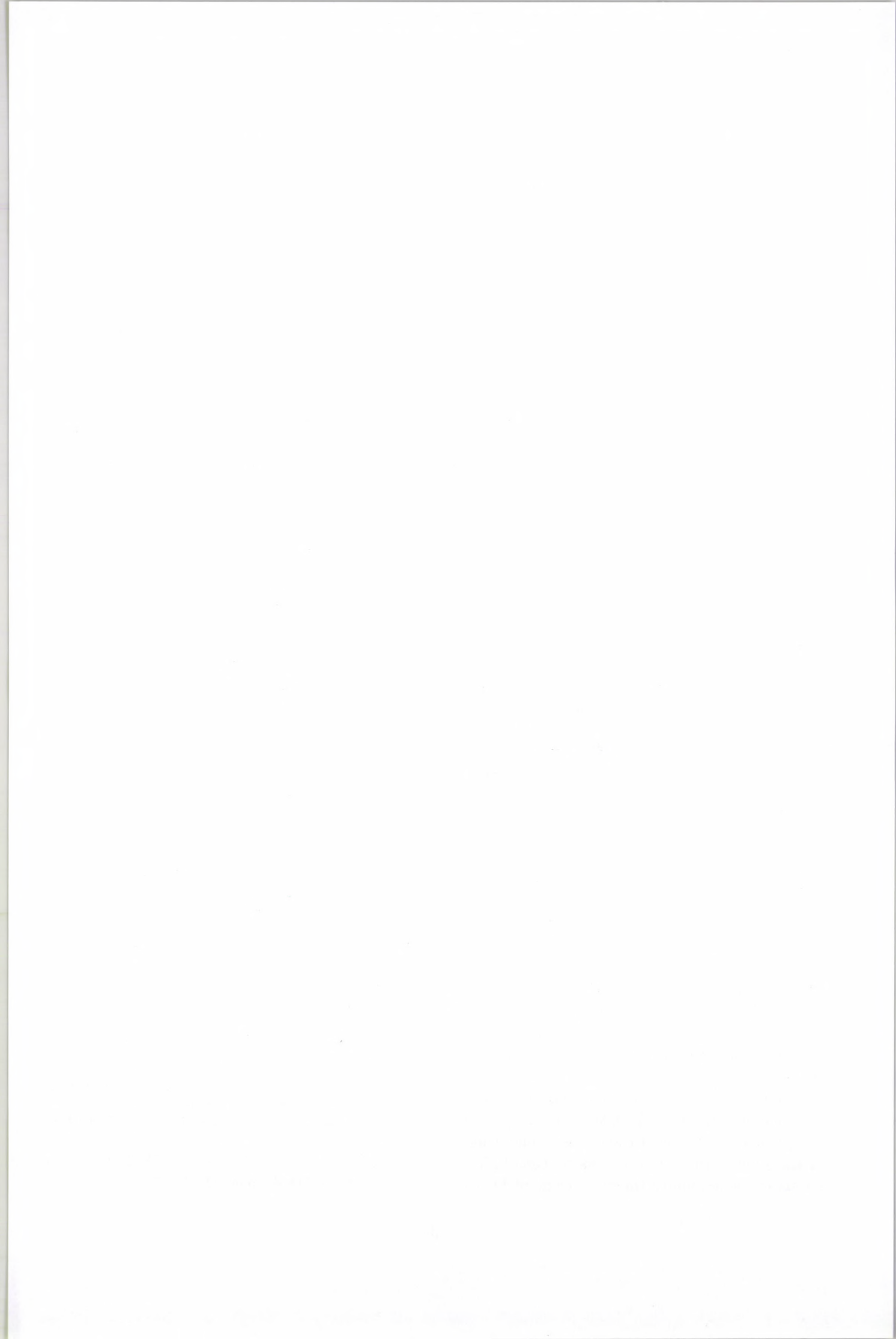


Figure 1. Comparison between experiment and CTMC calculations. Both data sets are divided by the PWBA target results, and integrated over forward (a) and backward (b) observation angles. Some typical error bars are also indicated [2].

This work is supported by OTKA Nos. T032942, M27839, T032306 and the grant "Magyary".

[1] E. Fermi, *Phys. Rev.* **75** (1949) 1169.

[2] Sulik *et al.*, *Phys. Rev. Lett.* **88** (2002) 73201.



3.15 Auger-electron lineshapes in electron impact ionization

B. Paripás^{a)}, G. Vitéz^{a)}, Gy. Víkor^{b)}, K. Tőkési, and L. Gulyás

The distortion effects of the post-collision interaction (PCI) on argon $L_{2,3}M_{2,3}M_{2,3}$ Auger electron lineshapes at 2 keV electron and 3.6 MeV antiproton impact inner-shell ionization, where reliable experimental data are available, and where a discrepancy was found between theory and experiment, have been calculated [1]. The calculations were based on the model of Kuchiev and Sheinerman [2] applying our cross section data for secondary electrons, determined by a classical trajectory Monte Carlo (CTMC) method and a continuum distorted wave (CDW) method. We separated the effect of the ejected electron and the scattered projectile.

Fig. 1 shows the angular dependence of the average asymmetry parameter (ξ). The results show that the angular dependence of ξ is caused mainly by the scattered projectiles. When only the ejected electrons are taken into account the CTMC and the CDW based calculations result in an opposite (although very weak) angular dependence. The discrepancy between theory and experiment at $\vartheta_A = 90^\circ$ is probably caused by the underestimated cross sections of the slow ejected electrons. It really can happen because in the CTMC method the dipole interaction is neglected and in the CDW approach the cross section - because of computational reasons - breaks down under 10 eV. Then the decreased cross sections reduce the peak asymmetry in the whole angular interval. At the same time the cross sections of the high energy projectiles scattered in the forward direction (corresponding to the low energy ejected electrons) are also underestimated that reduces the angular dependence. The resultant of these two effects is that the peak asymmetry is underestimated only around $\vartheta_A = 90^\circ$. It is interesting that the

CTMC based calculations agrees better with the experiments when we - keeping the scattered electron projectile - exchange the cross sections to the ones concerning the antiproton projectiles.

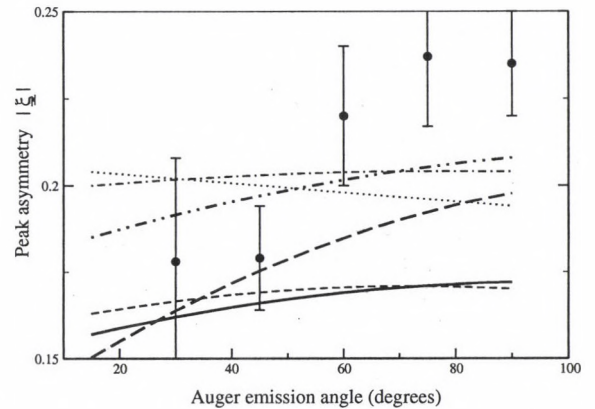


Figure 1. Angular dependence of the Auger peak asymmetry: (circle) experiment with electron projectile; thick lines: calculations when the scattered projectile is electron (with CTMC (solid line), CDW (long dashed line) and CTMC-antiproton (-.-) cross sections); c, thin lines: calculation - but the effect of the scattered projectile is omitted (CTMC (dashed line) and CDW (dotted line) cross sections) or the scattered projectile is antiproton with equivalent velocity (dashdotted line) (CTMC-antiproton cross sections).

This work is supported by OTKA No. T032306, the grant "Magyary".

a) Department of Physics, University of Miskolc, Hungary

b) Department of Atomic Physics, Stockholm University, Sweden

[1] B. Paripás, G. Vitéz, Gy. Víkor, K. Tőkési, and L. Gulyás, *J. Phys.* **B34** (2001) 3301.

[2] M.Yu. Kuchiev and S. Asheinerman, *Sov. Phys. Usp.* **32** (1989) 569.

3.16 Transmission of Ne^{7+} ions through nanocapillaries etched in polymer PET: Evidence for capillary guidance

N. Stolterfoht^{a)}, J.H. Bremer^{a)}, R. Hellhammer^{a)}, V. Hoffmann^{a)}, B. Sulik, K. Tőkési, A. Petrov^{a)}, and D. Fink^{a)}

Recently, we performed experiments in which slow highly charged ions are transmitted through capillaries with a large aspect ratio of about 100nm diameter in a $10\mu\text{m}$ thick PET polymer foil [1]. The nanocapillaries were produced by etching ion tracks in PET using NaOH. We measured the transmission of 3 keV Ne^{7+} ions whose final charge state and angular distribution were analyzed by means of an electrostatic deflector.

Similar studies have previously been performed using the method of x-ray spectroscopy [2]. In our experiments, particular emphasis was given to the angular distributions of the transmitted ions measured using highly insulating PET surfaces. The results are partially shown in Fig. 1. For PET foil tilted by 5° , the angular distribution of the Ne^{7+} is found to be relatively broad (FWHM of $\sim 6^\circ$) and the maximum is shifted by 5° . Similar results were obtained when the tilt angle was increased up to 20° . The results are completely different, when the capillaries are covered with Ag. In this case the angular distribution is as narrow as 1° HWHM, which is expected when no force acts on the ion within the capillaries.

The results are partially shown in Fig. 1. For PET foil tilted by 5° , the angular distribution of the Ne^{7+} is found to be relatively broad (FWHM of 6°) and the maximum is shifted by 5° . Similar results were obtained when the tilt angle was increased up to 20° . The results are completely different, when the capillaries are covered with Ag. In this case the angular distribution is as narrow as 1° HWHM, which is expected when no force acts on the ion within the capillaries.

Therefore, the PET results are highly unexpected. The observation that the angular distributions for PET has a peak equal to the tilt angle suggests a "guidance" of the Ne^{7+} ion within the capillary. This observation of

capillary guidance is surprising, since multiple scattering events are expected to change the charge state of the projectile, i.e. highly charged ions scattered by, e.g. 5° are neutralized when emerging from the surface [3]. The present finding of ion guidance provides evidence that the inner walls of the capillaries are charged in a self-supporting process and close collisions with the surface involving electron capture into the projectile are suppressed. Models will be discussed to describe the capillary guidance.

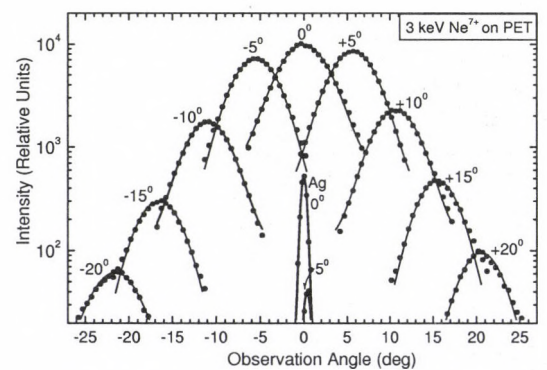


Figure 1. Angular distribution of Ne^{7+} ions transmitted through capillaries in PET. The foils were tilted by the angles as indicated in the figure. The solid lines represent Gaussian functions fitted to the data. The distinct peaks at 0° were obtained using capillaries covered with Ag. These silver data indicate that there is no guidance when the surface is conductive.

a) Hahn-Meitner-Institut Berlin GmbH, Glienickestr. 100, D-14109 Berlin, Germany, e-mail: stolterfoht@hmi.de

[1] N. Stolterfoht, J.H. Bremer, V. Hoffmann, D. Fink, A. Petrov, and B. Sulik, submitted for publication to Phys. Rev. Lett. (2001)

[2] Y. Yamazaki, Int. J. Mass Spec. **192** (1999) 437. and K. Tőkési *et al.*, Phys. Rev. **A61** (2000) 20901-1.

[3] W. Huang, H. Lebius, R. Schuch, M. Grether, N. Stolterfoht, Phys. Rev. **A58** (1998) 2962.

3.17 Electron emission in highly-charged ion collisions on Li surfaces

B. Sulik, J. Rangama^{a)}, J.-Y. Chesnel^{a)}, J.H. Bremer^{b)}, V. Hoffmann^{b)}, and N. Stolterfoht^{b)}

Electron emission following 4- and 30-keV Ne^{4+} ion impact on a Li surface was investigated. For Li, the valence band in the solid replaces the 2s atomic shell, while the 1s core remains essentially the same as for atomic Li. These changes lead to differences in the core excitation mechanisms, and may involve collective effects such as plasmon excitation [1].

To study these effects, first experiments were carried out using the ECR source at the Hahn-Meitner Institute, Berlin. The experiments were performed in a scattering chamber, where the pressure was 2×10^{-6} mbar. Thin lithium layers were build up, providing a solid Li target, by evaporating Li onto an aluminum substrate. The evaporation was maintained in order to renew the surface to a clean state. By refreshing the surface continuously, it was not necessary to operate in an ultra high vacuum environment.

With sufficiently fast renewal of the Li surface at 30 keV ion impact, the electron emission spectra exhibited a structure near 50 eV, due to Li K-Auger transitions following single excitation, demonstrating the feasibility of the present evaporation method that leads to rough but clean Li surfaces.

Fig. 1 shows a typical spectrum taken at lower projectile energies, where the Li K-Auger line intensity became smaller due to the decrease of the K-shell excitation cross section. Here, an intense Auger line has been observed near 22 eV [2], providing evidence for above-surface L-Auger electron emission from the Ne projectiles. Auger emission from Ne is a signature of electron capture in the incoming part of the projectile trajectory. Since Ne is much heavier than Li, the Ne beam is unexpected to be reflected at the Li surface. Thus, observation of Auger electrons from Ne indicates that the Ne projectiles capture electrons in an early stage of the collision so that their Auger decay takes place before they reach the surface.

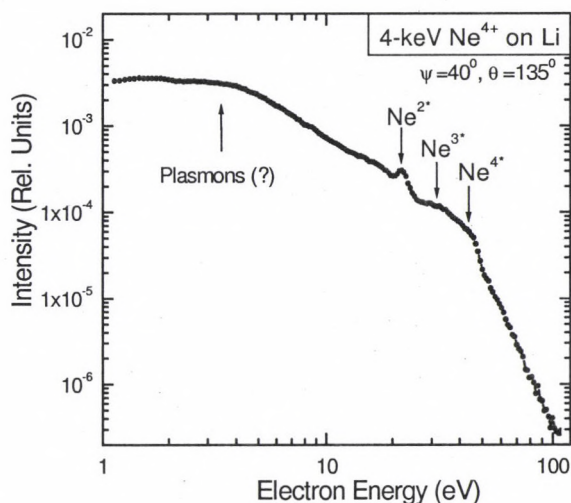


Figure 1. Electron spectrum from the impact of slow Ne^{4+} ions on Li. The distinct line at 22 eV originates from the doubly excited $1s^2 2s^2 2p^4 3s^2 \ ^1D$ state of neon atoms formed by a fourfold capture process along the incoming ion-path above the surface [2]. The strengths of that line at 40° incidence angle shows that the capture process start to take place at large distances from the surface. This can be related to the low value of the workfunction for Li (2.3 eV). The broader structures at higher energies belong to excited states with 3 or 4 L-shell vacancies [2].

Electron capture is also expected to be accompanied by plasmon excitation [1]. In the spectra, a structure near 6 eV might be attributed to plasmon creation. Experiments are under progress to confirm this interpretation.

Support: German-Hungarian ST Collaboration D17/99; French-German Cooperation Program PROCOPE (No. 02957RJ).

- a) CIRIL, Unit mixte CEA-CNRS-ISMRA-Univ. de Caen, 6 Bd Mar. Juin, F-14050 Caen, France
- b) Hahn-Meitner-Institut Berlin GmbH, Bereich Strukturforschung, D-14109 Berlin, Germany
- [1] D. Niemann, M. Grethér, M. Rösler, and N. Stolterfoht, Phys. Rev. Lett. **80** (2000) 3328.
- [2] N. Stolterfoht, J.H. Bremer, V. Hoffmann, M. Rösler, and R.A. Baragiola, Nucl. Instr. and Meth. **B182** (2001) 89.

4.1 Micro-RBS characterisation of the chemical composition and particulate deposition on Pulsed Laser Deposited $Si_{1-x}Ge_x$ thin films

A. Simon, Z. Kántor^{a)}

Formation and deposition of particulates upon Pulsed Laser Deposition (PLD) of $Si_{1-x}Ge_x$ semiconductor alloy thin films were investigated by Rutherford-backscattering spectrometry at the nuclear microprobe facility of ATOMKI.

Large-area AFM images showed that depending on the position approx. 10 to 20% of the substrate surface was covered by different kinds of particulates. However, there were droplet-free zones up to $25\mu\text{m}$ diameter distributed over the surface, thus by collecting point spectra with a 2MeV He^+ beam of $2\mu\text{m}^2$ size we were able to give the accurate quantitative elemental composition of the $Si_{1-x}Ge_x$ film and that of the particulates itself, separately. Elemental maps and tomographic images were generated for the identification of different kinds of particulates.

Regarding the mechanism of the deposition and solidification of the film in the PLD, one would expect that each droplet is enclosed between the two parts of the thin layers condensed before and after the deposition of the given droplet. However, such structures were not found *at all*, in any of the investigated ar-

reas. There is an absence of the PLD layer beneath the droplet. Furthermore, the evaluation of the micro-RBS spectra revealed that there is a distribution of the Ge elemental concentration in depth with a decreasing Ge fraction toward the surface.

A plausible explanation of the absence of the PLD layer beneath the droplet is that due to the high temperature of the arriving droplet, the existing film melted and mixed with the droplet material. As the substrate extracted heat from the molten material, solidification is set on first at the interface and gradually toward the free surface. Upon the movement of the solidification front, the germanium most likely moves towards the surface, resulting in a continuously increasing Ge content.

Further discussion on mechanisms, including elemental maps and tomographic images can be found in [1].

a) Research Group on Laser Physics of the Hungarian Academy of Sciences, Szeged, P.O.Box 406, H-6701, Szeged, Hungary.

[1] A. Simon, Z. Kántor, Nucl. Instr. and Meth B, in press

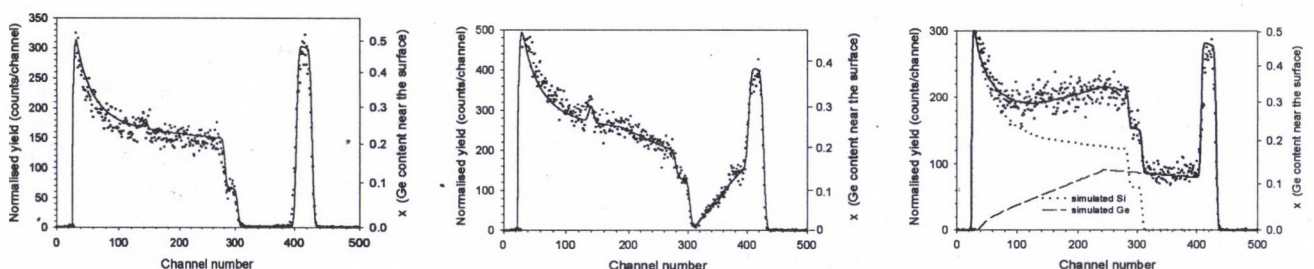


Figure 1. Micro-RBS spectra (dots: measured; lines: simulated) collected on particulate-free area (160 nm nominal film thickness), 640 nm and 2300 nm thick particulates, respectively.

4.2 Formation and Stability of Metastable Pd(Zr) Solid Solution Developed During Ball Milling and/or Heat-Treatment of Pd₃Zr

G.L. Katona^{a)}, M. Kis-Varga and D.L. Beke^{a)}

There are indications in the literature, that nanocrystallinity can lead to the stabilisation of a coexisting mixture of solid solution and ordered compound [1,2] instead of a homogeneous ordered equilibrium phase, or to the stabilisation of the homogeneous solid solution instead of a mixture of two equilibrium solid solutions [3].

Formation of nanocrystalline solid solution induced by ball milling and/or subsequent annealing of the Pd₃Zr intermetallic compound was studied. The single phase initial compound was milled in a medium energy vibrating mill under vacuum for various time periods. The structural characterization was made by X-ray diffraction with monochromatic CuK_{α1} radiation. The starting material showed the *hcp* equilibrium phase structure of the Ni₃Ti-type intermetallic compound with a preferred orientation of (004) lattice planes. 46 h milling led to nanocrystalline single phase Pd₃Zr with a mean crystallite size of 10-12 nm, which is in good agreement with the results of [1], obtained by milling with a SPEX 8000 shaker mill for 1 h in Ar atmosphere. The formation of Pd(Zr) solid solution during annealing was observed by X-ray diffraction. At higher temperatures the phase fraction of Pd(Zr) reached a maximum between 800 and 900 °C, then it decreased and finally the reflections of disordered phase disappeared from XRD spectrum at 1330 °C indicating the return to the single phase ordered state. The temperature range of the coexistence of the two phases is higher by 100-150 °C than that of published in [1]. We also observed that ball milling of Pd₃Zr for longer periods (up to 300 h) resulted in single phase nanocrystalline Pd(Zr) solid solution, with a grain size of 8 nm and with a Zr

molar fraction of 0.21. Annealing of these samples most of the intermetallics transformed to solid solution with moderate grain coarsening. The crystallite size increased from 8 nm to 20-80 nm and the disordered state proved to be stable even at high temperatures.

In accordance with [1], the behaviour of the shortest milled sample can be explained by nanocrystalline character of the material and by the segregation of Zr at grain boundaries. By longer milling we were able to transform the compound to single phase nanocrystalline solid solution which proved to be very stable against annealing. This is in contrast with the statement of [1], i.e. the Pd₃Zr can not be disordered by ball milling. Our results however coincide with the conclusions of the authors of [4], who observed the formation of solid solution induced by ball milling of many ordered alloys. It can be concluded that the nanocrystalline character and the grain boundary segregation plays important role in the phase transformation induced by ball milling and/or subsequent heat-treatment of Pd₃Zr, but the oxidation/contamination may also have an influence on the process by stabilising the phases and changing their compositions.

a) Department of Solid State Physics, University of Debrecen, Hungary

- [1] J. Weissmüller, H. Ehrhardt, Phys. Rev. Lett. **81**, 1114 (1998).
- [2] Cs. Cserhádi, H. Bakker, D.L. Beke, Surface Science **290**, 345 (1993).
- [3] D.L. Beke, Z. Erdélyi, P. Bakos, Cs. Cserhádi, I.A. Szabó, Proc. of International Conference on Solid-Solid Phase Transformations '99 (JIMIC-3), Kyoto pp. 1293 (1999).
- [4] H. Bakker, G.F. Zhou, H. Yang, Prog. Mater. Sci. **39**, 159 (1995).

4.3 Non-linearity of diffusion in amorphous Si-Ge multilayers

A. Csik, D.L. Beke^{a)}, G.A. Langer^{a)}, Z. Erdélyi^{a)}, L. Daróczi^{a)}, K. Kapta^{a)}, M. Kis-Varga

Multilayers and superlattices are of considerable industrial interest because of their specific properties and many promising areas of application in microelectronics or optics [1,2]. However, the multilayers as compositionally modulated materials are not equilibrium structures. Thus the knowledge of interdiffusion mechanisms is highly desired for understanding the physical properties of these materials, especially for the amorphous semiconductors.

For the understanding of the mechanism of diffusion in amorphous semiconductors a considerable number of factors must be controlled and taken into account [3]. First of all the diffusion asymmetry and non-linearity (manifested in the strong concentration dependence of the interdiffusion coefficients) [4], the significant pore formation during the diffusional mixing [5], stresses, which are known to affect interdiffusion in crystals, may become more significant in the course of the interdiffusion. The diffusional effects in Si-Ge system were theoretically studied by Beke and his co-workers [4] using finite element calculations. It was shown, that - due to the strong concentration dependence of D - the initially sharp interface does not flatten but shifts, consuming the Si layer and with increasing Si content the process of intermixing slows down at longer time. This strong concentration dependence leads to a significant initial curvature on the $\ln(I/I_0)$ vs. t curve, as well (I/I_0 is the normalized height of the first order small angle X-ray diffraction peak, t is the time).

In accordance with theoretical results detailed experimental measurements were carried out and it was shown by Auger depth profiling technique [6] that the concentration profile at the initially sharp Si/Ge interface in

amorphous Si/Ge multilayers shifted but remained still sharp after a heat treatment at 680 K for 100 hours. At the same time the fast diffusion of Si resulted in the formation of an almost homogeneous Ge(Si) amorphous solution, while there was practically no diffusion of Ge into Si layer. Similar results could be obtained from the Rutherford backscattering measurements [7], from which the change of the concentration of Ge at the center of the originally pure Ge layer can be determined. By the use of small angle X-ray diffraction technique, the concentration dependence of the interdiffusion coefficient in Si-Ge multilayers has been evaluated. It has been found that the interdiffusion coefficient is expressible in the Arrhenius form with the preexponential term $D(0)=1.3 \cdot 10^{-16} \text{m}^2 \text{s}^{-1}$ and $D(0.25)=7.9 \cdot 10^{-7} \text{m}^2 \text{s}^{-1}$ at 0 and 0.25 at% Si. The activation energy at 0 and 0.25 at% Si are $1.0 \pm 0.2 \text{ eV}$ and $2.3 \pm 0.7 \text{ eV}$, respectively.

a) Department of Solid State Physics, University of Debrecen, Hungary

- [1] Multicomponent and multilayered Thin Films for Advanced Microtechnologies: Techniques, Fundamentals and Devices, Vol.234, ed. O. Auciello and J. Engemann, NATO ASI Series 1989.
- [2] A. Fert, Mater. Sci. Forum **59/60** (1990) 439.
- [3] S.M. Prokes and F. Spaepen, Appl. Phys. Lett. **47** (1985) 234.
- [4] D.L. Beke, P. Nemes, Z. Erdélyi, I.A. Szabó and G.A. Langer, Proc. of MRS Spring Meeting, San Francisco, USA, 99 (1998) 528.
- [5] L. Daróczi, D.L. Beke, G. Langer, Gy. Radnóczy and Zs. Czigány, J. Magn. Magn. Mat. **156** (1996) 417.
- [6] A. Csik, G.A. Langer, D.L. Beke, Z. Erdélyi, M. Menyhárd and A. Sulyok, J. Appl. Phys. **89** (2001) 804.
- [7] A. Simon, A. Csik, F. Pászti, A.Z. Kiss, D.L. Beke, L. Daróczi, Z. Erdélyi, G.A. Langer, Nucl. Inst. and Meth. **B161-163** (2000) 472-476.

4.4 Magnetic relaxation and disordered magnetic phase in partially oxidized bulk nanocrystalline iron

L. Kerekes, J. Hakl, S. Mészáros, K. Vad, P. Gurin, M. Kis-Varga, I. Uzonyi, S. Szabó^{a)}, D.L. Beke^{a)}

Vibration ball milled nanocrystalline iron powder with 20 nm and 30 nm average grain size has been prepared using pure Fe powder (99.95% purity) under 1 bar helium gas atmosphere (sample A) and under 10^{-6} mbar vacuum (sample B). After preparation the samples were aged on air.

The comparison of XRD, PIGE and PIXE results showed, that atmospheric oxygen has penetrated in substantial amounts into the interfacial layers of the milled samples with memory effect to the milling conditions.

Low field magnetization measurements revealed a clear breaking point in the zero-field-cooled (ZFC) magnetization at about $T_{br} = 42$ K. For sample with lower oxygen content the step in derivative is much pronounced, than for sample A. In a wide temperature range around T_{br} the ZFC magnetization curves can be well fitted with two, $M_a - M_b \exp(-\alpha T)$ type exponentially saturating functions (see Fig. 1.).

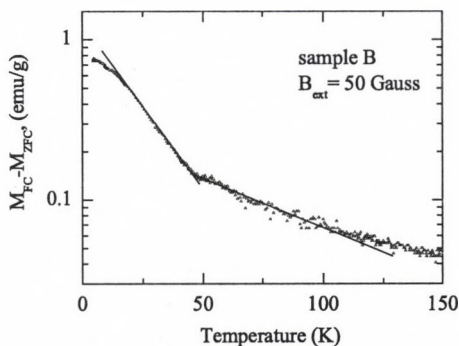


Figure 1. The difference of field-cooled and zero-field-cooled magnetizations at 50 Gauss external magnetic field for sample B. The lines are to guide the eyes.

At 5 T field the temperature dependence of the magnetization fits the Bloch's $T^{3/2}$ law. The fitted value of Bloch's constant is $8 \times 10^{-6} \text{ K}^{-3/2}$, which is 2.4 times larger than the temperature coefficient of bulk Fe.

The time dependence of magnetization after a sudden field step at a given temperature showed logarithmic character. The measurements indicate magnetically frozen, partially disordered state with a low field linear regime, where the relaxation rate is independent of the starting field and depends only on the field step (see Fig. 2.).

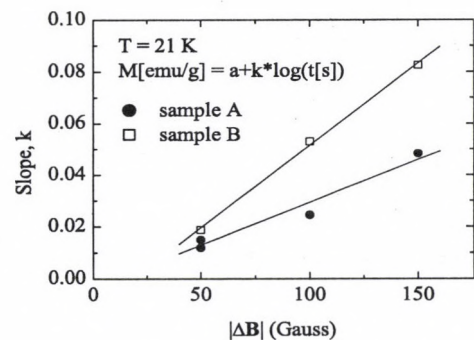


Figure 2. The dependence of k coefficient on the external magnetic field step.

The relaxation and exponential type $M(T)$ curves at low fields and $T^{3/2}$ scaled magnetization at high fields show the presence of blocked ferromagnetism, explained by an exchange interaction, which is mediated by interfacial oxides of the sample.

a) Department of Solid State Physics, Debrecen University, H-4010 Debrecen, P.O.B. 2, Hungary

4.5 Friction force of the highly charged ions at large distances from the metal surfaces

K. Tórkési, X-M. Tong^{a)}, and J. Burgdörfer^{b)}

We have studied the dissipative component of the force acting on the moving highly charged ions in front of the solid surface. When a charged particle (ion) travels along the surface, the electrons in the surface and the bulk will be polarized and build up induced charge density. This induced charge density can be visualized as image charge. The image charge is located inside the solid at the same distance from the surface as the ion but with opposite sign. Therefore, the interaction between the charged particle and its image charge is attractive and the particle will accelerate towards to surface. When the charged particle is moving with finite velocity \vec{v} , the induced charge density will lag behind the ion leading to an additional force in the direction opposite to that of the ion velocity. This force is the so-called friction force (stopping power) which is responsible for the energy loss of the charged particle.

During the last 80 years continuous interest manifest for studies of stopping power of atoms, molecules and solids by numerous projectiles. The works have been inspired because the accurate knowledge of the interaction between charged particle and matter has considerable importance in many different areas of research and technology such as, for example, surface diagnostics and spectroscopy.

In order to study the energy loss of charged particles in distant collisions it is required to know the asymptotic form of the stopping power. In many applications of ion-surface scattering a simplified classical dielectric response picture, the so called "specular reflection model (SRM)" is very powerful tool. But, the crude description of the induced charge density within this approach fails to account the realistic potential distribution in the vicinity of the surface. The time dependent density functional theory (TDDFT), however provide an accurate model. So far the analysis of stopping power at large distances by TDDFT is not

available, therefore we have performed calculations for the first time. The comparison between our TDDFT and SRM calculations are shown in Fig. 1, where the Fig. 1a displays the distance-dependent stopping power due to the plasmon excitations and Fig. 1b displays it due to the particle-hole excitations. The distance dependences are similar for SRM and TDDFT and are given by c_{pl}/d^3 for plasmon excitation and c_{p-h}/d^4 for particle-hole excitation but the coefficients (c_{pl}, c_{p-h}) are significantly larger for TDDFT.

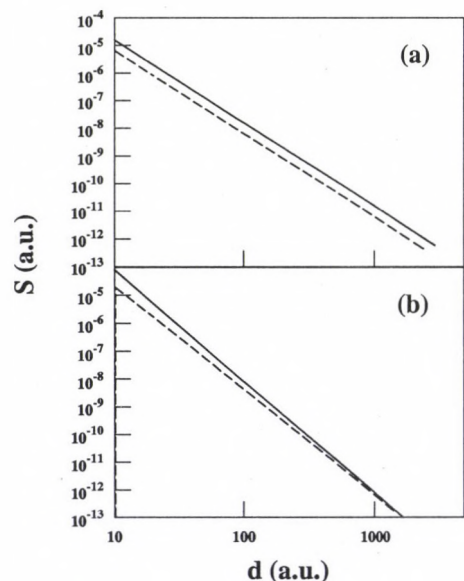


Figure 1. Distance-dependent stopping power due to the plasmon (a) and particle-hole excitation (b) for a proton moving in a parallel trajectory with velocity $v=0.29$ a.u. in front of an Al surface. Solid line: TDDFT, dashed line: SRM.

This work is supported by FWF, OTKA No. T032306, the grant "Magyary", and the "Stiftung Aktion Österreich-Ungarn" (45öu6).

a) Department of Physics, Kansas State University, Manhattan, USA

b) Institute for Theoretical Physics, Vienna University of Technology, Austria.

5.1 Geological and Biomedical Applications of Ion Beam Analysis Techniques

Z. Elekes, G.Á. Sziki, I. Uzonyi, A. Simon, P. Rózsa^{a)}, J. Simulák^{a)}, Gy. Szöör^{a)}, Á.Z. Kiss

Different types of magnetic spherules with various geological locations in the Carpathian Basin were studied in our earlier work [1] and recently revealed the signs of a meteoritic impact event in SW-Hungary [2] using micro-PIXE technique. The light components of the samples are usually measured worldwide by charged particle detection via deuteron induced reactions. Nevertheless, we previously demonstrated that gamma-ray detection could be also efficient in the quantitative analysis of carbon, nitrogen and oxygen [3].

In the current study [4] we measured the excitation function of the reaction $^{12}\text{C}(d,p\gamma)^{13}\text{C}$ in the bombarding energy of 1.4 – 1.9 MeV. In conclusion we could state that for analytical purposes 1.8 MeV can be suggested when thick targets are measured. The recommended energy for thin targets was found to be 1.792 MeV. The resonance at 1.4495 MeV can be used for depth profiling in specific cases.

By the measurement of standard samples it was pointed out that deuteron induced gamma-ray technique can provide quantitative data on carbon and oxygen contents with an accuracy of 10 % and minimum detection limits of 90 and 70 $\mu\text{g/g}$ respectively.

Moreover, our studies suggested that accurate determination of iron-oxide phases and carbon content of metallic spherules and/or other impact materials could serve as an efficient tool for the identification and clarification of their genesis (Figure 1).

The nitrogen constituent of materials plays relevant role in many fields of science and technology. For example, it is significant to the determination of the organic fingerprint in rock samples and more widely the behaviour of nitrogen contributes to diagenetic and metamorphic processes. Because nitrogen is an essential element in all living matter, its determination

in biomedical samples is of basic importance.

In our second systematic study of the experimental conditions affecting the minimum detection limit attainable by Deuteron Induced Gamma-Ray Emission (DIGE) method in the case of nitrogen determination in carbon matrix was carried out. As a result, an optimal experimental set-up was realized with the use of plate glass linings of the transport tube and chamber close to the target and using copper diaphragms for shaping the beam. The necessity of the reduction of electronic pile-up and the cosmic background is also discussed in our recent paper [5]. The best detection limit obtained was 130 $\mu\text{g/g}$.

a) Department of Mineralogy and Geology, University of Debrecen, Debrecen, Hungary

[1] I. Rajta *et al.*, Nucl. Instr. and Meth. **B118** (1996) 437.

[2] Gy. Szöör *et al.*, Nucl. Instr. and Meth. **B181** (2001) 557.

[3] Z. Elekes *et al.*, Nucl. Instr. and Meth. **B168** (2000) 305.

[4] Z. Elekes *et al.*, Nucl. Instr. and Meth. B (in press)

[5] G.Á. Sziki *et al.*, Nucl. Instr. and Meth. B (in press)

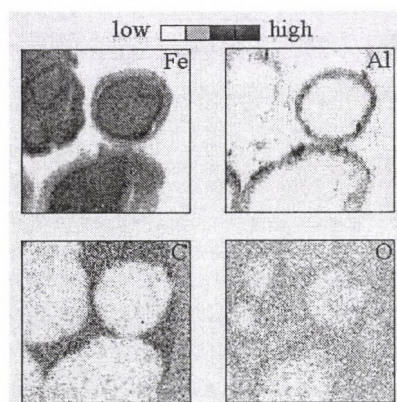


Figure 1. Fe, Al (PIXE), C and O maps (DIGE) taken on Arizona metallic spherules (scan size: $1000 \times 1000 \mu\text{m}^2$)

5.2 Radon exhalation of limestone bedrock and cave deposits

Z. Dezső^{a)}, J. Hakl, L. Molnár^{b)}

Sources of airborne radon have been investigated *in situ* in the Baradla-cave (Aggtelek karst, NE Hungary) using active radon detection technique.

The exhalation of radon from clay deposits as well as from limestone bedrock was measured in several *in situ* experiments using specially designed exhalation chambers. The obtained radon time series have been fitted to model calculations which were based on simple theoretical considerations on radon diffusion.

The result show that under normal climatic conditions in caves, the effective diffusion length of radon in clay is large enough to play a significant role in feeding the cave atmosphere with radon gas. This is further enhanced by the relatively high radium-226 concentration and extremely small grain size of clay minerals resulting in emanation power of

44 %. Limestone, in turn showed very weak emanation power, 2.5 %, which, together with its low radium content, resulted in two orders of magnitude less exhalation rate compared to clay.

These results provide a clear evidence that the source of radon in karstic caves is clay deposit.

The support of OTKA 023181, MKM 0146/1999 and Karst and Cave Foundation is highly acknowledged.

- a) Department of Environmental Physics, University of Debrecen - Institute of Nuclear Research of the Hungarian Academy of Sciences, 4001 Debrecen Pf. 51.
- b) Regional laboratory of HBM ÁEÉÁ, 4002 Debrecen Pf. 137.

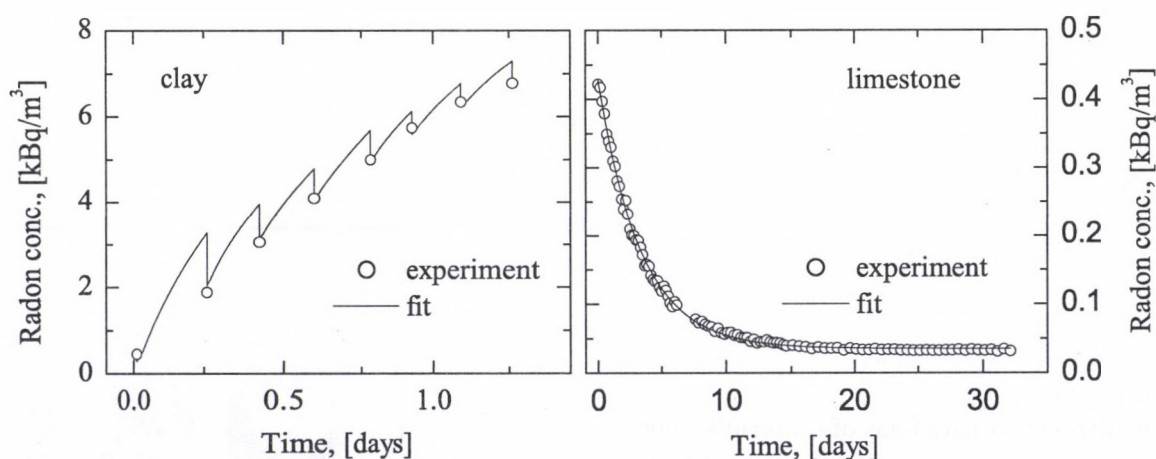


Figure 1. *Left:* The exhalation of radon from clay deposit increases radon concentration under the accumulation hemisphere. The data characterizing the subsoil radon transport can be extracted from the numerical fit. The fit beside saturating part reflects periodical dilution caused by the grab sampling mode of the detection. *Right:* The exhalation from a limestone sample measured in continuous mode in a closed accumulation vessel sealed *in situ* at the beginning of the experiment. The decreasing tale of radon time series reflects insufficient emanation power of limestone to feed the exhalation vessel with radon.

5.3 Representative indoor radon survey in Gyergyóremete, Romania

I. Csige and S. Csegzi^{a)}

The primary goal of the Gyergyóremete radon programme was to pilot a representative indoor radon survey in Romania, that can be done in other places of the country. The 1992 census counted 2406 houses and 6550 residents in the village. Almost all houses are single floor wooden made houses without cellar. Representativity of the sample was ensured by random pull of 120 houses from the stock (hypergeometric statistical model). Etched track type radon detectors [1] (Radamon) were used to measure long time average ^{222}Rn concentration. Measurements were done in sleeping rooms at pillow level.

The detectors were distributed and collected by 10 to 14-years-old children of the local primary school with the help of some of their teachers. The children's group (called Rutherford Group) was divided into subgroups with three or four children in a subgroup. Each subgroup was responsible for 12 houses. In afternoon courses the children were trained on the very basics of the radon phenomena. The public was also informed about the planned survey through the local media (cable television and newspaper). Before the distribution of the detectors the children visited all the selected houses to check readiness of the residents to accept the detectors. Then the distribution, and later on the collection, of the detectors could be done almost in single day campaigns.

Exposure lasted from January to July 1999. The half year exposure time was chosen to reduce the number of lost detectors (known to increase linearly with exposure time), and to keep participating childrens and publics interest alive (likely to fall exponentially with exposure time). The starting and ending dates of the exposure period were selected to minimize biasing effect of seasonal variation of radon in homes. At the end 115 samples could be collected and were evaluated.

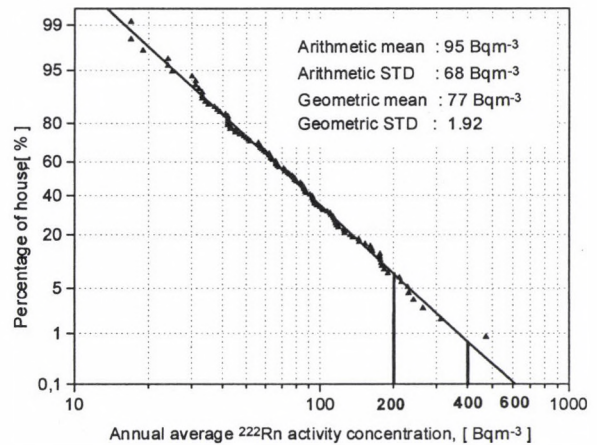


Figure 1. Complementary (downwards) cumulative distribution of annual average ^{222}Rn activity concentration measured in a representative (random pull) sample of the Gyergyóremete housing stock. The solid line is the lognormal distribution fit to the experimental data.

Figure 1 summarizes the results of our survey. We have found that the distribution of indoor ^{222}Rn activity concentration can be very well fitted with lognormal distribution. The correlation coefficient of linear fitting on linearized scales was $k = -0.9980$. The arithmetic mean (95 Bq m^{-3}) and the distribution together suggests that, though ^{222}Rn in Gyergyóremete's houses may have been significantly higher than estimated world average (about 40 Bq m^{-3}), but still, the area should not be classified as a radon prone area. The percentages of houses expected to have annual average ^{222}Rn activity concentration higher than 400 Bq m^{-3} is less than 1 %, and of those higher than 600 Bq m^{-3} can be estimated to be around 0.1 %.

OTKA T-029306 supported this work.

a) Str. Cornesti nr. 68/A, 4300 Tirgu Mures, Romania
[1] I. Csige and S. Csegzi, Radiation Measurements
34(1-6) (2001) 437-440.

5.4 The origin of water in the vicinity of Püspökszilágy RWTDS

M. Molnár, Zs. Szántó, I. Futó L. Palcsu, É. Svingor

The Püspökszilágy Radioactive Waste Treatment and Disposal Site (RWTDS) is located about 30 km NE of Budapest on the top of a hill between Némedi and Szilágyi streams, near two villages, Püspökszilágy and Kisnémedi (Fig. 1).

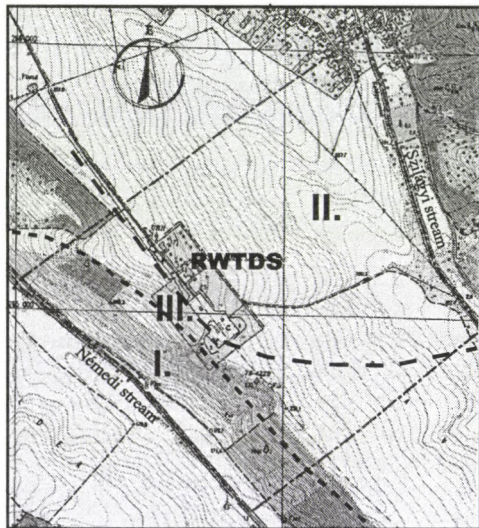


Figure 1. The location of Püspökszilágy RWTDS

Within the framework of the safety assessment program for the Püspökszilágy site, water quality and stable isotope investigations were carried out. The aim of this investigation was to get information about the origin of water, the mixing of water bodies and the influence of recharge.

There was a large range in the ages calculated from the ^{14}C content of the waters. On the Némedi side of the hill (steep slope, I. in Fig. 1, the groundwater appears to be old, while on the top and on the Szilágyi side of the hill (gentle slope, II. in Fig. 1, young virtual ages are dominant. The question is that this difference reflects different origins or different mixing rates of the two water bodies.

Correlations can be seen between the radiocarbon content, water chemistry, stable isotope and tritium data. The water in wells with low ^{14}C

concentration contains large amount of sulphate, HCO_3 , Mg, and their conductivity is high. The negative $\delta^{34}\text{S}$ values of the sulphate in these wells can be explained by their old age as well. These wells are on the Némedi side of the hill (region I.). The wells on the top and on the Szilágyi side of the hill are characterized by higher ^{14}C concentrations, smaller amounts of sulphate, HCO_3 , Mg, low conductivity and positive $\delta^{34}\text{S}$ values. The differences suggest different origins for the two water bodies.

The calculated ^{14}C ages of water in region I. are more than 8000 years. The averages of the measured tritium concentrations in these wells are 1-2 TU. This is too high for such old waters therefore we can not exclude the presence of a small amount of modern water. This means that the closed-system condition has not been fulfilled, and the calculated 'ages' can be interpreted as an upper limit (youngest value) for the water age.

The 'age' of the water in several wells on the Némedi side of the hill near the ridge (region III.) is about 5500 years, the water chemistry data show a transition from the old water body to the younger one. The tritium content was constant and less than 1 TU. This water likely comes from a mixture of the old and young water and the recharge is probably very limited.

The water level in the wells on the top of the hill (around the repository) is very deep: 20 - 26 m below the surface. The water in these wells has low conductivity and their tritium content varies in a wide range. Some of these wells contain little water and have long refilling time. In these wells, the radiocarbon concentration was large more than 80 pMC. A possible explanation may be the following: During the construction of the facility, a large amount of fresh precipitation might have infiltrated to the deep soil. Taking into consideration the poor hydraulic conductivity and the low porosity of the bedrock, we can expect restricted mixing and dilution. As a result, the infiltrated water remained under the repository.

5.5 Excess tritium in observation wells around Püspökszilágy RWTDS

L. Palcsu, Zs. Szántó

Tritium activity of water samples taken from the streams and observation wells around Püspökszilágy Radioactive Waste Treatment and Disposal Site (RWTDS) was measured quaternary during the period of July 1999 - December 2000. In most of the wells the tritium concentration in the water was less than 2 TU (TU= tritium unit, which is defined as 1 tritium atom per 10^{18} atoms of hydrogen, which corresponds to 0.118 Bq/l water). In wells with water level 3-5 m below the surface, the tritium concentrations were changed between 3 - 6 TU. Taking into account that the average of tritium concentration measured in the streams was 7-8 TU, the amount of tritium measured in these wells was typical of shallow groundwaters. All of the wells discussed above showed only small fluctuations in their tritium concentration during the measurement period.

In 4 wells the tritium concentration exceeded the tritium activity of present-day surface waters. The water in three of them showed only a small tritium excess and a small fluctuation in its tritium content could be observed during the monitoring period.

We compared our findings to the average of the tritium content of the wells measured by VITUKI in 1991-1993 [1]. The first columns in Fig. 1 show the values measured by VITUKI. The second columns show the tritium content of the wells expected in 2000, calculated from the tritium decay without additional (external) tritium and accepted the values measured by VITUKI as initial activities. The last columns represent the average of the tritium content measured in 1999-2000.

The small tritium excesses in wells Psz-29 and Psz-69 may be of atmospheric origin (shallow water level, the tritium concentration less than in surface water). Excess tritium can be observed in wells C, Psz-54, Psz-11 and Psz-63.

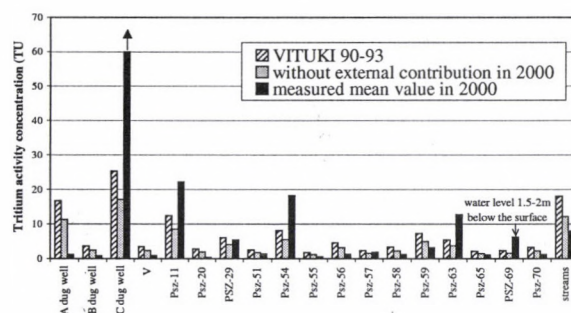


Figure 2. Comparison of the tritium concentration measured in 1990-1993, values calculated for 2000 and values measured in 2000

The highest tritium activity, 2400 TU (cc. 280 Bq/l) was detected in C dug well at the top of the hill. During the sampling period a continuous growing of tritium activity could be observed in it with a maximum in December 2000. The tritium content of the water in this well was measured every second week in 2001 (Fig. 2). The tritium content decreased at a level of 50 Bq/l by September then it remained constant. This amount of tritium is cc. ten times more than it was in this well in 1999 and 50 times more than the tritium content of the surface water (streams) near the repository.

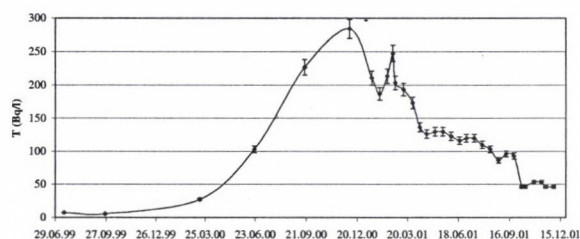


Figure 2. Tritium content of the water in C well measured in 1999-2001

[1] VITUKI, 1993. Püspökszilágyi RHFT Kutatási Program. Izotóphidrológiai Vizsgálatok

5.6 Modeling of the groundwater movement at Püspökszilágy RWTDS

É. Svingor, Zs. Szántó, M. Molnár, L. Palcsu, I. Futó

The Püspökszilágy Radioactive Waste Treatment and Disposal Site (RWTDS) has been in use since 1976 and it was intended to serve labs, industry and hospitals but as there is no disposal site for the Paks NPP its L/ILW has also gone to this site. The RWTDS of Püspökszilágy has got an interim operational licence, on condition that a safety assessment has to be completed.

For the safety assessment it is essential to determine the main pathways by which radionuclides from the facility may migrate to the environment. The groundwater pathway is one of the most important routes. In a complex system, it is not always possible to identify all of the routes by which radionuclides might be transported in groundwater from the facility to the surface. Hydrogeological modelling can help to identify these paths, usually applying a pathline approach in which particles are released from the facility and tracked through the model.

A hydrogeological model was constructed by MODFLOW, a finite-difference groundwater flow and transport code. The constructed model consists of 3 main layers: top soil, Pleistocene sandy-clayey layer, Oligocene clay. The surface of the layers was constructed from borehole logs. The Pleistocene layer was divided into 3 sublayers on the basis of geophysical measurements. The hydraulic conductivity changes within the layers, sand and gravel lenses as well as clay lenses were inserted on the basis of borehole logs.

Constant head boundaries were defined at the northern and southern part of the modelled area. The Szilágyi and Némedi streams form the eastern and western boundaries.

The detailed description of the model can be found in [1]. The near-site relief map of the repository can be seen in [2] in Fig. 1.

The key features of the groundwater flow field at the site by the calibrated model are the following:

- In the vicinity of the repository, the groundwater divide is not in the centre of the ridge, it is displaced towards the Némedi side (region III. in [2]).
- The water table on the Némedi side (region I. and III. in [2]) is generally located in the Oligocene layer.
- The water table on the Szilágyi side and the top of the ridge (region II. in [2]) is located in the upper and middle Pleistocene sublayers.
- Clayey rocks dominate along the ridge, almost continuous sand and gravel should be supposed along the hill side toward the Szilágyi stream (abandoned stream bed).
- The recharge is only 2-7% of the mean yearly precipitation.
- The streams have strong influence on the water level.
- The majority of the groundwater flows toward the Szilágyi stream in the upper and middle Pleistocene sublayers. The travel time is about 300 years in this direction. There is a very limited discharge to the Némedi stream in the Oligocene layer with a travel time of several thousand years.
- No discharge was found in the small valley between the site and Püspökszilágy village.

[1] A Püspökszilágyi Radioaktív Hulladék Feldolgozó és Tároló biztonsági elemzéséhez szükséges vizsgálatok elvégzése. No. P400V-4-06/99 Földtani kutatási zárójelentés, IV. kötet, 12. fejezet: Vízmozgás, ill. tríciumtranszport modellezések. ATOMKI, 2001.

[2] M. Molnár *et al.*, in this issue

5.7 Isotopic analysis of Hungarian thermal waters

Zs. Szántó, É. Svingor, I. Futó, L. Palcsu, M. Molnár

As a result of the agreement between the Ministry of Environmental Protection (KÖM) and The Geological Institute of Hungary (MÁFI) the Laboratory of Environmental Studies (KAL) was invited to take part in an extended survey of the present condition of Hungarian groundwaters with special emphasis on baseline condition of thermal waters.

The main goal of the two-years project was the estimation of the environmental impact of contaminated water originating from hydrocarbon mining activity on groundwater from specially designated areas. The main task of the work was a qualitative and quantitative analysis of micro and macro components present in the thermal water.

The Laboratory of Environmental Studies performed stable isotope analysis, tritium and noble gas measurements. Stable isotope ratios (δD , $\delta^{18}O$, $\delta^{15}N$, $\delta^{34}S$, $\delta^{13}C$) were measured by a mass spectrometer developed in the Institute. Low-level tritium concentrations were measured using the 3H - 3He method, He, Ne, Ar, Kr and Xe concentrations were determined using VG 5400 noble gas mass spectrometer. In some cases a qualitative and quantitative analysis of the gas components was made a Balzers Omnistar type quadruple spectrometer in order to detect and interpret the different processes that occurred during the formation of

thermal waters.

Even if these measurements cannot directly prove the presence or absence of artificially introduced components into the water body (components like methanol or glycol), but they could give us a hint about the mechanisms governing the water-rock interactions and might explain the differences observed between the content of the thermal waters situated in different regions of the country.

In most of the cases correlation between temperature and depth versus stable isotope ratio and tritium content was found and results were in accordance with the theoretical calculation.

In some cases isotope fractionation processes, bacterial sulphate reduction or surface water infiltration was detected.

The results of the work have been summarized [1] and constitute the main part of a complex hydrological database of the surveyed areas. The compilation will be distributed on CD during the next year and will represent a valuable tool for the scientists dealing with hydrological and hydrogeological modelling.

- [1] Termálvizek izotópanalitikai vizsgálata, Kutatási jelentés, Szerződésszm: 27266005, (2001) 20.

5.8 ^{226}Ra in bottled mineral waters of Hungary

E. Baradács^{a)}, Z. Dezső^{a)}, I. Hunyadi

More than two third of Hungary's territory hide huge amount of high temperature artesian and karstic waters in the depth. This phenomenon is a result of two favourable geological component jointly present in the Carpathian Basin. One is that in the Triassic period some thousand metres thick carbonate deposit (successive layers of limestone and dolomite) was formed in the region. In the subsequent periods of the historical geology the earlier deposit karstified, was covered by layers of clay, marl, sand and sandstone, and due to tectonic movements overthrust, lateral displacements, uplift and subsidence of huge carbonate blocks occurred. The other favourable component is the anomalous geothermal gradient of Hungary, which is 15-18 m/°C (50-70 °C/km). This is extremely high even by international comparison, the continental average is 33 m/°C (30 °C/km). The higher water temperature causes a greater quantity of mineral matter to be dissolved, with the result that waters with high levels of minerals and mineral salts are particularly beneficial for health.

Hungarian thermal waters have been used on a large scale for bathing, drinking and medical purposes since centuries, while the consumption of bottled mineral waters is steeply increasing recently. Today, there are nearly 80 wells and springs producing certified natural mineral waters in Hungary, and the water of 21 of these is bottled commercially.

In this work ^{226}Ra content of some commercially available bottled mineral waters, originat-

ing from different regions of Hungary, was studied by etched track detector method developed in the Radon Group of the Institute of Nuclear Research [1] and by destructive gamma-spectrometric method developed in the University of Debrecen by Z. Dezső.

The majority of the studied bottled mineral waters have moderate ^{226}Ra activity concentration, as can be seen in Table 1 (next page). According to the aquifers the radium content of the studied waters can be arranged roughly in two groups. It can be seen that mineral waters, which arise from Triassic dolomite and limestone, have higher radium content than those waters, which originate from Upper Pannonian sediment. The highest value exceeded 2 kBq m⁻³ in the case of the Apenta mineral water, which is a popular brand in Hungary, as well as in Europe and North America. The German owned company which bottle and sell Apenta has lately introduced a radium removal process to avoid consumers from increased health risk due to consumption of this water. The comparison of the applied methods showed good agreement for ^{226}Ra determination in mineral waters.

Acknowledgements This work was supported by OTKA Contract T022985 and T029306.

a) Department of Environmental Physics, University of Debrecen-Atomki, H-4001 Debrecen, POB. 51.

[1] I. Hunyadi *et al.*, *Radiat. Meas.* **31** (1999) 301-306.

Table 1. ^{226}Ra activity concentration [Bqm^{-3}] of Hungarian bottled mineral waters by different analytical methods

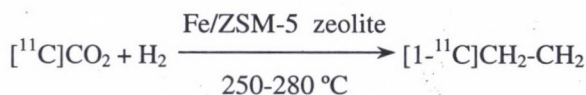
Brand name	Aquifer	^{226}Ra by SSNTD	^{226}Ra by gamma
Bonaqua	-	5±2	-
Szentkirályi ásványvíz	Upper Pannonian	7±2	13
Aqua, Spring water of Mátra Mtn	-	8±2	-
Mineralis 305	-	8±2	-
Parádi Ásványvíz	Upper Pannonian Upper Oligocene	10±2	27
Pannon Aqua	Upper Pannonian	12±2	13
Borsodi ásványvíz	-	19±3	-
Balfi Ásványvíz	Miocene, Badenian stage limestone	-	85
Theodora Quelle	Lower Triassic, Limestone	64±7	77
Óbudai Gyémánt	Upper Triassic, Limestone	111±11	110
Visegrádi Ásványvíz	Upper Triassic Dolomite	186±18	204
Margitszigeti Kristályvíz	Upper Eocene Limestone	451±42	518
Gellérthegyi Kristályvíz	Upper Triassic, Dolomite	1135±104	704
Apenta			
sparkling		2865±264	2780
still	Upper Triassic	-	2770
gently carbonated	clastic dolomite	2911±268	2890
tonic		-	2450

6.1 Reduction of [^{11}C]carbon dioxide to [^{11}C]olefin over zeolite catalyst by hydrogenation

É. Sarkadi-Pribóczki, Z. Kovács

The zeolites are effective catalysts for partial oxidation of hydrocarbons in the presence of oxidants and even for reduction of carbon dioxide in the presence of reductant. In our earlier experiments Fe/ZSM-5 zeolite was used for partial oxidation of [^{11}C]methane to [^{11}C]methanol [1]. Currently Fe/ZSM-5 zeolite catalyst is applied for reduction of [^{11}C]carbon dioxide by H_2 reductant to [^{11}C]ethene. The method is known only for ^{14}C -labelled or inactive compounds [2]. In this work no-carrier added ^{11}C -labelled carbon compounds were used therefore it was not necessary to correct the radiochemical yield of products for natural carbon impurities and the radio-method sensitive was enough to detect already few millimoles of carbon compounds. The [^{11}C]ethene product may serve as new and useful precursor for synthesis of PET-radiopharmaceuticals but until now the [^{11}C]ethene was produced only by long chemical processes [3]. We suggest here a simple catalysis method to form [^{11}C]ethene using zeolite and H_2 reductant.

The Fe/ZSM-5 zeolite was prepared [4] and conditioned in a stainless steel tube before the radioactive experiment. The [^{11}C]carbon dioxide was produced in N_2 gas target containing 1% O_2 by $^{14}\text{N}(\text{p},\alpha)^{11}\text{C}$ reaction. The [^{11}C]carbon dioxide was effectively trapped on the catalyst and the catalyst was flushed and fed by H_2 gas. The catalyst tube was closed and heated to 250-280 °C and kept for 10 min.



After reaction the radio-gas products were analysed by radio-gas chromatography (Molecular Sieve 5A column, TCD- and scintillation detector). In virtue of first experiments [^{11}C]ethene (EOB radiochemical yield 20-40%) and unchanged $^{11}\text{CO}_2$ were detected. The radiochemical yields of reactions at different temperatures of the iron-zeolite catalyst were as follow: [^{11}C]ethene was not detected at 190 °C, 20% was measured at 250 °C and 40% at 280 °C.

In summary the radiochemical yield mainly depends on the condition- and regeneration ways of iron-zeolite catalyst. Our aim is to optimize the parameters of experiments for higher radiochemical yield and also to determine further radiochemical intermediers ([^{11}C]methanol, [^{11}C]dimethylether or [^{11}C]ethane and others) by other analysis method what may form at lower temperature (200-150-100 °C), analogously to inactive experiments known.

This work was financially supported by the Hungarian Scientific Research Fund No. T031764. Fe/ZSM-5 zeolite was prepared by Applied Chemistry Department of Szeged University, Hungary.

- [1] É. Sarkadi-Pribóczki, Ph. Elsinga *et al.*, *J. Lab. Comp. and Radiophar.* **44**,1 (2001) 1026-1028.
- [2] M. Stöcker, *Microporous and Mesoporous Materials* **29** (1999) 3-48.
- [3] F. Shah, V.W. Pike *et al.*, *Appl. Rad. Isot.* **48**,7 (1997) 931-941.
- [4] P. Fejes *et al.*, *Applied Catalysis A: General* **190** (2000) 117-135.

7.1 Activities at the Van de Graaff Accelerator Laboratory

L. Bartha and E. Somorjai

During 2001 the beam time of the VdG-1 machine amounted to 126 hours. The accelerator delivered proton (46.8 %) and helium (53.2 %) beam used for low energy atomic physics experiments.

The 5 MV Van de Graaff machine was operating for 1321 hours during this period. Proton (53.0 %), D^+ (31.0 %) and He^+ (16.0 %) particles were accelerated.

The beam time was distributed among different research subjects as it is shown in Table 1.

Table 1. Time distribution among different research activities at VdG-5

Field	Hours	%
Atomic physics	281	21.3
Nuclear astrophysics	114	8.6
Analytical studies	490	37.1
Analyses on the microprobe	401	30.4
Machine tests	35	2.6
Total	1321	100

7.2 Status Report on the Cyclotron

Z. Kormány

The operation of the cyclotron in 2001 was again concentrated to the usual 9 months; January, July and August were reserved for maintenance and holidays. The overall working time of the accelerator was 4300 hours, the breakdown periods amounted to 66 hours last year. The cyclotron was available for users during 3751 hours, the effectively used beam-on-target time is summarized in Table 1. The total time required for machine setup and beam tuning or spent waiting for the start of an irradiation was 272 hours.

The control of the adjustable collimators applied in the beam transport system of the cyclotron was renewed during the winter maintenance period. They have been connected to the programmable logic controllers (PLC) and their new control code frees the operators from the long and slow manual setting process. The

successful renewal of the control of this and other subsystems (cyclotron and beam transport power supplies) made lots of adjusting and measuring elements on the original control desk needless. To provide more space for the control PCs and remove all unnecessary devices, the unused part of the control desk has been dismantled.

The short beam line used mainly for radiation hardness studies was equipped with a new oil-diffusion vacuum system during the summer maintenance. Its components are also connected to the PLC and the same automatic control has been provided like for the other vacuum stands of the beam transport system. Another short beam line - basically a mirror image of the first one - has also been installed and successfully tested by trial irradiations.

Table 1. Distribution of the irradiation (beam-on-target) time

Projects	Beam time (hours)	%
Nuclear spectroscopy	138	7
Nuclear astrophysics	923	51
Radiation hardness	147	8
Nuclear data	29	2
Neutron physics	13	1
Isotope production	553	31
Total	1803	100

7.3 3D Proton Beam Micromachining

I. Rajta, F. Watt^{a)}, A.A. Bettiol^{a)}, J.A. van Kan^{a)}

The miniaturisation of machines, sensors and actuators etc. and the integration of these micromechanical components with electronic devices (microelectromechanical systems - MEMS), is considered to be a new high-technology growth area of enormous potential. The demand for microstructures and MEMS is expected to grow similarly to what we have witnessed in IC production over the last few decades [1].

The majority of sub-micron machining procedures involve two types of interaction: electromagnetic radiation (e.g. optical, UV or X-ray photons) or charged particles (electrons, low energy heavy ions, high energy light ions). In general electromagnetic radiation based micromachining procedures require masks. In mask processes a selective pattern of radiation is transmitted through a structured mask on to a resist material, which is chemically developed subsequently thus produces microstructures. The use of a mask has significant advantages in mass production, masks usually contain multiple repeat patterns, and they can be re-used over many irradiations.

The use of a mask with charged particles is not so convenient, since in general greater energy is deposited in the mask during exposure. This can cause mask instabilities (heat expansion, stress and damage). The use of charged particle techniques for micromachining therefore is essentially limited to direct write processes, where a focused charged particle beam is scanned over a material in a specific pattern to produce microstructures.

Focused high energy ion beam micromachining is the newest of the micromachining techniques. The others include e.g. optical lithography, X-ray lithography (LIGA), UV lithography, E-beam writing, focused ion beam milling and laser beam micromachining. There are about 50 scanning proton microprobe facilities worldwide, but so far only few of them showed activity in this promising

field [e.g. 2, 3]. High energy light ions have a well defined penetration in matter with small lateral spread (except at the end of range). High energy ion beam micromachining using a direct-write scanning *MeV* ion beam is therefore capable of producing 3D microstructures and components with well defined lateral and depth geometry (e.g. Fig. 1). The achievable aspect ratios are as high as 100 [4], with potential lateral resolutions down to 100 nm and below, representing the current state-of-the-art performance for 2 MeV protons.

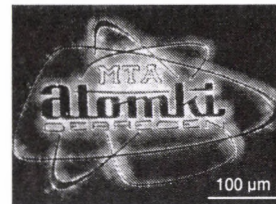


Figure 1. The Atomki logo made by Proton Beam Micromachining, using the PBM facility at the National University of Singapore. The structure is made in 30 μm thick SU-8 (beamsize: 0.5 μm , scan size: 400 μm , 1024 pixels).

The technique has high potential in the manufacture of 3D molds, stamps, and masks for LIGA, and also in the rapid prototyping of microcomponents either for research purposes (e.g. fluid flow properties in microchannels, friction properties, wear characteristics of moving parts, inertial properties of cantilevers, bio-activity of micro implants, etc.) or for components testing prior to batch production.

Preparatory work introducing PBM has begun in our laboratory.

- a) Research Centre for Nuclear Microscopy, Dept. of Physics, National University of Singapore, Singapore 119260
- [1] F. Watt, Nucl. Instr. and Meth. **B158** (1999) 165.
 - [2] S.V. Springham *et al.*, Nucl. Instr. and Meth. **B130** (1997) 155.
 - [3] D.G. de Kerckhove *et al.*, Nucl. Instr. and Meth. **B136-138** (1998) 379.
 - [4] J.L. Sanchez *et al.*, Nucl. Instr. and Meth. **B136-138** (1998) 385.

7.4 Application for the excitation of medium energy (up to 10 keV) photoelectron and Auger lines used in the study of surface analytical applications*

J. Tóth, Gy. Molnár^{a)}, D. Varga, I. Cserny, L. Kövér, J. Kiss, I. Gál, A. Nagy, A. Domonyi, Zs. Kertész, J. Mosolygó, G. Tarr, G. Pethő^{a)}, I. Szabó^{a)}, Y. Ould-Metidji^{b)}, B. Gruzza^{b)}, L. Bideux^{b)}, V. Matolin^{c)}, A. Sulyok^{a)} and M. Menyhárd^{a)}

A combination of specially designed XPS-XAES sources for the excitation of Auger lines of the few keV energy range is presented, including the main parameters of the home made X-ray tubes.

A home-made XPS-XAES-REELS instrument [1], based on an electron spectrometer with energy range of 10-10000 eV and high energy resolution by fixed retardation ratio k ($k=E_{kin}/E_{pass}$) of 2-100, has been used for studying of different materials: semiconductors [2], [3]; 3d elements and their alloys [4]; conducting polymers [5], [6], [7]; inorganic compounds; etc. The instrument is equipped with the mentioned X-ray sources with excitation photons of 1253-8048 eV energy and bremsstrahlung up to 25-30 keV.

Parameters of the "Henke type" XPS-XAES X-ray sources: Anode materials: Mg, Al, W, Cu, Mo, Ag. Anode voltage: 15 kV for Al, Mg; 25 kV for Cu, Mo, Ag, W; (max: 30 kV). Emission current: 10-20 mA; (max: 32 mA); Cooling water: deionised, closed loop, 1.2 l/min. Vacuum: better than 1.5 times 10^{-9} mbar in the measurement chamber of ESA-31 HSA based electron spectrometer [1]. Mounting flange: UHV CF 40.

XAES: A) Si KLL DETECTION WITH HIGH SENSITIVITY: An example of the high sensitivity detection of silicon by the help of Mo excited Si KLL Auger line was published (ECASIA-91 Budapest) [1]. The X-ray excitation source is one of the key parts of the above mentioned hemispherical analyzer based, high energy resolution electron spectrometer equipped with a specially designed input electron lens system [1]. **B) STUDY OF RADIATIVE AUGER EFFECT:** Recently the direct Auger lines originating from the XAES spectra were compared with high resolution X-ray spectra to study the radiative Auger effect (see Ref. 8 and References therein).

XPS: STUDIES OF THE NATURAL LINE WIDTH OF ATOMIC INNER SHELLS BY PAX (Photo-electrons from Absorption of X-rays) METHOD: By the help of the XPS X-ray excitation sources of the ESA-31 instrument [1] the PAX method was also used to study the natural line widths of atomic inner shells [9], [10], [11].

XPS AND XAES: DETERMINATION OF IMFP (Inelastic Mean Free Path) OF PHOTO- AND AUGER ELECTRONS AND LAYER THICKNESS OF THIN LAYERS

The ESA-31 electron spectrometer, with different methods of XPS-XAES-REELS, is an important tool in the "experimental" determination of IMFP of electrons by EPES method [12], [14]. In the IMFP studies, the specimen in-depth compositional homogeneity can be tested by different excitation energy X-rays. The high energy resolution quantitative EPES (QEPEPES: [See Ref 13 and References therein]) was used in the determination of IMFP (vs. energy of the primary electron beam) of III-V type compound semiconductors [2], [3] and synthetic metal (conductive polymer) films [5], [6], [7].

The energy calibration method by the help of the relatively high energy X-ray excited photoelectron lines ($E_{kinetic} \sim 7$ keV) [15] is also mentioned.

GaN specimens, generated from GaAs (100) by a new type of a radio frequency plasma source developed by Matolin, were characterized by MgK_{α} excited XPS, AES and EELS [16].

Sensitive detection of CuK_{α} excited Si 1s line, below from 10-20 nm thick layers, and determination of the layer thicknesses of 10-40 nm thick 3d metals from the high energy XPS and XAES spectra by QUASES method (developed by Tougaard) [17] is also presented.

*NOTE: the paper was presented at the 9th Eur. Conf. on Appls. of Surface and Interface Anal. (ECASIA'01.) 30 Sep-5 Oct, 2001 Avignon, France. Book of Abstr. pp 293. TU-P-TDE07.

a) Res. Inst. for Techn. Physics and Mats. Sci., H-1525 Budapest, P.O.Box. 49.

b) LASMEA-UMR 6602 CNRS, Blaise Pascal University, F-63177 Aubierre, France

c) Dept. of Electronics and Vac. Phys., Charles University, V. Holesovickach 2, 18000 Prague

[1] L. Kövér, D. Varga, I. Cserny, J. Tóth, K. Tőkési, *Surface and Interf. Anal.* **19** (1992) 9.

[2] M. Krawczyk, A. Jablonski, S. Tougaard, J. Tóth, D. Varga, G. Gergely, *Surface Science* **402-404** (1998) 491-495.

[3] G. Gergely, M. Menyhárd, S. Gurban, Zs. Benedek, Cs. Daróczi, V. Rakovics, J. Tóth, D. Varga, M. Krawczyk, A. Jablonski, *Surface and Interface Anal.* **30** (2000) 195-198.

[4] L. Kövér, I. Cserny, J. Tóth, D. Varga, T. Mukoyama, *J. of El. Spectr. & Rel. Phen.* **114-116** (2001) 55-61.

[5] B. Lesiak, A. Kosinski, M. Krawczyk, L. Zommer, A. Jablonski, J. Zemek, P. Jiricek, L. Kövér, J. Tóth, D. Varga, I. Cserny, *Appl. Surf. Sci.* **144-145** (1999) 168-172.

[6] B. Lesiak, A. Kosinski, A. Jablonski, L. Kvr, J. Tóth, D. Varga, I. Cserny, *Surf. and Interf. Anal.* **29** (2000) 614-623.

[7] B. Lesiak, A. Kosinski, M. Krawczyk, L. Zommer, A. Jablonski, L. Kövér, J. Tóth, D. Varga, I. Cserny, J. Zemek, P. Jiricek, *Polish Journal of Chem.* **74** (2000) 847-865.

[8] I. Abrahams, L. Kövér, J. Tóth, D.S. Urch, B. Vrebos, M. West, *J. of El. Spectr. & Rel. Phen.* **114-116** (2001) 925-931.

[9] J.L. Campbell, T. Papp, *X-ray Spectrometry* **24** (1995) 307.

[10] T. Papp, J.L. Campbell, D. Varga, *AIP Conf. Proc.* **389** (1997) 431.

[11] T. Papp, J.L. Campbell, D. Varga, G. Kalinka, *Nucl. Instr. and Meth.* **A412** (1998) 109-122.

[12] G. Gergely, *Surf. and Interface Anal.* **3** (1981) 203; G. Gergely, *Scanning* **8** (1986) 203.

[13] C.J. Powell and A. Jablonski, *J. Phys. Chem. Ref. Data.* **28** (1999) 19.

[14] A. Jablonski P. Mrozek, G. Gergely, M. Menyhárd, A. Sulyok, *Surf. and Interface Anal.* **6** (1984) 291.

[15] J. Tóth, *J. of Surf. Anal.* **1** (1995) 101.

[16] L. Bideux, Y. Ould-Metidji, B. Gruzza and V. Matolin, *Book of Abstr. of 9th Eur. Conf. on Appl. of Surf. and Interf. Anal.* (Sep 30-Oct 5 2001, Avignon, France), TU-P-TFC(inorg.) 05 p.233.

[17] L. Kövér, S. Tougaard, J. Tóth, L. Daróczi, I. Szabó, G. Langer, M. Menyhárd, *Surf. and Interf. Anal.* **31** (2001) 271.

7.5 Modeling and calibration of a double-crystal spectrometer for absolute x-ray wavelength measurements

Cs. Szabó, E. Takács^{a,b}, Z. Berényi, J. D. Gillaspay^b, L. Hudson^b

Highly charged ions generated in the Electron Beam Ion Trap (EBIT) of the National Institute of Standards and Technology (NIST) emit most of their radiation in the x-ray region. High-resolution wavelength measurements using crystal spectrometers require tedious calibration work. To provide quick, and absolute x-ray wavelengths we have implemented a method that uses two reflecting crystal surfaces. We developed a Ge double crystal spectrometer that uses a CCD camera as a detector.

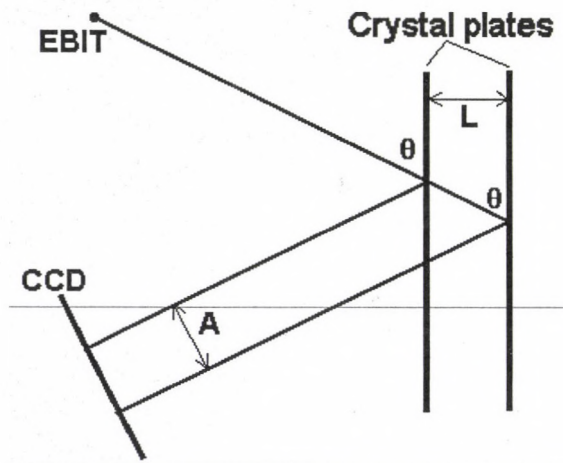


Figure 1. Setup of the crystal spectrometer

The spectrometer consists of a monolithic Ge crystal with two parallel surfaces. From the source x-rays of the wavelength λ are incident with a certain angle Θ on each of the crystal plates are reflected when Θ fulfills the Bragg equation (ignoring finer corrections):

$$\lambda = 2d \sin \Theta. \quad (1)$$

The detector face (CCD) is perpendicular to the direction of the reflected x-rays. On the

CCD camera we get a double spectrum of the source each reflected from one of the crystal plates. The crystal planes are in a distance of $L = 10$ mm from each other. The unknown wavelength λ can be evaluated from the shift of the two corresponding images. If the separation is A , then from the geometry:

$$\cos \Theta = \frac{A}{2L}, \text{ and} \quad (2)$$

$$\lambda = 2d \sqrt{1 - \left(\frac{A}{2L}\right)^2}. \quad (3)$$

With the precise knowledge of L the shift (A) between each of the peaks of the two spectra reflected by the two crystal plates will define the absolute wavelength.

As a first step of our design we modeled the Ge double-crystal step. The geometrical modeling procedure allowed us to select the final dimensions of the Ge crystal. The crystal was precision cut and analyzed at NIST. For in-situ calibrations we developed a calibration source built onto the EBIT port opposite to the spectrometer. The calibration was performed with the K_α and K_β lines of 5 different metals. The analysis of the spectra is on the way, and it will provide wavelength measurement capabilities for highly charged ion spectra.

Acknowledgment

During the work one of the authors (Cs. Szabó) was supported by the Soros Foundation and the Fulbright Commission.

a) Experimental Physics Department, University of Debrecen, Hungary

b) National Institute of Standards and Technology (NIST), Gaithersburg, MD, USA

7.6 Off-line production of ^7Be radioactive ion beam

L. Gialanella^{a,c,e}), U. Greife^b), N. De Cesare^{c,e}), A. D'Onofrio^{d,e}), M. Romano^{c,e}),
L. Campajola^{c,e}), A. Formicola^a), Zs. Fülöp, Gy. Gyürky, G. Imbriani^{c,e}), C. Lubritto^{d,e}),
A. Ordine^{c,e}), V. Roca^{c,e}), D. Rogalla^a), C. Rolfs^a), M. Russo^c), C. Sabbarese^{d,e}), E. Somorjai,
F. Strieder^a), F. Terrasi^{d,e}), H.P. Trautvetter^a)

The production of intense ^7Be radioactive ion beam ($T_{1/2}=53\text{ d}$) is presently absorbing considerable efforts in several laboratories [1]. Due to the long half-life, ^7Be ion beam can be produced either in an on-line mode (ISOL) or an off-line mode. We report here on the off-line mode, where ^7Be formation was carried out at the cyclotron in ATOMKI, Debrecen, the radiochemistry at the Isotop-Labor of the Ruhr-Universität Bochum, and the ^7Be acceleration at the TTT3 tandem in Naples.

The ^7Be nuclides were formed via the $^7\text{Li}(p,n)^7\text{Be}$ reaction at $E_p=11.4\text{ MeV}$, with $I_p=20\ \mu\text{A}$. In the activation process a metallic ^7Li disk was fixed in a copper holder. The absence of oxygen allowed a more efficient ^7Be production due to the higher areal density of Li for a given energy loss in the target. Moreover, the beam power could be dissipated in a much larger volume by direct water cooling on the bottom of the holder and by He-gas-flow cooling on the upper surface of the Li target separated by a thin foil-window from the vacuum-system. Usually, the Li disks were activated in two weeks using a pneumatically operated automatic irradiation chamber, and the resulting average ^7Be activity reached 20 GBq.

In order to extract the ^7Be nuclides from the Li matrix we adopted and improved the procedure of Kavanagh [2]. The irradiated Li targets of the order of 1 g mass with an average activity of 5 GBq each, corresponding to 0.4 mg of ^7Be , were processed at the Isotop-Labor of the Ruhr-Universität Bochum.

Several cathode geometries have been tested with stable Be and with low activity cathodes. The adopted geometry was of an inverted triangular shape, matching the sputter-

ing geometrical profile of the ion source. The cavity surfaces were coated with a chemically deposited silver layer to reduce the ^7Be diffusion into the copper bulk of the cathode during the operation in the accelerator source. The cathodes were used in Naples to produce an 8 MeV ^7Be ion beam: the sputter source delivered a 23 keV $^7\text{BeO}^-$ beam that was injected in the tandem accelerator and accelerated to a terminal voltage of 2.414 MV. The interaction with the carbon stripper foil, $5\ \mu\text{g}/\text{cm}^2$ thick, in the terminal of the accelerator broke the $^7\text{BeO}^-$ molecular ions and produced ^7Be positive ion beam in all its possible charge states. The 3+ charge state, $^7\text{Be}^{3+}$, was selected in order to reach the desired energy of 8.0 MeV. To suppress the accompanying $^7\text{Li}^{3+}$ beam, due to the presence of some residual lithium in the cathodes (sputtered as $^7\text{LiO}^-$), a post stripper carbon foil, $10\ \mu\text{g}/\text{cm}^2$ thick, was used before the analysing magnet, to form the 4+ charge state of ^7Be .

The ^7Be beam production is now routinely used several times per year. In view of the continuing need of ^7Be ion beam, the automatization of most of the steps during extraction is in progress. The automated procedure will allow a reduction (down to zero) of the doses received by the operators and will open the possibility to increase the number of preparations per year.

a) Ruhr-Universität Bochum, Bochum, Germany

b) Colorado School of Mines, Golden, CO, USA

c) Università Federico II, Napoli, Italy

d) Seconda Università di Napoli, Caserta, Italy

e) INFN, Napoli, Italy

[1] W. Bradfield-Smith *et al.*, Nucl. Instr. and Meth. **A425** (1999) 1.

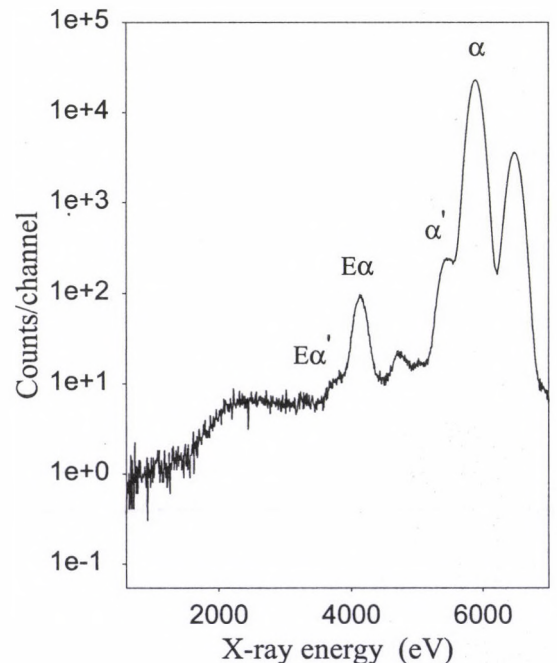
[2] R.W. Kavanagh, Nucl. Phys. **15** (1960) 411.

7.7 Spectral Artefacts with a Si-pin Photodiode X-Ray Detector: I. The Low Energy Case

G. Kalinka, T. Papp

In the last decade X-ray detectors based on thermoelectrically cooled, small sized Si-pin photodiodes have become very popular (see e.g. [1][2]). These diodes have low leakage current and moderate capacitance, are cheap and reliable and are suitable to build input stages with ≤ 200 eV energy resolution. We have carried out detailed investigations of a Hamamatsu S1223 photodiode (oxide-p⁺-n-n⁺ structure, 7 mm² × 0.2 mm) with X- and γ - rays of various energy (1.5-60 keV) and degree of collimation. Artefacts in the spectra, namely low energy side shoulder peaks of different nature and origin have been observed both at lower (up to ≈ 10 keV) and higher (from ≈ 10 keV) energies. The low energy artefact is insensitive to lateral position on the detector surface, however the background can be significantly reduced by collimation, enhancing the effect investigated. A MnK spectrum taken with 1 mm diameter collimation at 140 V bias is shown here for illustration. α denotes true MnK α photopeak, α' the shoulder one, while E α and E α' the corresponding escape peaks. The intensity ratio of E α / α is 0.4 % as expected, while that of E α' / α' is $\approx 2.4\% \approx \omega_{SiK}/2$, which is a strong indication of surface origin. A systematic investigation from 1.5 to 11 keV revealed that the relative energy displacement of the shoulder peak α' relative to α is 7 % and is largely independent of bias voltage, while from the α'/α relative intensity ratios the affected surface layer thickness is $\approx 0.3 \mu\text{m}$, i.e. on the order of front p⁺-region thickness. The reduced charge (electron) collection in this subsurface region, a problem here for low energy X-rays, has long been an obstacle for the construction of high efficiency UV-photodiodes using oxide-p⁺-n-n⁺ structure [3]. Thermal oxidation to create antireflective oxide, although reduces surface recombination, brings about a deleterious

boron redistribution [4]. This, and the positive oxide charge both create adverse electric fields which enhance Auger recombination in the p⁺-region and steer minority carriers to the oxide-Si interface where they recombine. A remedy to overcome this problem is either to use o-n⁺-p-p⁺ structure [5], where the oxidation has favourable effect on near surface electric field distribution or to apply proper oxidation/oxide deposition technology [6] in order to reduce surface recombination velocity rather drastically.



- [1] <http://www.amptek.com>
- [2] A.C. Huber *et al.*, Nucl. Instr. and Meth. **B99** (1995) 665.
- [3] J. Geist *et al.*, J. Appl. Phys. **52** (1981) 4879.
- [4] R. Korde and J. Geist, Solid State Electron. **30** (1987) 89.
- [5] G. Thungström *et al.*, Nucl. Instr. and Meth. **A460** (2001) 165.

7.8 Spectral Artefacts with a Si-pin Photodiode X-Ray Detector: II. The High Energy Case

G. Kalinka, T. Papp, G. Hegyesi

The Hamamatsu S1223 Si pin photodiode used as an X-ray detector has shown another type of artefact satellite peak structure for higher (≥ 10 keV) energies as well, dissimilar in nature and origin to those typically observed at low energies and discussed in the previous article [1]. This is illustrated in the figure below for two different bias voltages at 20 μ s peaking time.

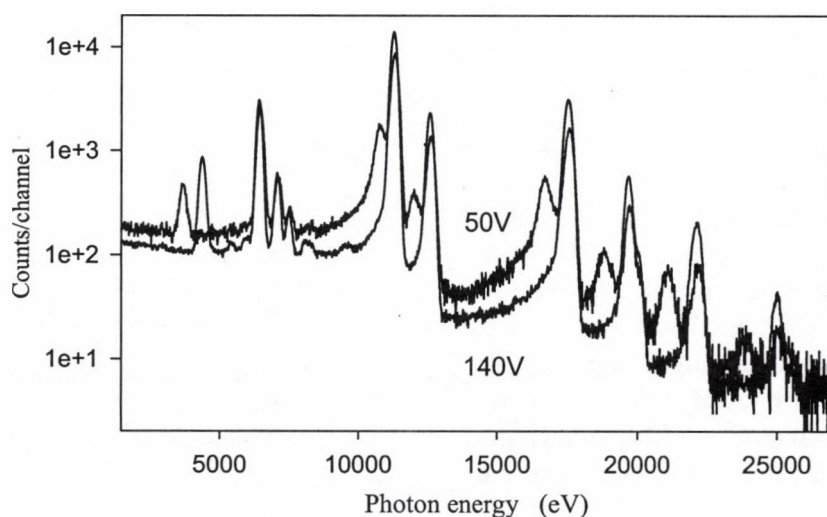
As deduced from C-V measurement, this diode is expected to be fully depleted at ≈ 220 V, but since breakdown voltage is ≈ 150 V, the detector is only always partially depleted. Using photons of various energy, front and rear side irradiation, sideways scanning with a microbeam and varying the bias voltage, it has been established that the true photopeak is related with depleted region events, while the satellite peak at the low energy side with undepleted region events, much the like the peaks observed in e.g. HP Ge detectors [2].

An additional pulse shape analysis has revealed that such undepleted region events produce detector current signals with long (max. 30 μ s) exponential tails. Therefore the amplitude loss of the satellite peak is a virtual one, caused by ballistic deficit effect. Between the

satellite and the true peaks there is a continuum (hardly noticeable in this figure) related to split events, since due to the finite photo- and Auger-electron ranges there is a finite probability of simultaneous energy deposition in two (or more) adjacent regions of the whole vacuum-oxide- p^+ -depleted n-undepleted $n-n^+$ -vacuum structure to be considered in this respect.

The narrowly distributed exponentially decaying detector signals from purely undepleted region energy deposition can be explained with the model described in [3], assuming that the rear $n-n^+$ junction behaves as a perfect mirror for holes. In this case the detector current risetime, though depends on the depth of photon interaction, at any degree of depletion is (much) shorter than the decay time determined by the (depletion region capacitance \times undepleted region series resistance) product.

- [1] G. Kalinka and T. Papp, in this Annual Report, p.62.
- [2] R.D. Baertsch, IEEE Trans. Nucl. Sci. NS-20, No.1 (1973) 488.
- [3] G.G. Pavlov and J.A. Nousek, Nucl. Instr. and Meth. A428 (1999) 348.



7.9 Scintillation Detectors with Multilayer Polymer Mirror Reflector Based on Giant Birefringent Optics

G. Kalinka, J.N. Scheurer^{a)}, G. Hegyesi, B.M. Nyakó, J. Gál

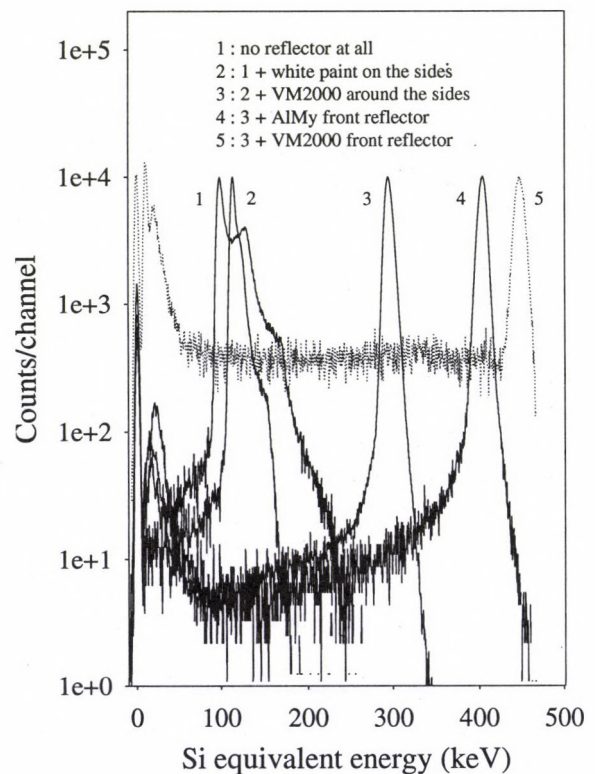
Photons created by incident radiation in scintillation detectors suffer multiple reflection and refraction before reaching photodetector. To increase light collection, therefore reflectors surrounding the optical system are necessary, which are efficient in a wide range of wavelength, incidence angle and polarization. These requirements are best met by using finely dispersed systems, as e.g. MgO, TiO₂, teflon tape, etc., exhibiting $\geq 95\%$ reflectivity. Metallic mirrors, though being robust, possess somewhat lower reflectivity.

Multilayer interference mirrors based on optically isotropic dielectric materials can have much higher value ($\geq 99\%$), but only for a narrow range of the above parameters. This limitation comes primarily from the fact that reflection at a material's interface for p-polarized light vanishes for a specific (Brewster's) angle. This can be overcome by using anisotropic (birefringent) polymers, for which Brewster's angle can be anywhere between 0-90°, or even imaginary. This enables the design of interference mirrors with unprecedented performance if birefringence is on the order of the change of the in-plane refractive index between adjacent polymeric layers (giant birefringent optics, GBO) [1].

Multibounce reflections, as e.g. in scintillation detectors, require broadband mirrors, which can be constructed by a stack of birefringent polymer films, whose refractive index in the direction perpendicular to their plane is matched. Such a mirror, with $\geq 98\%$ reflectivity in the visible, the VM2000 film [2] was used to upgrade the performance of the DIAMANT charged particle detector system [3] built up from CsI(Tl) scintillators coupled to Si-pin photodiodes. Retaining the previously used aluminized Mylar (AlMy) front reflector foil and the very efficient thin white underpaint layer [4,5], the outer teflon tape wrapping has

been changed for this GBO mirror film.

The evolution of the performance for 5.5 MeV α -particles in different stages of the completion is shown below. Light collection efficiency for the completed charged particle detector can reach 75 %, and by replacing the front reflector as well (enabling γ -detection only), 80 % is achievable.



- a) CENBG, Université de Bordeaux, F-33175 Gradignan Cédex, France
- [1] M.F. Weber *et al.*, *Science* **287** (2000) 2451.
[2] <http://www.3M.com/lightmanagement>
[3] J.N. Scheurer, *Int. Conf. Future of Nuclear Spectroscopy*, Aghia Pelagia, Crete, World Scientific (1993), p.371
[4] G. Kalinka *et al.*, *Atomki Ann. Rep.* 1994, (1995) 81.
[5] G. Kalinka *et al.*, *Atomki Ann. Rep.* 1996, (1997) 75.

7.10 Production of multiply charged fullerene and carbon cluster beams by the ECR ion source

S. Biri, A. Valek, L. Kenéz, A. Jánossy^{a)}

Endohedral fullerenes (where an alien atom is placed into the centre of the C₆₀, C₇₀ and other carbon balls) have been in the focus of interest for the last 5-6 years. If this alien atom is nitrogen then one can produce N@C₆₀ hybrid giant molecules. The neutral nitrogen atom is a sensitive probe to explore its environment by electron-spin-resonance (ESR) spectroscopy, thus N@C₆₀ can inform us on molecular distortions, molecular motions in internal fields and it monitors exohedral chemical addition reactions.

We report our results on study of normal and endohedral fullerene plasmas and beams produced by the 14.5 GHz Electron Cyclotron Resonance (ECR) Ion Source of ATOMKI. A mixed plasma of mainly N, N₂, and C₆₀ was produced in the plasma chamber using a homemade low-temperature oven. Then a beam was extracted from the plasma at U=700 V extraction voltage (Fig.1). The plasma consists mostly of C₆₀⁺ and C₆₀⁺⁺ with certain N₂⁺ and a smaller quantity of water. Left from the large C₆₀⁺ peak smaller C₅₈⁺, C₅₆⁺, C₅₄⁺,... down to C₃₂⁺ peaks appear together with similar structures at the left of C₆₀⁺⁺ and C₆₀⁺⁺⁺. Between n=30 and n=60 (n: number of the C atoms in the molecule) only even-numbered fullerenes are observed. The left side of the spectrum is the base plasma (C⁺, N⁺, O⁺, H₂O⁺, N₂⁺ etc.). Between the base plasma and the C₆₀⁺⁺⁺ peak many C_n^{Q+} cluster peaks are observable, where n=2...15 and Q=1 or 2. It is easy to tune the ECR ion source for optimal 1⁺, 2⁺, 3⁺ etc. production (Fig.1 represents a tuning for 1⁺). The highest beam intensities obtained and recorded in our laboratory in 2001 are: 410 nA of C₆₀⁺, 245 nA of C₆₀⁺⁺ and 105 nA of C₆₀⁺⁺⁺. These numbers exceed all values we found in the published literature and prove the suitability of ECR source to produce high intensity fullerene beams [1].

It became quickly clear that the method developed to obtain high intensity C₆₀^{Q+} beams

is suitable to produce carbon cluster beams, as well. We obtained easily several tens of nA of C_n^{Q+} beams (n=2...15, Q=1...2) sometimes more than 100 nA.

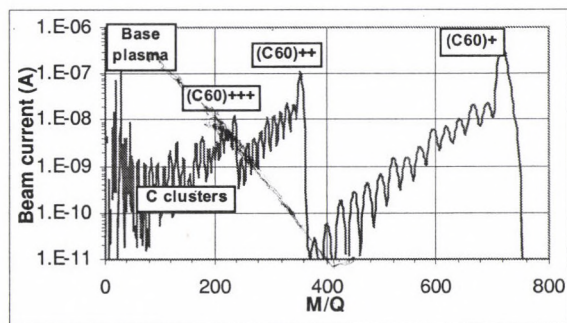


Figure 1. Typical fullerene spectrum at U=700 V extraction voltage

The main goal of the experiment was to produce high intensity of N@C₆₀ beams and so high quantity of N@C₆₀ bulk material. The mass of N@C₆₀ is 734 and is quite close to C₆₀ (720), NC₅₉ (722) and C₆₂ (744). The resolution of our bending magnet is not high enough to fully separate these heavy ions. Nevertheless, we successfully deposited macroscopic quantities of solid solution of N@C₆₀ and C₆₀ mixture within the ECR ion source. The N@C₆₀/C₆₀ ratio measured off-line using electron-spin-resonance spectroscopy was higher than typical values using conventional, non-ECR techniques [1].

The research proved the ECR ion source is able to deliver high intensity single and multicharged fullerene, endohedral fullerene and large carbon cluster plasmas and beams. The method is suitable to produce bulk quantities of endohedral fullerenes.

a) Tech. Univ. of Budapest, Dept. Exp. Phys., H-1521 Budapest, PO Box 91, Hungary

[1] S. Biri, A. Valek, L. Kenéz, A. Jánossy, A. Kitagawa, Production of multiply charged fullerene and carbon cluster beams by a 14.5 GHz ECR ion source. 9th Int. Conf. Ion Sources (ICIS01). Oakland, USA, Sept. 3-7, 2001. Accepted for publication in the Rev. Sci. Instr. **73**(2) (2002 February).

7.11 Langmuir-probe data analysis including the complex nature of the ECR plasma

L. Kenéz, S. Biri, J. Karácsony^{a)}, A. Valek

Electron Cyclotron Resonance (ECR) plasmas have already been studied in many ways, mainly by x-ray and UV measurements. Langmuir-probes, however, have proven useful for other kind of plasmas, and have rarely been used to explore the ECR plasma. A diagnostics setup has been built at the 14.5 GHz ATOMKI-ECRIS. Results of the cold plasma region measurements are shown.

Theory. A new formula for the electron density was deduced [1], which includes the multi-component multiply charged nature of the plasma.

- Single-Component Singly Charged approximation (SCSCh) (1) where, n_e is the electron density, M the ion mass, A the normal area of the probe with respect to the magnetic field lines, e the elementary charge, k the Boltzmann constant, j the charge state; the saturation ion current and T_e the parallel electron temperature, determined from the mean square fit of the characteristics; the mean stripping of the beam and β_j the percentage composition of the beam, determined experimentally from the beam spectra.
- Multi-Component Multiply Charged approximation (MCMCh) (2), where k denotes the plasma components.

Experiment. Two series of probe on-axis characteristics measurements were carried out in Ar plasma when the biased-disc was On and Off, respectively [2].

Data evaluation. Electron densities were calculated using Eq. (1) and Eq. (2).

Discussion. Variation of the electron densities is presented in Fig.1.

- The electron density increases as the probe approaches to the ECR zone ($D_j > 80$ mm).
- The mean charges of the plasma ion component in the Disc On/Off cases

were 4.23 and 2.9, respectively, which shows that the charge state distribution changed substantially. However the differences between the electron density values calculated using the Disc On/Off series are below the error limit. This means that the cold plasma regions are not affected by electron injection into the plasma.

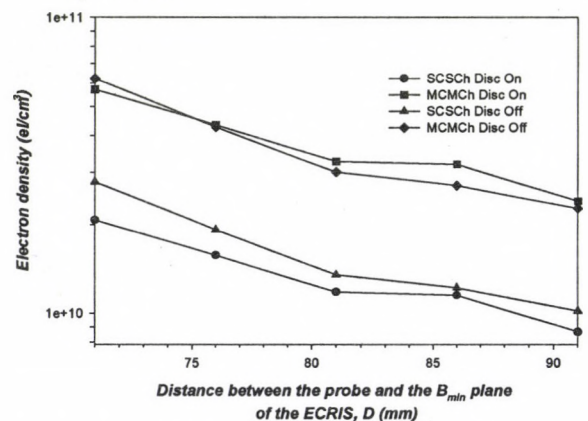


Figure 1. Electron density. Ar⁸⁺ optimized

- Differences between the electron densities calculated using the multiply charged and singly charged approximations are substantial.

Other experiments [1] have shown that as the mean charge of the ion component of the plasma is getting higher the difference between the original simple probe theories and our approximation is getting higher either. This is reasonable because higher optimized charge state means higher average stripping of the plasma.

The presented results show the necessary consideration of the MCMCh approximation when ECR electron densities are calculated.

a) Babes-Bolyai University RO-3400, Cluj-Napoca, Str. M Kogalniceanu Nr. 1, Romania

[1] L. Kenéz, S. *et al.*, Nucl. Instr. and Meth. **187(2)** (2002) 249.

[1] L. Kenéz, *et al.*, Accepted for publication in Rev. Sci. Instr. **73(2)** (2002)

8.1 Papers Published in 2001

1. Abbiendi G., Dienes B., Horváth D., Trócsányi Z., et al.: Two Higgs Doublet Model and model independent interpretation of neutral Higgs boson searches. *SCI European Physical Journal C* 18 (2001) 425.
2. Abbiendi G., Dienes B., Horváth D., Trócsányi Z., et al.: Production rates of $b\bar{b}$ quark pairs from gluons and $b\bar{b}b\bar{b}$ events in hadronic Z^0 decays. *SCI European Physical Journal C* 18 (2001)447.
3. Abbiendi G., Dienes B., Horváth D., Trócsányi Z., et al.: Measurement of triple gauge boson couplings from $W+W^-$ production at LEP energies up to 189 GeV. *SCI European Physical Journal C* 19 (2001)1.
4. Abbiendi G., Dienes B., Horváth D., Trócsányi Z., et al.: Measurement of W boson polarizations and CP-violating triple gauge couplings from $W+W^-$ production at LEP. *SCI European Physical Journal C* 19 (2001)229.
5. Abbiendi G., Dienes B., Horváth D., Trócsányi Z., et al.: A study of B_0 s meson oscillation using D-s-lepton correlations. *SCI European Physical Journal C* 19 (2001)241.
6. Abbiendi G., Dienes B., Horváth D., Trócsányi Z., et al.: Charged multiplicities in Z decays into u, d, and s Quarks. *SCI European Physical Journal C* 19 (2001)257.
7. Abbiendi G., Dienes B., Horváth D., Trócsányi Z., et al.: Precise determination of the Z resonance parameters at LEP: "Zedometry". *SCI European Physical Journal C* 19 (2001)587.
8. Abbiendi G., Dienes B., Horváth D., Trócsányi Z., et al.: A study of one-prong Tau decays with a charged kaon. *SCI European Physical Journal C* 19 (2001)653.
9. Abbiendi G., Dienes B., Horváth D., Trócsányi Z., et al.: A search for a narrow radial excitation of the D^{*+} meson. *SCI European Physical Journal C* 20 (2001)445.
10. Abbiendi G., Dienes B., Horváth D., Trócsányi Z., et al.: A simultaneous measurement of the QCD colour factors and the strong coupling. *SCI European Physical Journal C* 20 (2001)601.
11. Abbiendi G., Dienes B., Horváth D., Trócsányi Z., et al.: Precision neutral current asymmetry parameter measurements from the Tau polarization at LEP. *SCI European Physical Journal C* 21 (2001)1.
12. Abbiendi G., Dienes B., Horváth D., Trócsányi Z., et al.: Bose-Einstein correlations in K^+K^+ pairs from Z^0 decays into two hadronic jets. *SCI European Physical Journal C* 21 (2001)23.
13. Abbiendi G., Dienes B., Horváth D., Trócsányi Z., Ujvári B., et al.: Measurement of $\langle V_{ub} \rangle$ using b hadron semileptonic decay. *SCI European Physical Journal C* 21 (2001)399.
14. Abbiendi G., Dienes B., Horváth D., Trócsányi Z., Ujvári B., et al.: Determination of the b quark mass at the Z mass scale. *SCI European Physical Journal C* 21 (2001)411.
15. Abbiendi G., Dienes B., Horváth D., Trócsányi Z., et al.: Search for the standard model Higgs boson in e^+e^- collisions at $\sqrt{s} = 192 - 209$ GeV. *SCI Physics Letters B* 499 (2001)38.
16. Abbiendi G., Dienes B., Horváth D., Trócsányi Z., et al.: Searches for prompt light gravitino signatures in e^+e^- collisions at $\sqrt{s} = 189$ GeV. *SCI Physics Letters B* 501 (2001)12.

17. Abbiendi G., Dienes B., Horváth D., Trócsányi Z., et al.: Measurement of the mass and width of the W boson in e+e- collisions at 189 GeV. *SCI Physics Letters B* 507 (2001)29.
18. Abbiendi G., Dienes B., Horváth D., Trócsányi Z., Ujvári B., et al.: Angular analysis of the muon pair asymmetry at LEP 1. *SCI Physics Letters B* 516 (2001)1.
19. Abbiendi G., Dienes B., Horváth D., Trócsányi Z., et al.: Measurement of the branching ratio for D-s → tau-nū-tau decays. *SCI Physics Letters B* 516 (2001)236.
20. Abbiendi G., Dienes B., Horváth D., Trócsányi Z., Ujvári B., et al.: Search for lepton flavour violation in e+e- collisions at sqrt(s) = 189-209 GeV. *SCI Physics Letters B* 519 (2001)23.
21. Abbiendi G., Dienes B., Horváth D., Trócsányi Z., Ujvári B., et al.: Measurement of the branching ratio for the process b → tau-nū-tauX. *SCI Physics Letters B* 520 (2001)1.
22. Abbiendi G., Dienes B., Horváth D., Trócsányi Z., Ujvári B., et al.: Search for single top quark production at LEP2. *SCI Physics Letters B* 521 (2001)181.
23. Abbiendi G., Dienes B., Horváth D., Trócsányi Z., Ujvári B., et al.: Genuine correlations of like-sign particles in hadronic Z0 decays. *SCI Physics Letters B* 523 (2001)35.
24. Abrahams I., Kövér L., Tóth J., Urch D. S., Vrebos B., West M.: Absorption in emission: radiative Auger spectra in silica, phosphate and sulfate. *SCI Journal of Electron Spectroscopy and Related Phenomena* 114 (2001)925.
25. Acciarri M., Baksay G., Raics P., Szillási Z., Sztaricskai T., Zilizi Gy., et al.: Search for R-parity violating decays of supersymmetric particles in e+e- collisions at sqrt(s) = 189 GeV. *SCI European Physical Journal C* 19 (2001)397.
26. Acciarri M., Baksay G., Raics P., Szillási Z., Sztaricskai T., Zilizi Gy., et al.: Study of Z boson pair production in e+e- interactions at sqrt(s) = 192-202 GeV. *SCI Physics Letters B* 497 (2001)23.
27. Acciarri M., Baksay G., Raics P., Szillási Z., Sztaricskai T., Zilizi Gy., et al.: Light resonances in K0sK+- pi+ and eta pi+ pi- final states in gamma gamma collisions at LEP. *SCI Physics Letters B* 501 (2001)1.
28. Acciarri M., Baksay G., Raics P., Szillási Z., Sztaricskai T., Zilizi Gy., et al.: Ks0Ks0 final state in two-photon collisions and implications for glueballs. *SCI Physics Letters B* 501 (2001)173.
29. Acciarri M., Baksay G., Raics P., Szillási Z., Sztaricskai T., Zilizi Gy., et al.: Search for excited leptons in e+e- interactions at sqrt(s) = 192-202 GeV. *SCI Physics Letters B* 502 (2001)37.
30. Acciarri M., Baksay G., Raics P., Szillási Z., Sztaricskai T., Zilizi Gy., et al.: Measurement of the cross sections for open charm and beauty production in gamma gamma collisions at sqrt(s) = 189-202 GeV. *SCI Physics Letters B* 503 (2001)10.
31. Acciarri M., Baksay G., Raics P., Szillási Z., Sztaricskai T., Zilizi Gy., et al.: Search for neutral Higgs bosons of the minimal supersymmetric standard model in e+e- interactions at sqrt(s) = 192-202 GeV. *SCI Physics Letters B* 503 (2001)21.
32. Acciarri M., Baksay G., Raics P., Szillási Z., Sztaricskai T., Zilizi Gy., et al.: Study of the e+e- → Z gamma gamma → qq- gamma gamma process at LEP. *SCI Physics Letters B* 505 (2001)47.

33. Acciarri M., Baksay G., Raics P., Szillási Z., Sztaricskai T., Zilizi Gy., et al.: Measurement of the tau branching fractions into leptons. *SCI Physics Letters B* 507 (2001)47.
34. Acciarri M., Baksay G., Raics P., Szillási Z., Sztaricskai T., Zilizi Gy., et al.: Search for the Standard Model Higgs boson in e+e- collisions at sqrt(s) up to 202 GeV. *SCI Physics Letters B* 508 (2001)225.
35. Acciarri M., Baksay G., Raics P., Szillási Z., Sztaricskai T., Zilizi Gy., et al.: Measurement of the charm production cross section in gamma gamma collisions at LEP. *SCI Physics Letters B* 514 (2001)19.
36. Acciarri M., Baksay G., Raics P., Sztaricskai T., Szillási Z., Zilizi Gy., et al.: Total cross section in gamma gamma collisions at LEP. *SCI Physics Letters B* 519 (2001)33.
37. Achard P., Baksay G., Nagy S., Raics P., Szillási Z., Tarján P., Veszprémi V., Zilizi Gy., et al.: Search for heavy isosinglet neutrino in e+e- annihilation at LEP. *SCI Physics Letters B* 517 (2001)67.
38. Achard P., Baksay G., Nagy S., Raics P., Szillási Z., Tarján P., Veszprémi V., Zilizi Gy., et al.: Search for heavy neutral and charged leptons in e+e- annihilation at LEP. *SCI Physics Letters B* 517 (2001)75.
39. Achard P., Baksay G., Nagy S., Raics P., Szillási Z., Tarján P., Veszprémi V., Zilizi Gy., et al.: Standard model Higgs boson with the L3 experiment at LEP. *SCI Physics Letters B* 517 (2001)319.
40. Achard P., Baksay G., Nagy S., Raics P., Szillási Z., Tarján P., Veszprémi V., Zilizi Gy., et al.: Measurement of the topological branching fractions of the tau lepton at LEP. *SCI Physics Letters B* 519 (2001)189.
41. Afanasiev S. V., Gál J., Molnár J., et al.: Event-by-event fluctuations of the kaon-to-pion ratio in central Pb + Pb collisions at 158 GeV per nucleon. *SCI Physical Review Letters* 86 (2001)1965.
42. Algara A., Cseh J., Hess P. O., Hunyadi M.: Clusterization of heavy nuclei from the microscopic point of view: Application of the U(3) selection rule to 252Cf. *SCI Acta Physica Hungarica New Series - Heavy Ion Physics* 13 (2001)145.
43. Aliotta M., Raiola F., Gyürky Gy., Formicola A., Bonetti R., Brogгинi C., Campajola L., Corvisiero P., Constantini H., D'Onofrio A., Fülöp Zs., Gervino G., Gialanella L., Gulielmetti A., Gustavino C., Imbriani G., Junker M., Moroni P. G. P., Ordine A., Prati P., Roca V., Rogalla D., Rolfs C., Romano M., Schümann F., Somorjai E., Straniero O., Strieder F., Terrasi F., et al.: Electron screening effect in the reactions 3He(d,p)4He and d(3He,p)4He. *SCI Nuclear Physics A* 690 (2001)790.
44. Arai K., Ogawa Y., Suzuki Y., Varga K.: Microscopic multicluster description of light exotic nuclei with stochastic variational method on correlated Gaussians. *SCI Progress of Theoretical Physics Supplement* 142 (2001)97.
45. Back T., Cederkall J., Cederwall B., Johnson A., Kerek A., Klamra W., van der Marel J., Molnár J., Novák D., Sohler D., Steén M., Uhlén P.: An educational tool for demonstrating the TOF-PET technique. *SCI Nuclear Instruments and Methods in Physics Research Section A: Accelerators, Spectrometers, Detectors and Associated Equipment* 471 (2001)200.

46. Balogh K., Cassola P., Pompilio M., Puglisi D.: Petrographic, geochemical and radiometric data on tertiary volcano-arenitic beds from the Sicilian Maghrebic Chain: Volcanic sources and geodynamic implications. *SCI Geologica Carpathica* 52 (2001)15.
47. Banerjee S., Dajkó G., Fenyvesi A., Molnár J., Trócsányi Z., Szillási Z., Zilizi Gy., et al.: Prospects of B-physics with CMS. *SCI Nuclear Instruments and Methods in Physics Research Section A: Accelerators, Spectrometers, Detectors and Associated Equipment* 462 (2001)196.
48. Baradács E., Hunyadi I., Dezső Z., Csige I., Szerbin P.: ²²⁶Ra in geothermal and bottled mineral waters of Hungary. *SCI Radiation Measurements* 34 (2001)385.
49. Barmore B., Kruppa A. T., Nazarewicz W., Vertse T.: A new approach to deformed proton emitters: non-adiabatic coupled-channels. *SCI Nuclear Physics A* 682 (2001)256.
50. Barton R. A., Gál J., Molnár J., et al.: Production of multi-strange hyperons and strange resonances in the NA49 experiment. *SCI Journal of Physics G Nuclear and Particle Physics* 27 (2001)367.
51. Bende A., Vibók Á., Halász G., Suhai S.: BSSE-free description of the formamide dimers. *SCI International Journal of Quantum Chemistry* 84 (2001)617.
52. Bonacorsi D., Dienes B., Horváth D., Trócsányi Z., et al.: QCD measurements at the highest LEP2 energies. *SCI Nuclear Physics B Proceedings Supplement* 92 (2001)313.
53. Brandolini F., Medina N. H., Ribas R. V., Lenzi S. M., Gadea A., Ur C. A., Bazzacco D., Menegazzo R., Pavan P., Rossi-Alvarez C., Algora A., de Angelis G., De Poli M., Farnea E., Marginean N., Martínez T., Napoli D. R., Ionescu-Bujor M., Iordachescu A., Cameron J. A., Kasemann S., Schneider I., Espino J. M., Sanchez-Solano J.: Electromagnetic transitions and structure in the Z=N nucleus ⁴⁶V. *SCI Physical Review C Nuclear Physics* 64 (2001)4307.
54. Bucurescu D., Cata-Danil Gh., Cata-Danil I., Ivascu M., Marginean N., Rusu C., Stroe L., Ur C. A., Gizon A., Gizon J., Nyakó B. M., Timár J., Zolnai L., Boston A. J., Joss D. T., Paul E. S., Semple A. T., Parry C. M.: High-spin states in the ⁹⁶Tc nucleus. *SCI European Physical Journal A* 10 (2001)255.
55. Cacciari M., Del Duca V., Frixione S., Trócsányi Z.: QCD radiative corrections to $\gamma^*\gamma^* \rightarrow$ hadrons. *SCI Journal of High Energy Physics*(2001)29.
56. Campbell J. L., Papp T.: Widths of the atomic K-N7 levels. *SCI Atomic Data and Nuclear Data Tables* 77 (2001)1.
57. Campbell J. L., McDonald L., Hopman T., Papp T.: Simulations of Si(Li) x-ray detector response. *SCI X-Ray Spectrometry* 30 (2001)230.
58. Caner A., Dajkó G., Fenyvesi A., Molnár J., Trócsányi Z., Szillási Z., Zilizi Gy., et al.: Performance of the all-silicon CMS tracker. *SCI Nuclear Instruments and Methods in Physics Research Section A: Accelerators, Spectrometers, Detectors and Associated Equipment* 462 (2001)270.
59. Catani S., Dittmaier S., Trócsányi Z.: On-loop singular behaviour of QCD and SUSY QCD amplitudes with massive partons. *SCI Physics Letters B* 500 (2001)149.
60. Cavallari F., Dajkó G., Fenyvesi A., Molnár J., Trócsányi Z., Szillási Z., Zilizi Gy., et al.: Progress in the CMS ECAL. *SCI Nuclear Instruments and Methods in Physics Research Section A: Accelerators, Spectrometers, Detectors and Associated Equipment* 461 (2001)368.

61. Civitarese O., Liotta R. J., Vertse T.: Temperature dependent BCS-gap equations in the continuum. *SCI Physical Review C Nuclear Physics* 64 (2001)7305.
62. Csatlós M., Krasznahorkay A., van der Berg A. M., Harakeh M. N., van der Werf S. Y., Hagemann M., de Huu M., Akimune H., Fujimura H., Fujiwara M., Hara K., Ishikawa T.: A new methods to measure the neutron skin. *SCI Acta Physica Hungarica New Series - Heavy Ion Physics* 13 (2001)203.
63. Csige I., Csegi S.: The Radamon radon detector and an example of application. *SCI Radiation Measurements* 34 (2001)437.
64. Csík A., Malyovanik M., Dorogovich J., Kikineshi A., Beke D. L., Szabó I. A., Langer G. A.: Photo-stimulated structural transformations and optical recording in amorphous semiconductor multilayers. *SCI Journal of Optoelectronics and Advanced Materials*(2001)33.
65. Csík A., Langer G. A., Beke D. L., Erdélyi Z., Menyhárd M., Sulyok A.: Interdiffusion in amorphous Si/Ge multilayers by Auger depth profiling technique. *SCI Journal of Applied Physics* 89 (2001)804.
66. Csík A., Beke D. L., Langer G. A., Erdélyi Z., Daróczy L., Kapta K., Kis-Varga M.: Non-linearity of diffusion in amorphous Si-Ge multilayers. *SCI Vacuum* 61 (2001)297.
67. Darai J., Gyarmati B., Kónya B., Papp Z.: Variational separable expansion scheme for two-body Coulomb-scattering problems. *SCI Physical Review C Nuclear Physics* 63 (2001)7001.
68. Dekov V. M., Damyanov Z. K., Kamenov G. D., Bonev I. K., Rajta I., Grime G. W.: Sorosite (éta-Cu₆Sn₅)-bearing native tin and lead assemblage from the Mir zone (Mid-Atlantic Ridge, 26 degree N). *SCI Oceanologica Acta* 24 (2001)205.
69. Dienes B., Trócsányi Z.: A simultaneous measurement of the strong coupling and the QCD colour charges. *SCI Nuclear Physics B Proceedings Supplement* 96 (2001)40.
70. Dokhale P. A., Csikai Gy., Oláh L.: Investigations on neutron-induced prompt gamma ray analysis of bulk samples. *SCI Applied Radiation and Isotopes* 54 (2001)967.
71. Duchesneau D., Baksay G., Szillási Z., Zilizi Gy., Dienes B., Horváth D., Trócsányi Z., Raics P., Sztaricskai T., et al.: Studies of colour reconnection effects in hadronic W pair decays at LEP. *SCI Nuclear Physics B Proceedings Supplement* 96 (2001)13.
72. Elekes Z., Bíró K. T., Uzonyi I., Simon A., Kiss Á Z.: Analysis of prehistoric pottery finds from the Balaton region, Hungary. *SCI Nuclear Instruments and Methods in Physics Research Section B: Beam Interactions with Materials and Atoms* 181 (2001)670.
73. Erdélyi Z., Girardeaux Ch., Langer G. A., Beke D. L., Rolland A., Bernardini J.: Determination of grain-boundary diffusion of Ag in nanocrystalline Cu by the Hwang-Balluffi method. *SCI Journal of Applied Physics* 89 (2001)3971.
74. Fainstein P. D., Gulyás L.: State-selective multiple electron emission from argon by MeV proton impact. *SCI Journal of Physics B* 34 (2001)3003.
75. Formenti P., Andreae M. O., Lange L., Roberts G., Cafmeyer J., Rajta I., Maenhaut W., Holben N., Artaxo P., Lelieveld J.: Saharan dust in Brazil and Suriname during the Large-Scale Biosphere-Atmosphere Experiment in Amazonia (LBA) - Cooperative LBA regional Experiment (CLAIRE) in March 1998. *SCI Journal of Geophysical Research* 106 (2001)14919.

76. Futó I., Molnár M., Palcsu L., Svingor É., Szántó Zs.: Application of a noble gas mass spectrometric system in environmental studies. *SCI Vacuum* 61 (2001)441.
77. Fülöp Zs., Gyürky Gy., Máté Z., Somorjai E., Zolnai L., Galavíz D., Babilon M., Mohr P., Zilges A., Rauscher T., Oberhummer H., Staudt G.: $^{92}\text{Mo}(\alpha, \alpha)^{92}\text{Mo}$ scattering, the ^{92}Mo -alpha optical potential, and the $^{96}\text{Ru}(\gamma, \alpha)^{92}\text{Mo}$ reaction rate at astrophysically relevant energies. *SCI Physical Review C Nuclear Physics* 64 (2001)5805.
78. Galindo E., Hausmann M., Jungclaus A., Kast D., Lieb K. P., Müller G. A., Yordanov O., Brant S., Vretenar D., Algora A., Brandolini F., de Angelis G., De Poli M., Fahlander C., Gadea A., Martínez T., Napoli D. R., Dewald A., Peusquens R., Tiesler H., Górska M., Grawe H., Bizzeti P. G., Sona P., Bonsignori G.: Lifetime measurements of high-spin states in ^{101}Ag and their interpretation in the interacting boson fermion plus broken pair model. *SCI Physical Review C Nuclear Physics* 64 (2001)4304.
79. Gassmann D., Thierolf P. G., Mengel E., Habs D., Chromik M., Domscheit J., Gorgen A., Hauschild K., Hübel H., Hunyadi M., Krasznahorkay A., Lopez-Martens A., Neumann S., Neusser A., Pansegrau D., Reiter P., Scheit H., Schönwasser G., Schwalm D.: Conversion electron spectroscopy in the superdeformed minimum of ^{240}Pu . *SCI Physics Letters B* 497 (2001)181.
80. Gazdzicki M., Gál J., Molnár J., et al.: Evidence for Quark Gluon Plasma from hadron production in high energy nuclear collisions. *SCI Nuclear Physics A* 681 (2001)153.
81. Gergely Gy., Menyhárd M., Gurban S., Sulyok A., Tóth J., Varga D., Tougaard S.: Surface excitation effects in electron spectroscopy. *SCI Solid State Ionics* 141 (2001)47.
82. Gergely G., Menyhárd M., Benedek Zs., Sulyok A., Kövér L., Tóth J., Varga D., Berényi Z., Tókési K.: Recoil broadening of the elastic peak in electron spectroscopy. *SCI Vacuum* 61 (2001)107.
83. Gialanella L., Rogalla D., Strieder F., Theis S., Gyürky Gy., Agodi C., Alba R., Aliotta M., Campajola L., Del Zoppo A., D'Onofrio A., Figuera P., Greife U., Imbriani G., Ordine A., Roca V., Rolfs C., Romano M., Sabbarese C., Sapienza P., Schümann F., Somorjai E., Terrasi F., Trautvetter H-P.: The E1 capture amplitude in $^{12}\text{C}(\alpha, \gamma)^{16}\text{O}$. *SCI European Physical Journal A* 11 (2001)357.
84. Gialanella L., Aliotta M., Rogalla D., Rolfs C., Schümann F., Strieder F., Theis S., Trautvetter H-P., Campajola L., Imbriani G., Roca V., Romano M., D'Onofrio A., Sabbarese C., Terrasi F., Agodi C., Alba R., Del Zoppo A., Figuera P., Sapienza P., Spitaleri C., Gyürky Gy., Somorjai E., Greife U.: A new measurement of the E1 amplitude in $^{12}\text{C}(\alpha, \gamma)^{16}\text{O}$. *SCI Nuclear Physics A* 688 (2001)254.
85. Gizon A., Timár J., Gizon J., Weiss B., Barnéoud D., Foin C., Genevey J., Hannachi F., Liang C. F., Lopez-Martens A., Paris P., Nyakó B. M., Zolnai L., Merdinger J. C., Brandt S., Paar V.: Low-lying levels and collective bands in doubly-odd ^{124}Cs . *SCI Nuclear Physics A* 694 (2001)63.
86. Gruzza B., Merle S., Bideux L., Robert C., Kövér L., Tóth J., Matolin V.: UHV aluminium oxide on silicon substrates: electron spectroscopies analysis and electrical measurements. *SCI Applied Surface Science* 175 (2001)656.
87. Gulyás L., Fainstein P. D., Shirai T.: Multiple-scattering analysis of triply differential cross sections for electron emission in energetic ion-atom collisions. *SCI Journal of Physics B* 34 (2001)1473.

88. Gurin P., Gulácsi Zs.: $T_{\downarrow}=0$ properties of the infinitely repulsive Hubbard model for an arbitrary number of holes. *SCI Philosophical Magazine B* 81 (2001)321.
89. Gurin P., Gulácsi Zs.: Exact solutions for the periodic Anderson model in two dimensions: A non-Fermi-liquid state in the normal phase. *SCI Physical Review B* 64 (2001)5118.
90. Gyürky Gy., Somorjai E., Rauscher T., Harissopulos S.: Proton capture cross section of Sr isotopes. *SCI Nuclear Physics A* 688 (2001)90.
91. Gyürky Gy., Somorjai E., Fülöp Zs., Harissopulos S., Demetriou P., Rauscher T.: Proton capture cross section of Sr isotopes and their importance for nucleosynthesis of proton-rich nuclides. *SCI Physical Review C Nuclear Physics* 64 (2001)5803.
92. Gácsi Z., Csatlós M., Krasznahorkay A., Sohler D., Gulyás J., Timár J., Hunyadi M., Weil J. L., van Klinken J.: Low-lying, excited $K=0$ bands in ^{238}U . *SCI Physical Review C Nuclear Physics* 64 (2001)7303.
93. Gál J.: Double gated-integrator for shaping nuclear radiation detector signals. *SCI Nuclear Instruments and Methods in Physics Research Section A: Accelerators, Spectrometers, Detectors and Associated Equipment* 462 (2001)506.
94. Hannachi F., Korichi A., Wilson A. N., Lopez-Martens A., Rejmund M., Schueck C., Vieu Ch., Chmel G., Goergen A., Huebel H., Roszbach D., Schoenwasser S., Bergström M., Nyakó B. M., Timár J., Bazzacco D., Lunardi S., Rossi-Alvarez C., Bednarczyk P., Kintz N., Naguleswaran S., Astier A., Cullen D. Mc., Sharpey-Schafer J. F., Lauritsen T., Wadsworth R.: Collective excitations in the superdeformed well. *SCI Acta Physica Polonica B* 32 (2001)1083.
95. Harissopulos S., Galanopoulos S., Tzagari P., Demetriou P., Kuburas G., Paradellis T., Kunz R., Hammer J. W., Gyürky Gy., Somorjai E., Goriely S., Kasemann S., Dewald A., Zell K. O.: Cross sections of (p, gamma) reactions of $N=50$ nuclei relevant to p-process. *SCI Nuclear Physics A* 688 (2001)421.
96. Hashimoto T., Nakai K., Wakasaya Y., Tanihata I., Fülöp Zs., Kumagai H., Ozawa A., Yoshida K., Goswami R.: Half-life of ^{44}Ti . *SCI Nuclear Physics A* 686 (2001)591.
97. Hauke A., Dienes B., Horváth D., Trócsányi Z., et al.: A measurement of the tau mass and the first test of CPT-invariance with tau leptons. *SCI Nuclear Physics B Proceedings Supplement* 98 (2001)85.
98. Hawkings R., Baksay G., Szillási Z., Zilizi Gy., Dienes B., Horváth D., Trócsányi Z., Raics P., Sztaricskai T., et al.: LEP measurements of $|V_{cb}|$ and $|V_{ub}|$. *SCI Nuclear Instruments and Methods in Physics Research Section A: Accelerators, Spectrometers, Detectors and Associated Equipment* 462 (2001)126.
99. Hess E., Takács S., Scholten B., Tárkányi F., Coenen H. H., Qaim S. M.: Excitation function of the $^{18}\text{O}(p,n)^{18}\text{F}$ nuclear reaction from threshold up to 30 MeV. *SCI Radiochimica Acta* 89 (2001)357.
100. Hori M., Eades J., Hayano R. S., Ishikawa T., Sakaguchi J., Widmann E., Yamaguchi H., Torii H. A., Juhász B., Horváth D., Yamazaki T.: Sub-ppm laser spectroscopy of antiprotonic helium and a CPT-violation limit on the antiprotonic charge and mass. *SCI Physical Review Letters* 87 (2001)3401.

101. Hunyadi M., Gassmann D., Krasznahorkay A., Habs D., Csatlós M., Eisermann Y., Faestermann T., Graw G., Gulyás J., Hertzenberger R., Maier H. J., Máté Z., Metz A., Thierolf P. G., Chromik M., van der Werf S. Y.: Superdeformed rotational bands in ^{240}Pu . *SCI Acta Physica Polonica B* 32 (2001)699.
102. Hunyadi M., Gassmann D., Krasznahorkay A., Habs D., Thierolf P. G., Csatlós M., Eisermann Y., Faestermann T., Graw G., Gulyás J., Hertzenberger R., Maier H. J., Máté Z., Metz A., Chromik M.: Excited superdeformed $K\pi = 0^+$ rotational bands in beta-vibrational fission resonances of ^{240}Pu . *SCI Physics Letters B* 505 (2001)27.
103. Ivanov I. A., Mitroy J., Varga K.: Elastic positronium-atom scattering using the stochastic variational method. *SCI Physical Review Letters* 87 (2001)3201.
104. Iwasaki H., Motobayashi T., Sakurai H., Yoneda K., Gomi T., Aoi N., Fukuda N., Fülöp Zs., Futakami U., Gácsi Z., Higurashi Y., Imai N., Iwasa N., Kubo T., Kunibu M., Kurokawa M., Liu Z., Minemura T., Saito A., Serata M., Shimoura S., Takeuchi S., Watanabe Y., Yamada K., Yanagisawa Y., Ishihara M.: Large collectivity of ^{34}Mg . *SCI Physics Letters B* 522 (2001)227.
105. Jalilvand F., Eriksson L., Glaser J., Maliarik M., Mink J., Sandström M., Tóth I., Tóth J.: $\text{TlPt}(\text{CN})_5$ in the solid state - A multimethod study of an unusual compound containing inorganic wires. *SCI Chemistry - A European Journal* 7 (2001)2167.
106. Jordanova J., Oláh L., Fenyvesi A., Csikai Gy., Leshchenko B., El-Megrab A. M., Majdeddin A. D.: Measurements and calculations of neutron spectra modified by iron slabs bombarded by neutrons with energies up to 14 MeV. *SCI Applied Radiation and Isotopes* 54 (2001)307.
107. Juillet O., Fleck S., Theussl L., Richard J. -M., Varga K.: Lower bound on fermion binding energies. *SCI Physical Review B* 63 (2001)3102.
108. Kamada H., Nogga A., Glöckle W., Hiyama E., Kamimura M., Varga K., Suzuki Y., Viviani M., Kievsky A., Rosati S., Carlson J., Pieper S. C., Wiringa R. B., Navratil P., Barrett B. R., Barnea N., Leidemann W., Orlandini G.: Benchmark test calculation of a four-nucleon bound state. *SCI Physical Review C Nuclear Physics* 64 (2001)4001.
109. Kartvelishvili V., Dienes B., Horváth D., Trócsányi Z., et al.: Measurement of the low-x behaviour of the photon structure function. *SCI Nuclear Physics B Proceedings Supplement* 96 (2001)161.
110. Király B., Oláh L., Csikai Gy.: Neutron-based techniques for detection of explosives and drugs. *SCI Radiation Physics and Chemistry* 61 (2001)781.
111. Klint P. M., Baksay G., Szillási Z., Zilizi Gy., Dienes B., Horváth D., Trócsányi Z., Raics P., Sztaricskai T., et al.: Rare B decay at LEP. *SCI Nuclear Instruments and Methods in Physics Research Section A: Accelerators, Spectrometers, Detectors and Associated Equipment* 462 (2001)108.
112. Koncz Cs.: Double scattered electrons in ion-atom collisions: an impulse approximation. *SCI Journal of Physics B* 34 (2001)3879.
113. Korichi A., Wilson A. N., Hannachi F., Lopez-Martens A., Rejmund M., Schück C., Vieu Ch., Chmel G., Görgen A., Hübel H., Rossbach D., Schönwasser G., Bergström M., Nyakó B. M., Timár J., Bazzacco D., Lunardi S., Rossi-Alvarez C., Bednarczyk P., Kintz N., Naguleswaran S., Astier A., Cullen D. Mc., Sharpey-Schafer J. F., Lauritsen T., Wadsworth R.: Linear polarization

- measurement of interband transitions in superdeformed 190Hg: Model-independent evidence for octupole vibrational structures. *SCI Physical Review Letters* 86 (2001)2746.
114. Koroknai B., Horváth P., Balogh K., Dunkl I.: Alpine metamorphic evolution and cooling history of the Veporic basement in northern Hungary: new petrological and geochronological constraints. *SCI International Journal of Earth Science* 90 (2001)740.
 115. Krasznahorkay A., Habs D., Hunyadi M., Gassmann D., Csatlós M., Eisermann Y., Faestermann T., Graw G., Gulyás J., Hertenberger R., Maier H. J., Máté Z., Metz A., Ott J., Thierolf P. G., van der Werf S. Y.: Hyperdeformation and clusterization in the actinide region. *SCI Acta Physica Hungarica New Series - Heavy Ion Physics* 13 (2001)111.
 116. Krasznahorkay A., Habs D., Hunyadi M., Gassmann D., Csatlós M., Eisermann Y., Faestermann T., Graw G., Gulyás J., Hertenberger R., Maier H. J., Máté Z., Metz A., Ott J., Thierolf P. G., van der Werf S. Y.: Superdeformation, hyperdeformation and clustering in the actinide region. *SCI Acta Physica Polonica B* 32 (2001)657.
 117. Krasznahorkay A., Akimune H., Fujiwara M., Harakeh M. N., Janecke J., Rodin V. A., Urin M. H., Yosoi M.: Distribution of the Gamow-Teller strength in 90Nb and 208Bi. *SCI Physical Review C Nuclear Physics* 64 (2001)7302.
 118. Kruppa A. T., Varga K., Révai J.: Local realizations of contact interactions in two- and three-body problems. *SCI Physical Review C Nuclear Physics* 63 (2001)4301.
 119. Kruppa A. T., Heenen P. -H., Liotta R. J.: Resonances in the Hartree-Fock BCS theory. *SCI Physical Review C Nuclear Physics* 63 (2001)4324.
 120. Kun F., Wen W. J., Pál K. F., Tu K. N.: Breakup of dipolar rings under a perpendicular magnetic field. *SCI Physical Review E* 64 (2001)1503.
 121. Kövér L., Uda M., Csérny I., Tóth J., Végh J., Varga D., Ogasawara K., Adachi H.: Chemical effects on F KLL Auger spectra in fluorides. *SCI Journal of Vacuum Science and Technology A Vacuum, Surfaces and Films* 19 (2001)1143.
 122. Kövér Á., Paludan K., Laricchia G.: Triply differential ionization cross-section of H₂ by 50 eV impact-energy positrons. *SCI Journal of Physics B* 34 (2001)219.
 123. Kövér L., Csérny I., Tóth J., Varga D., Mukoyama T.: KLL Auger transitions in metallic Cu and Ni. *SCI Journal of Electron Spectroscopy and Related Phenomena* 114 (2001)55.
 124. Kövér Á., Laricchia G.: A parallel-plate analyser with time focusing. *SCI Measurement Science and Technology* 12 (2001)1875.
 125. Kövér L., Tougaard S., Tóth J., Daróczy L., Szabó I. A., Langer G. A., Menyhárd M.: Determination of overlayer thickness by QUASES analysis of photon-excited KLL Auger spectra of Ni and Cu films. *SCI Surface and Interface Analysis* 31 (2001)271.
 126. Ladrón de Guevara P., Baksay G., Raics P., Szillási Z., Zilizi Gy., et al.: First results from the L3+C experiment at CERN. *SCI Nuclear Physics B Proceedings Supplement* 95 (2001)237.
 127. Lagergren K., Cederwall B., Back T., Wyss R., Ideguchi E., Johnson A., Atac A., Axelsson A., Azaiez F., Bracco A., Cederkall J., Dombrádi Zs., Fahlander C., Gadea A., Million B., Petrache C. M., Rossi-Alvarez C., Sampson J. A., Sohler D., Weiszflog M.: Coexistence of superdeformed shapes in 154Er. *SCI Physical Review Letters* 87 (2001)2502.

128. Lenzi S. M., Marginean N., Napoli D. R., Ur C. A., Zuker A. P., de Angelis G., Algora A., Axiotis M., Bazzacco D., Belcari N., Bentley M. A., Bizzeti P. G., Bizzeti-Sona A. M., Brandolini F., von Brentano P., Bucurescu D., Cameron J. A., Chandler C., De Poli M., Dewald A., Eberth H., Farnea E., Gadea A., Garcés Narro J., Gelletly W., Grawe H., Isocrate R., Joss D. T., Podolyák Zs., et al.: Coulomb energy differences in T = mirror rotational bands in ^{50}Fe and ^{50}Cr . *SCI Physical Review Letters* 87 (2001)2501.
129. Leoni S., Bracco A., Camera F., Million B., Algora A., Axelsson A., Benzoni G., Bergström M., Blasi N., Castoldi M., Frattini S., Gadea A., Herskind B., Kmiecik M., Lo Bianco G., Maj A., Nyberg J., Pignanelli M., Styczen J., Vigezzi E., Zieblinski M., Zuchiatti A.: Quantum tunneling of the excited rotational bands in the superdeformed nucleus ^{143}Eu . *SCI Physics Letters B* 498 (2001)137.
130. Lesiak B., Kosinski A., Jablonski A., Kövér L., Tóth J., Varga D., Cserny I., Zagorska M., Kulszewicz-Bajer M., Gergely G.: Determination of the inelastic mean free path of electrons in polythiophenes using elastic peak electron spectroscopy method. *SCI Applied Surface Science* 174 (2001)70.
131. Lindroth E., Danared H., Glans P., Pesic Z., Tokman M., Víkor Gy., Schuch R.: QED effects in Cu-like Pb recombination resonances near threshold. *SCI Physical Review Letters* 86 (2001)5027.
132. Lugosi L., Gyémánt I. K.: A simple model for positronium formation in positron - hydrogen atom collisions. *SCI Acta Physica Hungarica New Series - Heavy Ion Physics* 14 (2001)267.
133. Lugosi L., Sarkadi L.: Calculation of the matrix elements of the Coulomb interaction involving relativistic hydrogenic wave functions. *SCI Computer Physics Communications* 141 (2001)73.
134. Lévai G., Cseh J., Van Isacker P.: Supersymmetry for nuclear cluster systems. *SCI European Physical Journal A* 12 (2001)305.
135. Lévai G., Cannata F., Ventura A.: Algebraic and scattering aspects of a PT-symmetric solvable potential. *SCI Journal of Physics A* 34 (2001)839.
136. Lévai G., Znojil M.: Conditions for complex spectra in a class of PT symmetric potentials. *SCI Modern Physics Letters A* 16 (2001)1973.
137. Mezei J. Zs., Mitroy J., Lovas R. G., Varga K.: Properties of some exotic five-particle systems. *SCI Physical Review A* 64 (2001)2501.
138. Mohr P., Babilon M., Galavíz D., Zilges A., Fülöp Zs., Gyürky Gy., Máté Z., Somorjai E., Zolnai L., Oberhammer H.: Alpha-nucleus potentials at astrophysically relevant energies. *SCI Nuclear Physics A* 688 (2001)424c.-426c.
139. Müller G. A., Jungclaus A., Yordanov O., Galindo E., Hausmann M., Kast D., Lieb K. P., Brant S., Krstic V., Vretenar D., Algora A., Brandolini F., de Angelis G., De Poli M., Fahlander C., Gadea A., Martínez T., Napoli D. R., Dewald A., Peusquens R., Tiesler H., Górska M., Grawe H., Bizzeti P. G.: High-spin structure and electromagnetic transition strengths in ^{104}Cd . *SCI Physical Review C Nuclear Physics* 64 (2001)4305.
140. Mészáros S., Vad K., Hakl J., Kerekes L., Gurin P., Kis-Varga M., Szabó S., Beke D. L., De Chatel P. F.: Identification of a disordered magnetic phase in pure nanocrystalline iron. *SCI Philosophical Magazine B* 81 (2001)1597.

141. Nagy Z., Trócsányi Z.: Multijet cross sections in deep inelastic scattering at next-to-leading order. *SCI Physical Review Letters* 87 (2001)2001.
142. Neumeister N., Dajkó G., Fenyvesi A., Molnár J., Trócsányi Z., Szillási Z., Zilizi Gy., et al.: CMS high-level triggering. *SCI Nuclear Instruments and Methods in Physics Research Section A: Accelerators, Spectrometers, Detectors and Associated Equipment* 462 (2001)254.
143. Palacz M., Fahlander C., Sohler D., Rudolph D., Blomqvist J., Kownacki J., Lagergren K., Norlin L. -O., Nyberg J., Algora A., Andreoiu C., de Angelis G., Atac A., Bazzacco D., Berglund L., Baeck T., Cederkall J., Cederwall B., Dombrádi Zs., Fant B., Farnea E., Gadea A., Górska M., Grawe H., Hashimoto-Saitoh N., Johnson A., Kerek A., Klamra W., Lenzi S. M., et al.: Investigations of neutron deficient nuclei close to 100Sn with EUROBALL. *SCI Acta Physica Polonica B* 32 (2001)999.
144. Palla F., Baksay G., Szillási Z., Zilizi Gy., Dienes B., Horváth D., Trócsányi Z., Raics P., Sztaricskai T., et al.: B0B oscillations at LEP. *SCI Nuclear Instruments and Methods in Physics Research Section A: Accelerators, Spectrometers, Detectors and Associated Equipment* 462 (2001)92.
145. Palsgard E., Ugarte M., Rajta I., Grime G. W.: The role of zinc in the dark-adapted retina studied directly using microPIXE. *SCI Nuclear Instruments and Methods in Physics Research Section B: Beam Interactions with Materials and Atoms* 181 (2001)489.
146. Papp Z., Filikhin I. N., Yakovlev S. L.: Integral equations for three-body Coulomb resonances. *SCI Few-Body Systems* 30 (2001)31.
147. Papp Z., Hu C. Y., Hlousek Z., Kónya B., Yakovlev S. L.: Three-potential formalism for the three-body scattering problem with attractive Coulomb interactions. *SCI Physical Review A* 63 (2001)2721.
148. Papp T., Campbell J. L.: Size and origin of the escape peak in various Si(Li) detectors. *SCI X-Ray Spectrometry* 30 (2001)77.
149. Paripás B., Vitéz G., Víkor Gy., Tókési K., Gulyás L.: Auger-electron lineshapes in electron impact ionization: a calculation for non-coincidence experiments. *SCI Journal of Physics B* 34 (2001)3301.
150. Paul E. S., Forbes S. A., Gizon J., Hauschild K., Hibbert I. M., Joss D. T., Nolan P. J., Nyakó B. M., Sampson J. A., Semple A. T., Wadsworth R., Walker L., Wilson J. N., Zolnai L.: Measurement of transition quadrupole moments of high-spin states in the $N=74$ isotopes 133Pr , 132Ce and 131La . *SCI Nuclear Physics A* 690 (2001)341.
151. Peeters F. M., Riva C., Varga K.: Trions in quantum wells. *SCI Physica B Condensed Matter* 300 (2001)139.
152. Perez G. E., Sohler D., Algora A., Dombrádi Zs., Nyakó B. M., Timár J., Zolnai L., Wyss R., Cederkall J., Johnson A., Kerek A., Klamra W., Norlin L. -O., Lipoglavsek M., Fahlander C., Likar A., Palacz M., Atac A., Nyberg J., Persson J., Gizon A., Gizon J., Boston A. J., Paul E. S., Grawe H., Schubart R., Joss D. T., Juutinen S., Makela E., et al.: Structure of high-spin states in 100Pd . *SCI Nuclear Physics A* 686 (2001)41.-63.
153. Petersen B., Baksay G., Nagy S., Raics P., Szillási Z., Tarján P., Veszprémi V., Zilizi Gy., et al.: First results from the L3+C experiment at CERN. *SCI Il Nuovo Cimento C* 24 (2001)751.

154. Pethes I., Sas B., Kriza Gy., Portier F., Williams F. I. B., Vad K., Mészáros S.: High-current differential resistance in Bi₂Sr₂CaCu₂O₈ single crystals. *SCI Synthetic Metals* 120 (2001)1013.
155. Pribóczki É., Elsinga Ph., Medema J., Vaalburg W., Horváth G., Kovács Z.: Novel oxidation method of (11C)carbon monoxide and (11C)methane on Fe/ZSM-5 zeolite. *SCI Journal of Labelled Compounds and Radiopharmaceuticals* 44 (2001)1026.
156. Raiola F., Gyürky Gy., Aliotta M., Formicola A., Bonetti R., Brogginì C., Campajola L., Corvisiero P., Constantini H., D'Onofrio A., Fülöp Zs., Gervino G., Gialanella L., Gulielmetti A., Gustavino C., Imbriani G., Junker M., Kavanagh R. W., Moroni P. G. P., Ordine A., Prati P., Roca V., Rogalla D., Rolfs C., Romano M., Schümann F., Somorjai E., Straniero O., Strieder F., et al.: Stopping power of low-energy deuterons in ³He gas. *SCI European Physical Journal A* 10 (2001)487.
157. Riva C., Peeters F. M., Varga K.: Magnetic field dependence of the energy of negatively charged excitons in semiconductor quantum wells. *SCI Physical Review B* 63 (2001)5302.
158. Riva C., Peeters F. M., Varga K.: Positively charged magnetoexcitons in a semiconductor quantum well. *SCI Physical Review B* 64 (2001)5301.
159. Roychoudhury R., Roy P., Znojil M., Lévai G.: Comprehensive analysis of conditionally exactly solvable models. *SCI Journal of Mathematical Physics* 42 (2001)1996.
160. Rudolph D., Gadea A., de Angelis G., Fahlander C., Algora A., Andreoiu C., Cardona R., Chandler C., Farnea E., Garcés Narro J., Nyberg J., Palacz M., Podolyák Zs., Steinhardt T., Thelen O.: The lifetime of the proton-decaying 8915 keV state in ⁵⁸Cu. *SCI Nuclear Physics A* 694 (2001)132.
161. Rudolph D., Fahlander C., Algora A., Andreoiu C., Cardona R., Chandler C., de Angelis G., Farnea E., Gadea A., Garcés Narro J., Nyberg J., Palacz M., Podolyák Zs., Steinhardt T., Thelen O.: Gamma-decay lifetime measurements in the second minimum of ⁵⁸Cu. *SCI Physical Review C Nuclear Physics* 63 (2001)2130.
162. Sarkadi L., Lugosi L., Tókési K., Gulyás L., Kövér Á.: Study of the transfer ionization process by observing the electron cusp in 100-300 keV He²⁺ + He collisions. *SCI Journal of Physics B* 34 (2001)4901.
163. Sarycheva L. I., Dajkó G., Fenyvesi A., Molnár J., Trócsányi Z., Szillási Z., Zilizi Gy., et al.: Heavy ion physics with compact muon solenoid at LHC. *SCI Nuclear Physics A* 681 (2001)229.
164. Seyboth P., Gál J., Molnár J., et al.: Results of the NA49 experiment on the search for the quark-gluon plasma at the CERN SPS. *SCI Acta Physica Hungarica New Series - Heavy Ion Physics* 14 (2001)361.
165. Seyboth P., Gál J., Molnár J., et al.: Correlations and fluctuations in Pb+Pb collisions. *SCI Nuclear Physics B Proceedings Supplement* 92 (2001)7.
166. Sheikh J. A., Kruppa A. T., Rowley N.: Chaos and isospin symmetry breaking in rotational nuclei. *SCI Nuclear Physics A* 694 (2001)233.
167. Simon A., Kántor Z., Rajta I., Szörényi T., Kiss Á Z.: Micro-RBS as a technique for the determination of the surface topography of Bi film prepared by pulsed laser deposition. *SCI Nuclear Instruments and Methods in Physics Research Section B: Beam Interactions with Materials and Atoms* 181 (2001)360.

168. Stolterfoht N., Sulik B., Hoffmann V., Skogvall B., Chesnel J. -Y., Rangama J., Frémont F., Hennecart D., Cassimi A., Husson X., Landers A. L., Tanis J. A., Galassi M. E., Rivarola R. D.: Evidence for interference effects in electron emission from H₂ colliding with 60 MeV/u Kr³⁴⁺ ions. *SCI Physical Review Letters* 87 (2001)3201.
169. Strieder F., Gialanella L., Gyürky Gy., Schümann F., Bonetti R., Brogginì C., Campajola L., Corvisiero P., Constantini H., D'Onofrio A., Formicola A., Fülöp Zs., Gervino G., Greife U., Guglielmetti A., Gustavino C., Imbriani G., Junker M., Moroni P. G. P., Ordine A., Prati P., Roca V., Rogalla D., Rolfs C., Romano M., Somorjai E., Straniero O., Terrasi F., Trautvetter H-P., Zavatarelli S.: Absolute cross section of ⁷Be(p, gamma)⁸B. *SCI Nuclear Physics A* 696 (2001)219.
170. Sulik B., Zouros T. J. M., Orbán A., Gulyás L.: Theoretical investigation of transfer-loss process in 0.2-2 MeV/u collisions of O⁵⁺ ions with H₂ and He targets. *SCI Journal of Electron Spectroscopy and Related Phenomena* 114 (2001)191.
171. Sulyok A., Gergely G., Menyhárd M., Tóth J., Varga D., Kövér L., Berényi Z., Lesiak B., Kosinski A.: Recoil effect in carbon structures and polymers. *SCI Vacuum* 63 (2001)371.
172. Szabó Cs., Biri S., Kenéz L., Suta T., Valek A.: Diagnostic reserach of highly ionized plasma generated by an ECR ion source. *SCI Vacuum* 61 (2001)391.
173. Szelecsényi F., Tárkányi F., Takács S., Hermanne A., Sonck M., Shubin Yu. N., Mustafa M. G., Youxiang Z.: Excitation function for the natTi(p,x)⁴⁸V nuclear process: Evaluation and new measurements for practical applications. *SCI Nuclear Instruments and Methods in Physics Research Section B: Beam Interactions with Materials and Atoms* 174 (2001)47.
174. Szelecsényi F., Suzuki K., Kovács Z., Takei M., Okada K.: Alpha beam monitoring via natCu+alpha processes in the energy range from 40 to 60 MeV. *SCI Nuclear Instruments and Methods in Physics Research Section B: Beam Interactions with Materials and Atoms* 184 (2001)589.
175. Szöör Gy., Elekes Z., Rózsa P., Uzonyi I., Simulák J., Kiss Á Z.: Magnetic spherules: Cosmic dust or markers of a meteoritic impact?. *SCI Nuclear Instruments and Methods in Physics Research Section B: Beam Interactions with Materials and Atoms* 181 (2001)557.
176. Söderman P. -O., Ringbom A., Blomgren J., Olsson N., Nilsson L., Bordewijk J. A., Brandenburg S., van't Hof G., Hofstee M. A., van der Ploeg H., van der Werf S. Y., Krasznahorkay A., Balanda A., Chmielewska D., Laurent H.: Neutron decay of deep hole states and isobaric analog states in ¹¹⁵Sn populated by the (³He, alpha) reaction at 102 MeV. *SCI Nuclear Physics A* 683 (2001)79.
177. Takeuchi S., Shimoura S., Motobayashi T., Akiyoshi H., Ando Y., Aoi N., Fülöp Zs., Gomi T., Higurashi Y., Hirai M., Iwasa N., Iwasaki H., Iwata Y., Kobayashi H., Kurokawa M., Liu Z., Minemura T., Ozawa S., Sakurai H., Serata M., Teranishi T., Yamada K., Yanagisawa Y., Ishihara M.: Isobaric analog state of ¹⁴Be. *SCI Physics Letters B* 515 (2001)255.
178. Takács E.4 , Berényi Z., Gillaspay J. D., Ratliff L. P., Minniti R., Pedulla J., Deslattes R. D., Stolterfoht N.: Separation of inner-shell vacancy transfer mechanisms in collisions of slow Ar¹⁷⁺ ions with SiO₂. *SCI Journal of Physics B* 34 (2001)1277.
179. Takács S., Szelecsényi F., Tárkányi F., Sonck M., Hermanne A., Shubin Yu. N., Dityuk A. I., Mustafa M. G., Youxiang Z.: New cross-sections and intercomparison of deuteron monitor reactions on Al, Ti, Fe, Ni and Cu. *SCI Nuclear Instruments and Methods in Physics Research Section B: Beam Interactions with Materials and Atoms* 174 (2001)235.

180. Terrasi F., Gialanella L., Imbriani G., Strieder F., Campajola L., D'Onofrio A., Greife U., Gyürky Gy., Lubritto C., Ordine A., Roca V., Rolfs C., Romano M., Rogalla D., Sabbarese C., Somorjai E., Trautvetter H-P.: Direct measurement of the absolute cross section of $p(7\text{Be}, \gamma)8\text{B}$. *SCI Nuclear Physics A* 688 (2001)539.
181. Thirof P. G., Gassmann D., Habs D., Chromik M., Eisermann Y., Graw G., Hertenberger R., Maier H. J., Metz A., Reiter P., Faestermann T., Krasznahorkay A., Hunyadi M., Csatlós M., Gulyás J., Máté Z., Pansegrau D., Scheit H., Schwalm D., Mengel E., Hübel H., Görden A.: Detailed spectroscopy in the superdeformed second minimum of 240Pu . *SCI Acta Physica Hungarica New Series - Heavy Ion Physics* 13 (2001)93.
182. Timár J., Gizon J., Gizon A., Sohler D., Nyakó B. M., Zolnai L., Cata-Danil Gh., Bucurescu D., Boston A. J., Joss D. T., Paul E. S., Semple A. T., Parry C. M., Brant S., Paar V.: Three-quasiparticle rotational bands in 101Rh : IBFBPM description and signature inversion of the $\pi 9/2$ orbital. *SCI Nuclear Physics A* 696 (2001)241.
183. Tougaard S., Krawczyk M., Jablonski A., Pavluch J., Tóth J., Varga D., Gergely G., Menyhárd M., Sulyok A.: Intercomparison of methods for separation of REELS elastic peak intensities for determination of IMFP. *SCI Surface and Interface Analysis* 31 (2001)1.
184. Tribedi L. C., Richard P., Gulyás L., Rudd M. E., Moshhammer R.: Two-center effect on low-energy electron emission in collisions of 1-MeV/u bare ions with atomic hydrogen, molecular hydrogen, and helium. I. Atomic hydrogen. *SCI Physical Review A* 63 (2001)2723.
185. Tribedi L. C., Richard P., Gulyás L., Rudd M. E.: Two-center effect on low-energy electron emission in collisions of 1MeV/u bare ions with atomic hydrogen, molecular hydrogen, and helium: II. H_2 and He. *SCI Physical Review A* 63 (2001)2724.
186. Turek K., Dajkó G.: Comparison of experimental and calculated responses of CR-39 to neutron spectra of Am-Be and 252Cf sources. *SCI Radiation Measurements* 34 (2001)625.
187. Tókési K., Wirtz L., Lemell C., Burgdörfer J.: Hollow-ion formation in microcapillaries. *SCI Physical Review A* 64 (2001)2902.
188. Uzonyi I., Rajta I., Bartha L., Kiss Á Z., Nagy A.: Realization of the simultaneous micro-PIXE analysis of heavy and light elements at a nuclear microprobe. *SCI Nuclear Instruments and Methods in Physics Research Section B: Beam Interactions with Materials and Atoms* 181 (2001)193.
189. Varga K.: Review of the recent applications of the stochastic variational method. *SCI Nuclear Physics A* 684 (2001)209.
190. Varga K., Navratil P., Usukura J., Suzuki Y.: Stochastic variational approach to few-electron artificial atoms. *SCI Physical Review B* 63 (2001)5308.
191. Varga D., Tókési K., Berényi Z., Tóth J., Kövér L., Gergely G., Sulyok A.: Energy shift and broadening of the spectra of electrons backscattered elastically from solid surfaces. *SCI Surface and Interface Analysis* 31 (2001)1019.
192. Vaupotic J., Csige I., Radolic V., Hunyadi I., Planinic J., Kobal I.: Methodology of radon monitoring and dose estimates in Postojna Cave, Slovenia. *SCI Health Physics* 80 (2001)142.
193. Vaupotic J., Hunyadi I., Baradács E.: Thorough investigation of radon in a school with elevated levels. *SCI Radiation Measurements* 34 (2001)477.

194. Viesti G., Rizzi V., Cinausero M., Gelli N., Gadea A., Bazzacco D., Algora A., Appelbe D., de Angelis G., Belcarì N., De Poli M., Drake T. E., Fabris D., Farnea E., Fioretto E., Galindo-Uribarri A., Królas W., Kröll T., Lucarelli F., Lunardi S., Lunardon M., Martínez T., Menegazzo R., Nayak B. K., Nebbia G., Napoli D. R., Nyakó B. M., Petrache C., Podolyák Zs., et al.: Observation of a double giant dipole resonance in fusion-evaporation reactions. *SCI Physical Review C Nuclear Physics* 63 (2001)4611.
195. Viesti G., Rizzi V., Fabris R., Lunardon M., Nebbia G., Cinausero M., Fioretto E., Prete G., Brondi A., La Rana G., Moro B., Vardaci E., Aiche M., Aleonard M. M., Barreau G., Boivin D., Scheurer J. N., Chemin J. F., Hagel K., Natowitz J. B., Wada R., Courtin S., Haas F., Rowley N., Nyakó B. M., Gál J., Molnár J.: Exploring the emission barriers in hot nuclei. *SCI Physics Letters B* 521 (2001)165.
196. Wagenbrunn R. F., Glozman L. Ya., Plessas W., Varga K.: Extended Goldstone-boson-exchange chiral quark model. *SCI Nuclear Physics A* 684 (2001)284.
197. Wilson A. N., Timár J., Ahmad I., Astier A., Azaiez F., Bergstrom M. H., Blumenthal D. J., Crowell B., Carpenter M. P., Ducroux L., Gall B. J. P., Hannachi F., Hübel H., Khoo T. L., Janssens R. V. F., Korichi A., Lauritsen T., Lopez-Martens A., Meyer M., Nisius D., Paul E. S., Porquet M. G., Redon N., Sharpey-Schafer J. F., Wadsworth R., Wilson J. N., Ragnarsson I.: Magnetic dipole bands in ^{190}Hg : first evidence of excitations across the $Z=82$ sub-shell in Hg nuclei. *SCI Physics Letters B* 505 (2001)6.
198. Yoneda K., Sakurai H., Gomi T., Motobayashi T., Aoi N., Fukuda N., Futakami U., Gácsi Z., Higurashi Y., Imai N., Iwasa N., Iwasaki H., Kubo T., Kunibu M., Kurokawa M., Liu Z., Minemura T., Saito A., Serata M., Shimoura S., Takeuchi S., Watanabe Y. X., Yamada K., Yanagisawa Y., Yogo K., Yoshida A., Ishihara M.: Deformation of ^{34}Mg studied via in-beam gamma-ray spectroscopy using radioactive-ion projectile fragmentation. *SCI Physics Letters B* 499 (2001)233.
199. Yuqian M. A., Baksay G., Raics P., Szillási Z., Zilizi Gy., et al.: Cosmic ray muon measurement by L3 Spectrometer at CERN. *SCI Modern Physics Letters A* 16 (2001)1667.
200. Znojil M., Lévai G.: Spontaneous breakdown of PT symmetry in the solvable square-well model. *SCI Modern Physics Letters A* 16 (2001)2273.
201. Znojil M., Lévai G., Roy P., Roychoudhury R.: Anomalous doublets of states in a PT symmetric quantum model. *SCI Physics Letters A* 290 (2001)249.

8.2 Conference contributions, talks and reports

1. de la Pena L. H., Hess P. O., Algora A., Lévai G.: Alpha-clustering in Be isotopes. *SCI Acta Physica Hungarica New Series - Heavy Ion Physics* 13 (2001)197.
2. de la Pena L. H., Hess P. O., Lévai G., Algora A.: Alpha-cluster structure in Be isotopes. *SCI Journal of Physics G Nuclear and Particle Physics* 27 (2001)2019.
3. Acciarri M., Baksay G., Raics P., Szillási Z., Sztaricskai T., Zilizi Gy., et al.: Moments of the charged particle multiplicity distribution in Z decays at LEP. *roceedings of 30th International Symposium on Multiparticle Dynamics (ISMD 2000). From e+e- to Heavy Ion Collisions. Tihany, Lake Balaton, Hungary, 9-15 Oct., 2000. Eds.: Csörgő T., Hegyi S. and Kittel W. Singapore, World Scientific* 0 (2001)312.
4. Arai K., Kruppa A. T.: Continuum level density in the microscopic cluster model: Parameters of resonances. *Few-Body Systems Supplement* 13 (2001)105.
5. Baksay L., Bencze Gy. L., Brunel L., Fenyvesi A., Molnár J., Molnár L., Novák D., Pszota G., Raics P., Szabó Zs.: Neutron radiation tolerance tests of optical and opto-electronic components for the CMS Muon Barrel Alignment. *roceedings of the Seventh Workshop on Electronics for LHC Experiments. Stockholm, Sweden, 10-14 Sept., 2001. Geneva, Sweden (CERN 2001-005, CERN/LHCC2001-034, 22 October 2001)* 0 (2001)132.
6. Balogh K., Pécskay Z.: K/Ar and Ar/Ar geochronological studies in the Pannonian-Carpathians-Dinarides (PANCARDI) region. *Acta Geologica Hungarica* 44 (2001)281.
7. Barczyk A. J., Baksay G., Raics P., Szillási Z., Zilizi Gy., et al.: Two photon collisions at LEP: K0(S) K0(S) final state, glueball searches and lambda antilambda production. *roceedings of 30th International Conference on High-Energy Physics (ICHEP 2000). Osaka, Japan, 27 July -Aug., 2000. Eds: C.S. Lim, T. Yamanaka. Singapore, World Scientific*(2001)369.
8. Beke D. L., Langer G. A., Csík A., Erdélyi Z., Kis-Varga M., Szabó I. A., Papp Z. M.: Diffusion and thermal stability in multilayers. *Defect and Diffusion Forum* 194 (2001)1403.
9. Berényi D.: Az atomfizika helye és szerepe a tudományban és a gyakorlatban. *Millennium az Akadémián. Közgyűlési előadások 2000. Szerk.: Glatz F. Bp., MTA*(2001)1695.
10. Biri S., Jánossy A., Kenéz L., Kitagawa A., Szabó Cs., Valek A.: Status and new developments at the 14.5 GHz ATOMKI-ECRIS. *roceedings of the Workshop on the Production of Intense Beams of Highly Charged Ions. Catania, 24-27 Sept., 2000. PIBHI-2000. Eds: S. Gammino and G. Ciavola. Bologna, INFN, LNS. (Conference Proceedings)* 72 (2001)73.
11. Brandolini F., Lenzi S. M., Ur C. A., Bazzacco D., Menegazzo R., Pavan P., Rossi-Alvarez C., Medina N. H., Ribas R. V., Marginean N., Napoli D. R., de Angelis G., De Poli M., Martínez T., Algora A., Gadea A., Farnea E., Bucurescu D., Ionescu-Bujor M., Iordachescu A., Cameron J. A., Kasemann S., Schneider I., Espino J. M., Poves A., Sanchez-Solano J.: Collective motions in the 1f7/2 shell. *Nuclear structure. Proceedings of the Conference: Bologna 2000. Structure of the Nucleus at the Dawn of the Century. 29 May -June, 2000. Bologna, Italy. Eds.: G.C.Bonsignori et al. New Jersey, etc., World Scientific*(2001)281.
12. Cseh J.: Clusterization and composite symmetries. *roceedings of International Symposium on Nuclear Structure Physics. Göttingen, Germany, 5-8 March, 2001. Eds: R. Casten, J. Jolie, U. Kneissl, at al. Singapore, World Scientific* 0 (2001)337.

13. Csikai Gy., Király B., Dóczy R.: Application of neutrons to plastic landmines detection. IAEA RCM (Research Co-ordination Meeting). St.Peterburg, Russia, Sept. 11-14, 2001. Proceedings. CD-ROM. IAEA/PS/RC-799-2. Vienna 0 (2001)46.
14. Dezső Z., Hakl J., Molnár L.: Barlangi kőzetek radon exhalációja. Karsztfejlődés. Szombathely, BDF Természetföldrajzi Tanszék. Szerk.: Veress M. 6 (2001)305.
15. Dóczy R., Király B., Fenyvesi A., Shtejer Diaz K., Csikai Gy.: Excitation functions of some neutron induced reactions. roceedings of the 3rd International Conference of PhD Students. University of Miskolc, Hungary, 13-19 Aug., 2001. Natural Science. Miskolc, Innovation and Technology Transfer Centre 0 (2001)127.
16. Etiopie G., Hakl J.: The "geogas" theory. roceedings of the 5th International Conference on Rare Gas Geochemistry. 30 Aug. -Sept., 1999, Debrecen, Hungary. Ed.: I. Hunyadi, I. Csige, J. Hakl. Debrecen, EP Systema 0 (2001)7.
17. Farnea E., Gadea A., Rubio B., Tain J. L., de Angelis G., Algora A., Belcari N., De Poli M., Fioretto E., Martínez T., Napoli D. R., Prete G. F., Spolaore P., Eberth J., Steinhardt T., Thelen O., Dewald A., Skoda S., Bazzacco D., Brandolini F., Isocrate R., Lenzi S. M., Lunardi S., Pavan P., Rossi-Alvarez C., Bizzeti P. G., Bizzeti-Sona A. M., Gelletly W., Petrache C. M.: Determination of the isospin impurity in ^{64}Ge . Nuclear structure. Proceedings of the Conference: Bologna 2000. Structure of the Nucleus at the Dawn of the Century. 29 May -June, 2000. Bologna, Italy. Eds.: G.C.Bonsignori et al. New Jersey, etc., World Scientific(2001)272.
18. Futó I., Hertelendi E., Szántó Zs., Vető I.: Isotope geochemistry of methane dissolved in formation waters of SE-Hungary. roceedings of the 5th International Conference on Rare Gas Geochemistry. 30 Aug. -Sept., 1999, Debrecen, Hungary. Ed.: I. Hunyadi, I. Csige, J. Hakl. Debrecen, EP Systema 0 (2001)89.
19. Galindo E., Hausmann M., Jungclaus A., Lieb K. P., Müller G. A., Yordanov O., Algora A., de Angelis G., Bizzeti P. G., Brandolini F., Dewald A., Fahlander C., Gadea A., Górska M., Grawe H., Martínez T., Napoli D. R., Peusquens R., De Poli M., Tiesler H.: Coincidence lifetime-measurements in ^{101}Ag . roceedings of International Symposium on Nuclear Structure Physics. Göttingen, Germany, 5-8 March, 2001. Eds: R. Casten, J. Jolie, U. Kneissl, at al. Singapore, World Scientific(2001)355.
20. Hakl J., Dezső Z., Somlai J., Várhegyi A.: Barlangászok radontól eredő sugárterhelése Magyarországon. Barlangkutatók szakmai találkozója. 2000. október 27-29. Pécs, Tudományegyetem. Szerk.: Sásdi L. Pécs, Pécsi Tudományegyetem, Magyar Karszt- és Barlangkutató Társulat 0 (2001)91.
21. Harissopoulos S., Demetriou P., Kokkoris M., Galanopoulos S., Tsagari P., Skreti E., Paradellis T., Kunz R., Hammer J. W., Somorjai E., Gyürky Gy., Fülöp Zs.: Cross section measurements of (p, gamma)-reactions relevant to the nucleosynthetic p-process. roceedings of International Symposium on Nuclear Structure Physics. Göttingen, Germany, 5-8 March, 2001. Eds: R. Casten, J. Jolie, U. Kneissl, at al. Singapore, World Scientific 0 (2001)359.
22. Hebbeker T., Baksay G., Nagy S., Raics P., Szillási Z., Tarján P., Veszprémi V., Zilizi Gy., et al.: First results from the L3+C experiment at CERN. roceedings of 30th International Conference on High-Energy Physics (ICHEP 2000). Osaka, Japan, 27 July -Aug., 2000. Eds: C.S. Lim, T. Yamanaka. Singapore, World Scientific(2001)1028.

23. Hertelendi E., Futó I., Palcsu L., Molnár M.: Isotope geochemistry of headspace gases of ground-water samples from the aleurit formation near Mecsek mountains, Hungary. roceedings of the 5th International Conference on Rare Gas Geochemistry. 30 Aug. -Sept., 1999, Debrecen, Hungary. Ed.: I. Hunyadi, I. Csige, J. Hakl. Debrecen, EP Systema 0 (2001)81.
24. Hess E., Takács S., Scholten B., Tárkányi F., Coenen H. H., Qaim S. M.: Nuclear data for ^{18}F -production via the $^{180}(\text{p},\text{n})^{18}\text{F}$ process with protons of energies up to 30 MeV. Journal of Labelled Compounds and Radiopharmaceuticals. Supplement 44 (2001)1055.
25. Ivanova J., Pécskay Z., Yanev Y.: K-Ar ages of the volcanic rocks from the paleogene Sheinovets Caldera, Eastern Rhodopes (Bulgaria). Comptes Rendus de l' Academie Bulgarie des Sciences. Geologie, Pétrographie 54 (2001)59.
26. Iwasaki H., Motobayashi T., Akiyoshi H., Ando Y., Fukuda N., Fujiwara H., Fülöp Zs., Hahn K. I., Higurashi Y., Hirai M., Hisanaga I., Iwasa N., Kijima T., Mengoni A., Minemura T., Nakamura T., Notani M., Ozawa S., Sagawa H., Sakurai H., Shimoura S., Takeuchi S., Teranishi T., Yanagisawa Y., Ishihara M.: Experimental studies of E1 and E2 transitions in ^{12}Be . RIKEN Review 39 (2001)42.
27. Kink I., Laming I. M., Takács E., Porto J., Gillaspay J. D., Silver E., Schnopper H. W., Bandler S. R., Barbera M., Brickhouse N. S., Murray S. S., Madden N., Landis D., Beeman J., Haller E. E.: Microcalorimeter/EBIT measurements of X-ray spectra of highly charged ions. hysica Scripta T 92 (2001)454.
28. Kirchner T., Gulyás L.: Differential net- and multiple-ionization cross sections in fast highly-charged ion collisions with atoms. hysica Scripta T 92 (2001)348.
29. Király B., Csikai Gy.: Location and identification of concealed objects using neutrons. roceedings of the 7th International Conference on Applications of Nuclear Techniques, Nuclear and Atomic Industrial and Analytical Applications. Crete, Greece, 17-23 June, 2001 (CD-ROM) 0 (2001)1.
30. Király B., Csikai Gy., Dóczy R.: Validation of neutron data libraries by differential and integral cross sections. roceedings of 2000 Symposium on Nuclear Data. JAERI, Tokai, Japan, 16-17 Nov., 2000. Vienna, IAEA. JAERI-Conf 2001-006, INDC(JPN)-188/4 0 (2001)283.
31. Koltay E.: Atommagfizika: utak, célok, hatások. Millennium az Akadémián. Közgyűlési előadások 2000. Szerk.: Glatz F. Bp., MTA(2001)1705.
32. Korichi A., Wilson A. N., Hannachi F., Lopez-Martens A., Rejmund M., Schüick C., Vieu Ch., Chmel G., Georgen A., Hübel H., Rossbach D., Schönwasser G., Bergström M., Nyakó B. M., Timár J., Bazzacco D., Lunardi S., Rossi-Alvarez C., Bednarczyk P., Kintz N., Naguleswaran S., Astier A., Cullen D. Mc., Sharpey-Schafer J. F., Lauritsen T., Wadsworth R.: Octopole vibration in the superdeformed well: First experimental evidence. Nuclear structure. Proceedings of the Conference: Bologna 2000. Structure of the Nucleus at the Dawn of the Century. 29 May -June, 2000. Bologna, Italy. Eds.: G.C.Bonsignori et al. New Jersey, etc., World Scientific(2001)312.
33. Krasznahorkay A., Hunyadi M., Csatlós M., Gulyás J., Máté Z., Habs D., Gassmann D., Graw G., Eisermann Y., Hertenberger R., Maier H. J., Metz A., Ott J., Thierolf P. G., Faestermann T., Harakeh M. N., van der Werf S. Y.: Super- and hyperdeformed states in the actinide region. Nuclear structure. Proceedings of the Conference: Bologna 2000. Structure of the Nucleus at the Dawn of the Century. 29 May -June, 2000. Bologna, Italy. Eds.: G.C.Bonsignori et al. New Jersey, etc., World Scientific(2001)306.

34. Krieger P., Dienes B., Horváth D., Trócsányi Z., Ujvári B., et al.: OPAL searches for prompt light gravitino production at LEP. *International Journal of Modern Physics A Supplement* 16 (2001)786.
35. Landers A. L., Pole D. L., Erickcek S., Ferguson S. M., Chesnel J. -Y., Sulik B., Tanis J. A.: Coherence in two-electron transfer in $F(8+) + Ne$ collisions. *Physica Scripta T* 92 (2001)354.
36. Lovas R. G., Tanaka N., Suzuki Y., Varga K.: Nuclear resonances by extrapolation of bound states. *Few-Body Systems Supplement* 13 (2001)76.
37. Lukic D. V., Focke P. R., Koncz Cs., Morozov V. A., Meyer F. W., Sellin I. A.: Autoionization of doubly and triply excited states of Li^+ and Li produced in Li^{3+} ion collision with $C60$, Ar and Xe . *Physica Scripta T* 92 (2001)174.
38. Lévai G., Cseh J., Van Isacker P.: Symmetry aspects of nuclear cluster systems. Nuclear structure. Proceedings of the Conference: Bologna 2000. Structure of the Nucleus at the Dawn of the Century. 29 May -June, 2000. Bologna, Italy. Eds.: G.C.Bonsignori et al. New Jersey, etc., World Scientific(2001)386.
39. Lévai G.: Correlations between cluster systems: a supersymmetric approach. Proceedings of International Symposium on Nuclear Structure Physics. Göttingen, Germany, 5-8 March, 2001. Eds: R. Casten, J. Jolie, U. Kneissl, et al. Singapore, World Scientific 0 (2001)369.
40. Maenhaut W., Fernández-Jiménez M. -T., Rajta I., Artaxo P.: Two-year study of atmospheric aerosols in Alta Floresta, Brazil: Multielemental composition, sources and source apportionment. *Journal of Aerosol Science Supplement* 32 (2001)469.
41. Mangeol D. J., Baksay G., Szillási Z., Zilizi Gy., et al.: Moments of the charged-particle multiplicity distribution in Z decays at LEP. Proceedings of 30th International Symposium on Multiparticle Dynamics (ISMD 2000). From e^+e^- to Heavy Ion Collisions. Tihany, Lake Balaton, Hungary, 9-15 Oct., 2000. Eds.: Csörgő T., Hegyi S. and Kittel W. Singapore, World Scientific 0 (2001)312.
42. Mindszenty A., Csoma A., Török Á., Hips K., Hertelendi E.: Flexura jellegű elötéri deformációhoz köthető karsztbauxitszintek a Dunántúli-középhegységben. *Földtani Közlöny* 131 (2001)107.
43. Molnár M., Palcsu L., Svingor É., Szántó Zs., Futó I., Ormai P.: Composition and activity variations in bulk gas of drum waste packages of Paks NPP. International Conference, Nuclear Energy in Central Europe. Portorz, Slovenia, 10-13 Sept., 2001. Proceedings, CD-ROM. Eds: I. Jencic, et al. Ljubljana, Nuclear Society of Slovenia 0 (2001)610.
44. Molnár M., Palcsu L., Pintér T., Patek G., Szántó Zs., Svingor É., Futó I.: Monitoring of steam generators by a portable QMS. Proceedings of the 5th International Seminar on Primary and Secondary Side Water Chemistry of Nuclear Power Plants. Eger, Hungary, 17-20 Sept., 2001 0 (2001)1.
45. Müller G. A., Galindo E., Hausmann M., Jungclaus A., Kast D., Lieb K. P., Yordanov O., Algora A., de Angelis G., Bizzeti P. G., Brandolini F., Brant S., Dewald A., Fahlander C., Gadea A., Górska M., Grawe H., Martínez T., Napoli D. R., Peusquens R., De Poli M., Tiesler H.: Competing collective and quasiparticle structures in the transitional nucleus ^{104}Cd . Proceedings of International Symposium on Nuclear Structure Physics. Göttingen, Germany, 5-8 March, 2001. Eds: R. Casten, J. Jolie, U. Kneissl, et al. Singapore, World Scientific(2001)385.

46. Novák D., Kerek A., Norlin L. -O., Dajkó G., Fenyvesi A., Molnár J., Székely G., Granholm L., Wallin S., Matilainen A., Virtanen A.: COTS DRAM's as Mass Memory for the European SMART-1 spacecraft. roceedings of the 5th European CMSE Commercialization Military and Space Electronics Conference and Exhibition. Nice, France, 17-20 Sept., 2001 0 (2001)18.
47. Palcsu L., Molnár M., Szántó Zs., Svingor É., Futó I., Pintér T.: Dissolved stable noble gas measurements from primary water of Paks NPP. International Conference, Nuclear Energy in Central Europe. Portorz, Slovenia, 10-13 Sept., 2001. Proceedings, CD-ROM. Eds: I. Jencic, et al. Ljubljana, Nuclear Society of Slovenia 0 (2001)612.
48. Palcsu L., Pintér T., Molnár M., Mogyorósi M., Szántó Zs., Svingor É., Futó I.: Dissolved stable noble gas measurements from primary water of Paks NPP. roceedings of the 5th International Seminar on Primary and Secondary Side Water Chemistry of Nuclear Power Plants. Eger, Hungary, 17-20 Sept., 2001 0 (2001)1.
49. Papp Z., Yakovlev S. L., Hu C. Y., Darai J., Filikhin I. N., Kónya B.: Resonant-state solution of the Faddeev-Merkuriev integral equations for three-body systems with Coulomb-like potentials. Few-Body Systems Supplement 13 (2001)152.
50. Podolyák Zs., Bizzeti P. G., Bizzeti-Sona A. M., Gadea A., Lunardi S., Bazzacco D., Dewald A., Algora A., de Angelis G., De Poli M., Farnea E., Kasemann S., Klug T., Kröll Th., Lenzi S. M., Martínez T., Napoli D. R., Petrache C., Peusquens R., Rossi-Alvarez C., Ur C. A., Kleinheinz P., Blomqvist J.: Competition between octupole and shell model states near the doubly closed 146Gd. roceedings of International Symposium on Nuclear Structure Physics. Göttingen, Germany, 5-8 March, 2001. Eds: R. Casten, J. Jolie, U. Kneissl, at al. Singapore, World Scientific(2001)391.
51. Pribóczki É., Kovács Z., Horváth G., Lehtikoinen P.: A modified method to form (11C)methanol on a column for synthesis of (11C)methyl iodide. roceedings of the 8th Workshop on Targetry and Target Chemistry. Ed: T. J. McCarthy. June 23-26, 1999. St.Louis, Missouri, USA 0 (2001)184.
52. Przybycien M., Dienes B., Horváth D., Trócsányi Z., et al.: Measurement of the cross-section for the process $E E \rightarrow E E \gamma^{(*)} \gamma^{(*)} \rightarrow EEX$ at $S^{**}(1/2) = 189$ GeV to 202 GeV. HOTON 2000: International Workshop on Structure and Interactions of the Photon Proceedings. Ambleside, Lake District, England, 26-31 Aug., 2000. Ed.: A.J. Finck. Melville, AIP. (AIP Confernece Proceedings 571) 571 (2001)147.
53. Puccio W., Lundin R., Lindblad Th., Janvier B., Kerek A., Klamra W., Norlin L. -O., Molnár J., Novák D., Székely G., Winningham J. D.: Hugin and Munin - Two Swedish nano-satellites based on COTS. roceedings of the 5th European CMSE Commercialization Military and Space Electronics Conference and Exhibition. Nice, France, 17-20 Sept., 2001 0 (2001)215.
54. Pécskay Z., Harkovska A., Zidarov N., Zagorchev I., Popov M., Panteva V.: K-Ar dating of the Tertiary volcanic rocks from Ograzden and Maleshevaska Mountains, South-Western Bulgaria. Comptes Rendus de l'Académie Bulgare des Sciences, Geologie, Volcanologie 54 (2001)71.
55. Ringkjøbing Jensen D., Hagemann G. B., Herskind B., Sletten G., Bergström M., Varmette P. G., Törmanen S., Nielsen B. S., Domscheit J., Hübel H., Ma W., Bracco A., Camera F., Demaria F., Frattini S., Million B., Napoli D. R., Maj A., Nyakó B. M., Joss D. T., Aiche M.: Co-existing coupling schemes for identical orbitals in 6-quasiparticle states. Nuclear structure. Proceedings of the Conference: Bologna 2000. Structure of the Nucleus at the Dawn of the

- Century. 29 May -June, 2000. Bologna, Italy. Eds.: G.C.Bonsignori et al. New Jersey, etc., World Scientific(2001)302.
56. Rosca A., Baksay G., Nagy S., Raics P., Szillási Z., Tarján P., Veszprémi V., Zilizi Gy., et al.: Search for a Higgs boson decaying into two photons with the L3 detector at LEP. *International Journal of Modern Physics A Supplement* 16 (2001)843.
57. Rosu E., Szakács A., Downes H., Seghedi I., Pécskay Z., Panaiotu C.: The origin of neogene calc-alkaline and alkaline magmas in the Apuseni Mountains, Romania: The Adakite connection. *Romanian Journal of Mineral Deposits Supplements* 79 (2001)3.
58. Schwengner R., Plettner C., Schnare H., Kaubler L., Dönauf F., Ragnarsson I., Afanasjev A. V., Algora A., de Angelis G., Gadea A., Napoli D. R., Eberth J., Steinhardt T., Thelen O., Hausmann M., Müller A., Jungclaus A., Lieb K. P., Jenkins D. G., Wadsworth R., Wilson A. N., Frauendorf S.: Signature inversion caused by triaxiality in ^{72}Br and band termination in ^{73}Br . Nuclear structure. Proceedings of the Conference: Bologna 2000. Structure of the Nucleus at the Dawn of the Century. 29 May -June, 2000. Bologna, Italy. Eds.: G.C.Bonsignori et al. New Jersey, etc., World Scientific(2001)276.
59. Seliger M., Tökési K., Reinhold C. O., Burgdörfer J., Takabayashi Y., Ito T., Komaki K., Azuma T., Yamazaki Y.: Relativistic electron transport through carbon foils. *Physica Scripta T* 92 (2001)211.
60. Simon M., Bohátka S.: Fringing field effect in prefiltered quadrupole mass spectrometer. *Advances in Mass Spectrometry* 15 (2001)483.
61. Ströbele H., Gál J., Molnár J., et al.: Particle production in Pb+Pb collisions at 158 GeV/nucleon in the Na49 detector. Nucleus-nucleus collisions. Proceedings of the Conference: Bologna 2000. Structure of the Nucleus at the Dawn of the Century. Bologna, Italy, May 29 - June 3, 2000. Eds: G.C. Bonsignori, et al. New Jersey etc., World Scientific(2001)99.
62. Sulik B., Tökési K., Koncz Cs., Kövér Á., Ricz S., Orbán A., Stolterfoht N., Chesnel J. -Y., Berényi D.: Multiple scattering of the emitted electrons in intermediate velocity C+ + Ne collisions: Search for Fermi-Shuttle acceleration in experiment and CTMC calculations. *Physica Scripta T* 92 (2001)463.
63. Szelecsényi F., Takács S., Tárkányi F., Sonck M., Hermanne A.: New cross section data on $^{nat}\text{Ti}(p,x)^{48}\text{V}$ nuclear process: Monitoring of proton beam and production of ^{48}V . Synthesis and applications of isotopically labelled compounds. Vol. 7.: Proceedings of the Seventh International Symposium, Dresden, Germany, 18-22 June 2000. Eds: Ulrich Pleiss and Rolf Voges. Chichester, etc., John Wiley and Sons, Ltd. 0 (2001)45.
64. Szántó Zs., Palcsu L., Futó I., Molnár M., Svingor É.: A vízbázisvédelem jelentősége, megvalósításának lépései - vízbázis sérülékenység vizsgálati módszerek. A földrajz eredményei az új évezred küszöbén. Magyar Földrajzi Konferencia. Szeged, 2001. október 25-27. 0 (2001)0.
65. Szántó Zs., Palcsu L., Futó I., Molnár M., Svingor É.: A vízbázisvédelem jelentősége, megvalósításának lépései - vízbázis sérülékenység vizsgálati módszerek. A földrajz eredményei az új évezred küszöbén. Magyar Földrajzi Konferencia. Szeged, 2001. október 25-27. Szegedi Tudományegyetem TTK Természeti Földrajzi Tanszéke. CD 0 (2001)1.
66. Szántó Zs., Szűcs Z., Svingor É., Molnár M., Palcsu L., Futó I., Vajda N., Molnár Zs., Kabai É.: Determination of ^{129}I in low level radioactive waste by two different methods. *International*

- Conference, Nuclear Energy in Central Europe. Portorz, Slovenia, 10-13 Sept., 2001. Proceedings, CD-ROM. Eds: I. Jencic, et al. Ljubljana, Nuclear Society of Slovenia 0 (2001)802.
67. Szántó Zs., Svingor É., Futó I., Palcsu L., Molnár M.: Application of carbon isotope analysis in food technology. *Studia Universitatis Babeş-Bolyai, Physica. Special Issue*(2001)124.
 68. Trigger I., Dienes B., Horváth D., Trócsányi Z., Ujvári B., et al.: Search for charginos and neutralinos by the OPAL collaboration at LEP. *International Journal of Modern Physics A Supplement* 16 (2001)778.
 69. Trigger I., Dienes B., Horváth D., Trócsányi Z., Ujvári B., et al.: Search for scalar partners of fermions by the OPAL collaboration at LEP. *International Journal of Modern Physics A Supplement* 16 (2001)807.
 70. Tőkési K., Tong X. -M., Lemell C., Burgdörfer J.: Surface dielectric properties probed by microcapillary transmission of highly charged ions. *Physica Scripta T* 92 (2001)27.
 71. Ur C. A., Rossi-Alvarez C., Bazzacco D., Kröll T., Lenzi S., Lunardi S., Pavan P., Spolaore P., Algora A., de Angelis G., De Poli M., Gadea A., Marginean N., Martínez T., Napoli D. R., Bucurescu D., Ionescu-Bujor M., Iordachescu A.: Study of the symmetric system $90\text{Zr} + 90\text{Zr}$ at GASP. Nuclear structure. Proceedings of the Conference: Bologna 2000. Structure of the Nucleus at the Dawn of the Century. 29 May -June, 2000. Bologna, Italy. Eds.: G.C.Bonsignori et al. New Jersey, etc., World Scientific(2001)205.
 72. Vallasek I., Erdélyi G., Langer G. A., Beke D. L.: Ni short circuit diffusion in alumina. *Defect and Diffusion Forum* 194 (2001)1033.
 73. Vossebeld J. H., Dienes B., Horváth D., Trócsányi Z., et al.: Recent results on particle production from OPAL. roceedings of 30th International Symposium on Multiparticle Dynamics (ISMD 2000). From $e+e-$ to Heavy Ion Collisions. Tihany, Lake Balaton, Hungary, 9-15 Oct., 2000. Eds.: Csörgő T., Hegyi S. and Kittel W. Singapore, World Scientific 0 (2001)125.
 74. Yordanov O., Galindo E., Hausmann M., Jungclaus A., Müller G. A., Lieb K. P., Brandolini F., Napoli D. R., Algora A., Martínez T., Gadea A., Górska M.: Lifetime measurements of a magnetic shears band in 104In . roceedings of International Symposium on Nuclear Structure Physics. Göttingen, Germany, 5-8 March, 2001. Eds: R. Casten, J. Jolie, U. Kneissl, at al. Singapore, World Scientific(2001)419.
 75. Zolnai L.: Tudománymetria és intézeti kollaboráció. *Fizikai Szemle* 51 (2001)264.

8.3 Theses

1. Elekes Z.: Ion beam based nuclear microanalysis of geological and archeological objects. Supervisor: A.Z. Kiss. Debrecen, University of Debrecen, Faculty of Sciences 0 (2001)114.
2. Gyürky Gy.: Magreakció vizsgálatok a nukleáris asztrofizika területén. Doktori (PhD) értekezés. Témavezető: Somorjai E. Debrecen, Debreceni Egyetem Természettudományi Kar 0 (2001)83.

8.4 Diploma work

1. Dobos E.: Detektálási módok kipróbálása a pásztázó transzmissziós ionmikroszkópia (STIM) módszerének megvalósításához az Atomki pásztázó nukleáris mikroszondájánál. Diplomamunka. Témavezető: Kiss árpád Zoltán. DETTK - Atomki Környezetfizikai Tanszék. 0 (2001)32.
2. Máté Z.: Számítógéppel segített adatgyűjtés és adatfeldolgozás ATOMKI ESA-31 típusú felületvizsgáló berendezésnél. Diplomamunka. Témavezető: Csery István. Debrecen, Atomki 0 (2001)50.
3. Papp H.: Gamma-átmenetek multipolaritásának meghatározása a ^{131}Ce atommag normáldeformált sávjaiban. Diplomamunka. Témavezető: Nyakó Barna. Debrecen, Atomki 0 (2001)36.
4. Rakos B.: Részecske-gamma koincidencia módszer alkalmazása extrém magdeformációk keresésében. Diplomamunka. Témavezető: Nyakó B. Debrecen, Atomki 0 (2001)43.
5. Szűcs N.: A felszín és a barlang kölcsönhatásának vizsgálata a Szemlő-hegyi-barlangban. Diplomamunka. Témavezető: Hunyadi Ilona, Csige István. Debrecen, DE, Atomki 0 (2001)42.

8.5 Book, chapter of book

1. Hermanne A., Gul K., Mustafa M. G., Nortier M., Oblozinsky P., Qaim S. M., Scholten B., Shubin Yu. N., Tárkányi F., Takács S., Youxiang Z.: Production cross-sections for diagnostic radioisotopes (Chapter 5). Gamma emitters (5.1). Charged particle cross-section database for medical radioisotope production: diagnostic radioisotopes and monitor reactions. Vienna, IAEA. IAEA-TECDOC-1211. (<http://www.nds.or.at/medical>)(e) 0 (2001)153.
2. Paripás B., Vitéz G., Víkor Gy., Tökési K.: Influence of post collision interaction on the line-shape of Auger-electron spectra in electron impact ionization. Many-particle spectroscopy of atoms, molecules, clusters, and surfaces. Eds.: J. Berakdar, J. Kirschner. New York, etc., Kluwer Academic - Plenum Publishers 0 (2001)149.
3. Qaim S. M., Tárkányi F., Takács S., Hermanne A., Nortier M., Oblozinsky P., Scholten B., Shubin Yu. N., Shubin Yu. N., Youxiang Z.: Production cross-sections for diagnostic radioisotopes (Chapter 5). Positron emitters (5.2). Charged particle cross-section database for medical radioisotope production: diagnostic radioisotopes and monitor reactions. Vienna, IAEA. IAEA-TECDOC-1211. (<http://www.nds.or.at/medical>)(e) 0 (2001)234.
4. Tárkányi F.: Experimental evaluation (Chapter 2). Compilation of experimental data (2.1). Analysis and selection of experimental data (2.2). Charged particle cross-section database for medical radioisotope production: diagnostic radioisotopes and monitor reactions. Vienna, IAEA. IAEA-TECDOC-1211 0 (2001)9.
5. Tárkányi F., Takács S., Gul K., Hermanne A., Mustafa M. G., Nortier M., Oblozinsky P., Qaim S. M., Scholten B., Shubin Yu. N., Youxiang Z.: Beam monitor reactions (Chapter 4). Charged particle cross-section database for medical radioisotope production: diagnostic radioisotopes and monitor reactions. Vienna, IAEA. IAEA-TECDOC-1211. (<http://www.nds.or.at/medical>)(e) 0 (2001)49.
6. Tárkányi F., Andó L., Szűcs Z., Mahunka I., Kovács Z.: Solid targets and irradiation facilities for production of diagnostic and therapeutic radionuclides at the Debrecen Cyclotron. Report on the 1st Research Co-ordination Meeting of the Co-ordinated Research Project on "Standardized High Current Solid Targets for Cyclotron Production of Diagnostic and Therapeutic Radionuclides." 27-30 Nov., 2000, Brussels, Belgium, IAEA, Vienna 0 (2001)1.

8.6 Edited work

1. Hunyadi I., Csige I., Hakl J.: Proceedings of the 5th International Conference on Rare Gas Geometry. 30 Augustus -September, 1999. Debrecen, Hungary. Edited by I. Hunyadi, I. Csige and J. Hakl. Debrecen, EP Systema 0 (2001)352.
2. Kruppa A. T., Lovas R. G.: Resonances in Few-Body Systems. Proceedings of the International Workshop. Sáropatak, Hungary, Sept., 4-8, 2000. Eds.: A.T. Kruppa and R.G. Lovas. Few-Body Systems Supplement 13 (2001)303.

8.7 Hebdomadal Seminars

1. January 25 *Charge particle reactions in practice* S. Takács
2. February 15 *Production of radio isotopes and radio farmacons for nuclear medicine* Z. Szűcs
3. March 1 *Micro analysis of geological and archeological samples by ion beam methods* Z. Elekes
4. April 5 *Nuclear reaction studies in nuclear astrophysics* Gy. Gyürky
5. April 12 *State of affairs* M. Pálincás, R. Lovas
6. April 19 *Safety analysis of radioactive waste storers I.* S. Mészáros, É. Svingor
April 23 *Wigner crystals classical and quantum* F.I.B Williams (Saclay)
7. April 26 *Safety analysis of radioactive waste storers II.* I. Csige, Z. Elekes
8. May 11 *Heavy element research in Japan* H. Kudo (Niigata University)
9. May 17 *A QCD toy model* P.O. Hess (UNAM, Mexico)
10. June 7 *The education system of Simon Bolivar University: Venezuela at the beginning of the third millenium* L. Sajo Bohus (Caracas)
11. June 27 *Hydrological model of water holding layers under the Paks NPP* É. Svingor
12. September 20 *Entry* I. Balogh, A. Csík, E. Dobos, Z. Máté, T. Ricsóka, G. Szíki
13. October 4 *MUNIN, SMART-I; Participation in satellite programs* J. Molnár, G. Székely
14. October 25 *Quantum localization of the kicked Rydberg atom* S.Yoshida (Vienna)
15. October 26 *Time-dependent DFT used as a tool to investigate electronic excitations at surfaces* C. Lemell (Vienna)
16. November 20 *Study of light exotic nuclei with the stochastic variational method* Y. Suzuki (Niigata University)
17. November 29 *Modern semiconductor detectors* G. Kalinka
18. December 6 *Quantum trajectories of stochastic Schrödinger equations* J. Burgdörfer (Vienna University of Technology)
19. December 7 *Stereo-microscope for atomic arrangement by circularly polarized X-ray photoelectron diffraction and three-dimensional band mapping with linearly polarized SR* H. Daimon (Nara Institute of Science and Technology)
20. December 13 *The history of the stochastic interpretation of quantum mechanics* P. Szegedi (ELTE)
21. December 17 *Excitations depending on atomic environment in Auger processes* L. Kövér

Author index

- Ahmad I. 18
Algora A. 9, 10, 13
Amorini F. 11
Andreoiu C. 10
de Angelis G. 10
Aoi N. 19
ASACUSA collaboration 26
Astier A. 18
Aszalós-Kiss B. 31, 32
Ata A. 10
Azaiez F. 11, 18
Azuma T. 34
- Baba H. 19
Bäck T. 10
Baiborodin D. 11
Baradács E. 52
Barnéoud D. 17
Bartha L. 55
Bauchet A. 11
Bazzacco D. 10
Becker F. 11
Beke D.L. 41, 42, 43
Belleguic M. 11
Berényi D. 36
Berényi Z. 31, 32, 60
Bergström M. 18
Bettioli A.A. 57
Bideux L. 58
Biri S. 65, 66
Blomqvist J. 10
Blumenthal D.J. 18
Borbély-Kiss I. 4
Borcea C. 11
Borge M.J.G. 13
Boston A.J. 16
Bourgeois C. 11
Brant S. 17
Bremer J.H. 38, 39
Bucurescu D. 16
Burgdörfer J. 34, 35, 44
- Campajola L. 61
Campeanu C. 20
Cano-Ott D. 13
Carpenter M.P. 18
- Căta-Danil Gh. 16
Cederkäll J. 10
Cederwall B. 10
Chesnel J.-Y. 39
Civitarese O. 6
Courtin S. 13
Crowelly B. 18
- Csatlós M. 8
Csegzi S. 47
Cseh J. 3, 9
Cserny I. 58
Csige I. 47
Csik A. 31, 32, 42
- Daróczi L. 42
De Cesare N. 61
Demetriou P. 4
Demichi K. 19
Dessagne Ph. 13
Dezső Z. 46, 52
Dlouhy Z. 11
Dombrádi Zs. 10, 11, 19
Domonyi A. 58
D'Onofrio A. 61
Donzaud C. 11
Dudu D. 20
Duprat J. 11
Ducroux L. 18
Duta E. 20
- Elekes Z. 19, 45
Erdélyi Z. 42
- Fahlander C. 10
Fant B. 10
Farnea E. 10
Fink D. 38
Foin C. 17
Formicola A. 61
Fraile L.M. 13
Fukuda N. 19
Fülöp Zs. 4, 5, 19, 61
Futó I. 48, 50, 51
- Gácsi Z. 8

- Gadea A. 10, 13
 Galanopoulos S. 4
 Gelberg A. 19
 Gál I. 58
 Gál J. 64
 Gall B.J.P. 18
 Gelletly W. 13
 Genevey J. 17
 Gialanella L. 61
 Gillaspay J.D. 60
 Girod M. 11
 Gizon A. 16, 17
 Gizon J. 16, 17
 Gomi T. 19
 Górska M. 10
 Grawe H. 10
 Greife U. 61
 Gruzza B. 58
 Guillemaud-Mueller D. 11
 Gulyás J. 8
 Gulyás L. 22, 23, 37
 Gurin P. 43

 Gyürky Gy. 4, 5, 61

 Hakl J. 43, 46
 Hannachi F. 17, 18
 Harissopoulos S. 4
 Hasegawa H. 19
 Hashimito-Saitoh N. 10
 Hegyesi Gy. 8, 63, 64
 Heil M. 8
 Hellhammer R. 38
 Hess P.O. 9
 Hoffmann V. 38, 39
 Hörndl M. 35
 Horváth D. 26
 Hubel H. 18
 Hudson L. 60
 Hunyadi I. 52

 Ibrahim F. 11
 Imai N. 19
 Imbriani G. 61
 Ishihara M. 19
 ISOLDE collaboration 13
 Ito T. 34
 Iwasaki H. 19

 Jánossy A. 65
 Janssens R.V.F. 18
 Johnson A. 10
 Joss D.T. 16
 Juhász B. 26
 Jungclaus A. 13

 Kaeppler F. 8
 Kalinka G. 62, 63, 64
 van Kan J.A. 57
 Kaneko E. 19
 Kanno S. 19
 Kántor Z. 40
 Kapta K. 42
 Karácsony J. 66
 Katona G.L. 41
 Kawasaki H. 19
 Kenéz L. 65, 66
 Kerek A. 10
 Kerekes L. 43
 Kertész Zs. 58
 Khoo T.L. 18
 Kishida T. 19
 Kiss Á.Z. 45
 Kiss J. 58
 Kis-Varga M. 41, 42, 43
 Klamra W. 10
 Kokkoris M. 4
 Komaki K. 34
 Koncz Cs. 36
 Kondo Y. 19
 Korichi A. 18
 Kormány Z. 56
 Kovács Z. 54
 Kövér Á. 22
 Kövér L. 31, 32, 58
 Kownacki J. 10
 Krasznahorkay A. 8
 Krasznahorkay A.Jr. 8
 Kubo T. 19

 Lagergren K. 10
 Langer G.A. 42
 Lauritsen T. 18
 Lenzi S.M. 10
 Lévai G. 1, 2
 Liang C.F. 17
 Likar A. 10
 Liotta R.J. 6

- Lipoglavšek M. 10
 Lopez M.J. 11
 Lopez-Martens A. 17, 18
 Lovas R.G. 12, 14, 15
 Lubritto C. 61
 Luca A. 20
 Lucas R. 11
 Lugosi L. 22, 23, 27, 29
 Lukyanov S.M. 11
 LUNA collaboration 5
- Maréchal F. 13
 Maslov V. 11
 Máté Z. 8
 Matolin V. 58
 Menyhárd M. 58
 Merdinger J.C. 17
 Mészáros S. 43
 Meyer M. 18
 Mezei J.Zs. 12
 Michimasa S. 19
 Miehé Ch. 13
 Minemura T. 19
 Miura M. 19
 Molnár Gy. 58
 Molnár L. 46
 Molnár M. 48, 50, 51
 Moore C. 11
 Mosolygó J. 58
 Moszyński M. 10
 Motobayashi T. 19
 Mrazek J. 11
- Nácher E. 13
 Nagy A. 58
 Nagy Z. 7
 Nakamura T. 19
 Napoli D.R. 10
 Nisius D. 18
 Norlin L.-O. 10
 Notani M. 19
 Nowacki F. 11
 Nyakó B.M. 11, 16, 17, 64
 Nyberg J. 10
- Ohnishi T. 19
 Ong H.J. 19
 Orbán A. 33, 36
 Ordine A. 61
- Ould-Metidji Y. 58
- Paar V. 17
 Palacz M. 10
 Palcsu L. 48, 49, 50, 51
 Papp T. 30, 62, 63
 Paripás B. 37
 Paris P. 17
 Parry C.M. 16
 Paul E.S. 16, 18
 Penionzhkevich Yu.-E. 11
 Perrot F. 13
 Pethó G. 58
 Petizon L. 11
 Petrov A. 38
 Poirier E. 13
 Porquet M.G. 18
- Ragnarsson I. 18
 Rajta I. 57
 Rangama J. 39
 Redon N. 18
 Reinfarth R. 8
 Reinhold C.O. 34
 Roca V. 61
 Rogalla D. 61
 Rolfs C. 61
 Romano M. 61
 Rossi-Alvarez C. 10
 Roth H.A. 10
 Roy P. 2
 Roychoudhury R. 2
 Rózsa P. 45
 Rubio B. 13
 Rudolph D. 10
 Russo M. 61
- Sabbarese C. 61
 Sahagia M. 20
 Saint-Laurent M.G. 11
 Saito A. 19
 Saitoh T. 10
 Sakurai H. 19
 Sarazin F. 11
 Sarkadi L. 22, 23, 24, 25, 29
 Sarkadi-Pribóczki É. 54
 Scarpaci J.A. 11
 Scheurer J.N. 64
 Seliger M. 34

Semple A.T. 16
Seweryniak D. 10
Sharpey-Schaferz J.F. 18
Shimoura S. 19
Simon A. 40, 45
Simulák J. 45
Skeppstedt "O. 10
Sletten G. 11
Sohler D. 10, 11, 16
Somorjai E. 4, 5, 55, 61
Sorlin O. 11
Stanoiu M. 11
Stodel C. 11
Stolterfoht N. 38, 39
Strieder F. 61
Sugimoto T. 19
Sulik B. 33, 36, 38, 39
Sulyok A. 58
Suzuki Y. 12, 14, 15
Svingor É. 48, 50, 51

Szabó Cs. 60
Szabó I. 58
Szabó S. 43
Szántó Zs. 48, 49, 50, 51
Sziki G.Á. 45
Szöör Gy. 45
Szűcs Z. 20

Tain J.L. 13
Takabayashi Y. 34
Takács E. 26, 60
Takeuchi S. 19
Tarr G. 58
Taylor M. 11
Tengblad O. 13
Terrasi F. 61
Theisen C. 11

Thirolf P.G. 8
Timár J. 8, 10, 11, 16, 17, 18
Tőkési K. 22, 27, 34, 35, 36, 37, 38, 44
Tong, X.M. 44
Török I. 30
Tóth J. 31, 32, 58
Trautvetter H.P. 61
Trócsányi Z. 7

Uzonyi I. 43, 45

Vad K. 43
Valek A. 65, 66
Varga D. 31, 32, 58
Varga K. 14, 15
Vertse T. 6
Viktor Gy. 37
Vitéz G. 37
Votolini G. 11

Wadsworth R. 18
Watanabe H. 19
Watt F. 57
Weiss B. 17
Weiszflog M. 10
Wilson A.N. 18
Wilson J.N. 18
Wolińska M. 10

Yamazaki Y. 34
Yoneda K. 19
Yoshida S. 35

Znojil M. 1, 2
Zolnai L. 16, 17
Zouros T.J.M. 33

Kiadja a
Magyar Tudományos Akadémia Atommagkutató Intézete
A kiadásért és szerkesztésért felelős
Dr. Lovas Rezső, az Intézet igazgatója
Sokszorosítás:
REXPO Kft. Nyomdaüzeme, Debrecen, Poroszlai u. 6.
Tel.: 52/452-555, Fax: 52/452-666
Felelős vezető: Rácz János
Debrecen, 2002. augusztus



